



Eigenvalues and delay differential equations: periodic coefficients, impulses and rigorous numerics

Kevin E. M. Church¹

Received: 29 April 2020 / Revised: 11 September 2020 / Accepted: 24 September 2020 /

Published online: 8 October 2020

© Springer Science+Business Media, LLC, part of Springer Nature 2020

Abstract

We develop validated numerical methods for the computation of Floquet multipliers of equilibria and periodic solutions of delay differential equations, as well as impulsive delay differential equations. Using our methods, one can rigorously count the number of Floquet multipliers outside a closed disc centered at zero or the number of multipliers contained in a compact set bounded away from zero. We consider systems with a single delay where the period is at most equal to the delay, and the latter two are commensurate. We first represent the monodromy operator (period map) as an operator acting on a product of sequence spaces that represent the Chebyshev coefficients of the state-space vectors. Truncation of the number of modes yields the numerical method, and by carefully bounding the truncation error in addition to some other technical operator norms, this leads to the method being suitable to computer-assisted proofs of Floquet multiplier location. We demonstrate the computer-assisted proofs on two example problems. We also test our discretization scheme in floating point arithmetic on a gamut of randomly-generated high-dimensional examples with both periodic and constant coefficients to inspect the precision of the spectral radius estimation of the monodromy operator (i.e. stability/instability check for periodic systems) for increasing numbers of Chebyshev modes.

Keywords Impulsive delay differential equations · Floquet multipliers · Chebyshev series · Rigorous numerics · Computer-assisted proofs

1 Introduction

Linearized growth and decay rates near steady states and invariant manifolds play a central role in the analysis of dynamical systems. When these manifolds have simple descriptions such as fixed points or periodic orbits, the computation of these growth rates is equivalent to an eigenvalue problem. For delay differential equations (or more generally, retarded functional

✉ Kevin E. M. Church
kevin.church@mcgill.ca

¹ Department of Mathematics and Statistics, McGill University, Burnside Hall, 805 Sherbrooke Street West, Montreal, QC H3A 0B9, Canada

differential equations), several authors have proposed solutions to the “delay eigenvalue problem”. For autonomous linear equations, these include methods based on discretization of the associated infinitesimal generator [3,4,18,33] and the solution operator [15]. In the scope of equations with periodic coefficients, there are several results concerning discretization and characteristic matrices [15,16,26,29,30].

Discretization schemes can provide strong convergence properties, but these still may not be able to provide mathematical proof concerning one or more approximate eigenvalues. For example, the spectral accuracy of the infinitesimal generator method with Chebyshev collocation [5] guarantees that each eigenvalue of the delay differential equation (DDE) is well-approximated by *some* eigenvalue of the discretized problem. Such convergence results exist also for methods based on the solution operator [16] and they can be summarized by the statement: every eigenvalue of the DDE is the limit of some eigenvalue of the discretized problem. However, one is often interested in a situation dual to this. That is, one wants to know when one or more eigenvalues of the *discretized problem* are close (or have the same relative location in the complex plane) as a pairing of eigenvalues of the DDE.

There has been progress recently on methods that can automatically prove (with the assistance of a computer and interval arithmetic) results concerning the location of eigenvalues of DDEs based on the eigenvalues of some discretization. We highlight the 2017 paper by Miyajima [23] on verified error bounds for particular eigenvalues, and the 2020 paper by Lessard and Mireles James [21] on validation of generalized Morse indices. These papers both concern autonomous problems, so one motivation of the present paper is to build on the results of Lessard and Mireles James to accommodate DDEs with periodic coefficients. Since we get a numerical discretization scheme for the monodromy operator (i.e. the period map) for free out of our analysis, we simultaneously get an alternative to the method of Gilsinn and Potra [16] for the computation of Floquet multipliers (the linearized stability-determining quantities) of DDEs with periodic coefficients.

In the case of autonomous DDEs, if the explicit location of an eigenvalue is required to high accuracy then there are several ways this can be accomplished [7,21,23]. Of mention is that in this case, the eigenvalues are precisely the zeroes λ of the characteristic equation $\det(\Delta(\lambda)) = 0$, where $\Delta(\lambda)$ is the *characteristic matrix* of the DDE. The characteristic equation is transcendental in λ , but the result is still a scalar (complex) zero-finding problem ($\Delta(\lambda)$ is a $d \times d$ matrix with d equal to the dimension of the DDE), so a given eigenvalue can be verified to a provable level of accuracy using the radii polynomial method; see Theorem 2.2 of [21] for a direct application of the method to the present situation. While characteristic matrices for periodic DDEs can be constructed [26,30] and the eigenvalues of these matrices are related to the Floquet multipliers, a discretization step must still be performed. Even if the characteristic matrix is explicitly available, such as when the delay is a multiple of the period [32], the computation of the matrix generally requires at least computing the Cauchy matrix of a time-periodic ordinary differential equation and computing weighted integrals involving this and the periodic coefficients. We have been unable to find publications concerning error estimates between the approximate eigenvalues of discretized characteristic matrices for periodic DDEs and the Floquet multipliers. As such, another goal of the present paper is to devise a strategy to validate the location of specific Floquet multipliers of DDEs with periodic coefficients.

Some physical systems are characterized by smooth evolution in addition to brief bursts of activity. This might be due to exogenous forcing or it might be an intrinsic property of the system. If these bursts of activity incur relatively large disturbances to the state and do not occur too frequently, it can be beneficial to model them as discontinuities. One mathematical formalism for such a construction is impulsive dynamical systems, which include impulsive

differential equations [2,20,25], impulsive evolution equations [13] and impulsive functional differential equations [8,28]. One of the simplest classes of impulsive dynamical system is one in which these discontinuities (hereafter called impulses) occur at fixed times. Even for more complicated classes of problems where impulses are triggered according to mixed spatio-temporal relations, the case of fixed (in time) impulses is still relevant since linear systems of this type arise linearization at bounded or periodic trajectories [2]. When the sequence of impulses has periodic structure and this is compatible with the continuous dynamics, the result is a periodic system. The Floquet theory has been developed for linear periodic impulsive retarded functional differential equations [10] and characteristic equations/matrices for special cases of periodic linear impulsive DDE [17,27] have been developed, but at present there is no rigorous numerical method to compute Floquet multipliers for a general class of such equations. Our approach in this paper will simultaneously address the approximation of Floquet multipliers for impulsive delay differential equations by way of a Chebyshev spectral method, computer-assisted proof of Floquet multiplier location, and computer-assisted proof of the count of the number of unstable Floquet multipliers (or generally, the number of Floquet multipliers having absolute value greater than some prescribed value). Formally, the most broad class of systems for which our numerical method applies is systems of the form

$$\begin{aligned} \dot{x} &= A(t)x(t) + B(t)x(t - q), & t \notin p\mathbb{Z} \\ \Delta x &= C_1x(t^-) + C_2x(t - q), & t \in p\mathbb{Z}, \end{aligned}$$

for (sufficiently regular) real matrix-valued functions $A(t)$ and $B(t)$, real matrices C_1 and C_2 , and natural numbers p (period) and q (delay). Necessary background on these systems appears in Sect. 2. More generally, we can treat systems with commensurate period and delay by way of a time scaling.

With the previous paragraph in mind, we will state and prove all results in the context of periodic impulsive delay differential equations. This class of equations includes delay differential equations with periodic coefficients by taking $C_1 = C_2 = 0$ in the displayed equation above, so our results can be applied to those equations as well. Finally, although this is an extreme level of reduction, the results also apply to ordinary and impulsive differential equations without delays. To give the reader a taste of the kinds of results that can be proven using our validated numerics framework, we still state two theorems that are consequences of results that appear in (and are proven in) Sect. 8.

Theorem *Let $\beta = 0.1$, $\rho = 1$, $K = 1$, $d_1 = 0.02$, $d_2 = 0.03$ in the following time-delay predator-prey model with impulsive harvesting*

$$\begin{aligned} \dot{x} &= rx(t)(1 - x(t)/K) - \beta x(t)y(t) \\ \dot{y} &= \rho\beta e^{-d_1\tau}x(t - \tau)y(t - \tau) - d_2y(t), & t \notin \mathbb{Z} \\ \Delta y &= -hy(t^-), & t \in \mathbb{Z}. \end{aligned}$$

The equilibrium $(K, 0) = (1, 0)$ enjoys the following properties for any $r > 0$:

- *its unstable manifold is one-dimensional if $h = 0.060$ and $\tau \in \{1, 2, 3\}$;*
- *it is locally asymptotically stable if $h = 0.075$ and $\tau \in \{1, 2, 3\}$;*
- *its unstable manifold is one-dimensional for all $h \in [0, 0.060]$ if $\tau = 1$;*
- *with $\tau = 1$, one of its Floquet multipliers crosses the unit circle at some $h \in [0.065, 0.066]$, and over this entire range of h there is exactly one eigenvalue whose absolute value is greater than 0.8.*

Theorem Consider the following two-dimensional delay equation modeled on the normal form of the Hopf bifurcation:

$$\begin{aligned}\dot{x} &= \beta x(t) - \pi y(t) - x(t)(x^2(t - \tau) + y^2(t)) \\ \dot{y} &= \pi x(t) + \beta y(t) - y(t)(x^2(t) + y^2(t - \tau)).\end{aligned}$$

For $\tau \in \mathbb{N}$, there is a nontrivial (i.e. nonzero) branch of periodic solutions parameterized by β . At parameter $\beta = \frac{3}{2}$ and $\tau = 1$, the unstable manifold of this periodic solution is at least two-dimensional.

1.1 Overview of the paper

The scope of this paper is fairly broad. It is therefore expected that many readers will only be interested in the numerical method and its applications to stability. Others, however, will want to see all the technical details concerning computer-assisted proofs. The difficulty is that the theory is intrinsically tied to the numerical method and its machine implementation. To ensure a sufficiently wide range of researchers are able to appreciate the content, we will overview the paper here with these points in mind.

The core of the numerical method is derived in Sects. 3 and 4 with the help of the background from Sect. 2. The first, Sect. 3, concerns an explicit representation of the monodromy operator. In Sect. 4.1 we review Chebyshev expansion and convolution, and in Sect. 4.2 we represent the monodromy operator on a sequence space by way of correspondence with Chebyshev series. The representation of the operator is on an infinite-dimensional space, and the explicit numerical method is obtained by projecting to a finite-dimensional subspace by mode truncation and projection. These mechanisms are described at the beginning of Sect. 4.3, in Sect. 4.4 and in Remark 6.3.1. The last remark involves some technical machinery, and a simplified implementation that would function *only* in the case of equal period p and delay q could be obtained by following Remark 6.1.1 from Sect. 6.1 instead. Once these details are ironed out, implementing the method for general period and delay amounts to simple matrix algebra and this is covered in Sect. 7.2, where some convergence guarantees are also discussed. Several examples featuring the double arithmetic implementation are provided in Sect. 9 to show how the implementation scales with respect to the dimension of the problem and the order of the method.

Concerning the rigorous numerics, we prove a few necessary results concerning Floquet theory in Sect. 2. Section 3 is devoted to an abstract functional-analytic representation of the monodromy operator. In Sect. 4 we transition from the abstract representation to a concrete representation of the monodromy operator in terms of Chebyshev series and establishes the basis for computer-assisted proof of eigenvalue location. Section 5 contains several auxiliary bounds of linear maps and operators that are needed later. Section 6 contains proofs of (computable) upper bounds for various abstract operators that are needed for computer-assisted proofs of eigenvalue location. We discuss MATLAB implementation in Sect. 7, while Sect. 8 is devoted to examples of computer-assisted proof.

We wrap up the paper with a conclusion in Sect. 10.

2 Preliminaries

In this section we will state relevant background concerning impulsive delay differential equations and Floquet multipliers. We will state some basic assumptions that will be needed

throughout the paper, and we will prove results concerning the regularity of the eigenfunctions that will be needed later.

2.1 Impulsive delay differential equations

In this paper, a *nonlinear periodic impulsive delay differential equation* will consist of of a delay differential equation together with a discrete-time update rule:

$$\begin{aligned} \dot{x} &= f(t, x(t), x(t - \tau)), & t \neq t_k & \quad (1) \\ \Delta x &= g(k, x(t_k^-), x(t_k - \tau)), & t = t_k. & \quad (2) \end{aligned}$$

The periodicity comes from the assumption that there exists some $n > 0$ and $T > 0$ such that $t_{k+n} = t_k + T$ for all integers k , while also $g(k + n, \cdot, \cdot) = g(k, \cdot, \cdot)$ and $f(t + T, \cdot, \cdot) = f(t, \cdot, \cdot)$. Equation (2) should be interpreted as

$$x(t_k) - x(t_k^-) = g(k, x(t_k^-), x(t_k - \tau)), \quad (3)$$

where $x(t^-)$ denotes the limit from the left at time t . Systems with multiple and time-varying delays can also be considered. More generally, impulsive retarded functional differential equations can be considered without periodicity assumptions. We refer the reader to [1,2,25,28] for background on impulsive differential equations. In future we will refer to (1)–(2) simply as a nonlinear IDDE, and will drop the reference to periodicity. In what follows we will assume that f is C^1 in its second and third variables and continuous from the right and bounded in its first, while g is C^1 in its second and third variables.

The following definitions are adapted from [8]. A *solution* (unconditional on any initial data) $x : \mathbb{R} \rightarrow \mathbb{R}^d$ of (1)–(2) is a function that is continuous from the right, possesses limits on the left, and satisfies both equations (1) and (2), with the derivative being interpreted as a right-hand derivative. These solutions are continuous from the right at times t_k with finite limits on the left. Any natural phase space for (1)–(2) with a vector space structure must therefore contain functions that have many discontinuities. To see why, observe that at each time t_k , the solution in \mathbb{R}^d will have a discontinuity, so the solution history $\theta \mapsto x_t(\theta)$ for $x_t : [-\tau, 0] \rightarrow \mathbb{R}^d$ and defined by $x_t(\theta) = x(t + \theta)$ will have a discontinuity at the lagged argument θ whenever $t + \theta = t_k$. This observation leads naturally to the choice of phase space

$$\begin{aligned} \mathcal{RCR}([-\tau, 0], \mathbb{R}^d) &= \{\phi : [-\tau, 0] \rightarrow \mathbb{R}^d : \phi \\ &\text{is continuous from the right and has limits on the left}\}. \end{aligned}$$

These are the *right-continuous regulated functions*. We will often write it simply as \mathcal{RCR} when there is no ambiguity. When equipped with the supremum norm $\|\phi\| = \sup_{\theta \in [-\tau, 0]} |\phi(\theta)|$ for $|\cdot|$ some norm on \mathbb{R}^d , \mathcal{RCR} becomes a Banach space. One can then define a *solution satisfying the initial condition* $x_s = \phi$ for some $(s, \phi) \in \mathbb{R} \times \mathcal{RCR}$ to be a function $x : [s - \tau, s + \beta) \rightarrow \mathbb{R}^d$ such that $x|_{(s, s + \beta)}$ satisfies (1)–(2) and $x_s = \phi$. Under the conditions described above, such a solution is guaranteed to exist and be unique for any $(s, \phi) \in \mathbb{R} \times \mathcal{RCR}$, and defined on a maximal interval of existence. Following this, an IDDE generates a (nonlinear) two-parameter semigroup on \mathcal{RCR} through the solution map in the usual way.

It is typical for nonlinear IDDE to possess no fixed points, and these will typically not be robust under perturbations of the vector field f and jump map g . This can be seen by observing that the problem of finding zeroes of the map $F : \mathbb{R}^d \rightarrow \mathbb{R}^d \times \mathbb{R}^d$ defined by

$F(x) = (f(x), g(x))$ is generally overdetermined. However, a generic periodic solution (of period jT for $j \in \mathbb{N}$) is robust under small T -periodic perturbations (this is a fairly direct consequence of Theorem 5.1.1 from [10], the Floquet theory and the implicit function theorem) of f and g , so in this regard periodic solutions are the simplest structurally stable invariant sets one can study in IDDE.

2.2 Monodromy operator and Floquet multipliers

The local stability of a periodic solution γ is determined by the trivial solution $y = 0$ of the linearization

$$\dot{y} = D_2f(t, \gamma(t), \gamma(t - \tau))y(t) + D_3f(t, \gamma(t), \gamma(t - \tau))y(t - \tau), \quad t \neq t_k \tag{4}$$

$$\Delta y = D_2g(k, \gamma(t^-), \gamma(t - \tau))y(t^-) + D_3g(k, \gamma(t^-), \gamma(t - \tau))y(t - \tau), \quad t = t_k. \tag{5}$$

If γ has period jT for some $j \in \mathbb{N}$, then (4)–(5) has period $\tilde{T} = jT$.

Let $t \mapsto y(t, s, \phi)$ denote the unique solution of (4)–(5) satisfying the initial condition $y_s(\cdot, s, \phi) = \phi$. Each (eventually compact) linear operator $M_t : \mathcal{RCR} \rightarrow \mathcal{RCR}$ defined by

$$M_t\phi = y_{t+\tilde{T}}(\cdot, t, \phi) \tag{6}$$

is called a *monodromy operator*. The spectrum of each monodromy operator is identical, so by convention we will usually refer to $M := M_0$ as *the* monodromy operator. γ is locally asymptotically stable if all eigenvalues of M are in the open ball $B_1(0) = \{z \in \mathbb{C} : |z| < 1\}$. When some eigenvalues have unit modulus but all others have modulus less than one, the stability of γ depends on some more algebraic properties (eg. whether the restriction of M to the direct sum of generalized eigenspaces associated to the eigenvalues of unit modulus has a diagonalizable representation) and dynamical properties (i.e. the flow on its centre manifold). If any eigenvalue has modulus greater than one, γ is unstable. The eigenvalues of M are called *Floquet multipliers*.

The computation of Floquet multipliers is important for several reasons. Apart from verifying stability or instability of a periodic solution, the number of Floquet multipliers outside of the disc $\overline{B_1(0)}$ together with the dimension of their generalized eigenspaces dictates the dimension of the unstable manifold of γ . The classification of a bifurcation in a parameter-dependent system depends on the structure of the centre fibre bundle in addition to higher-order normal form data, all of which depends on the Floquet multipliers on the unit circle and their associated eigenfunctions. For these reasons, we will now dispense with the explicit dependence on γ and consider the more general linear periodic impulsive delay differential equation

$$\dot{y} = A(t)y(t) + B(t)y(t - \tau), \quad t \neq t_k \tag{7}$$

$$\Delta y = C_1(k)y(t^-) + C_2(k)y(t - \tau), \quad t = t_k. \tag{8}$$

We will refer to such a system as a linear periodic IDDE (impulsive delay differential equation). The periodicity here means that there exists $T > 0$ and $n > 0$ such that $A(t+T) = A(t)$, $B(t+T) = B(t)$, $C_1(k+n) = C_1(k)$, $C_2(k+n) = C_2(k)$, and $t_{k+n} = t_k + T$.

2.3 Eigenfunctions are densely nonsmooth

Our approach to rigorous computation of Floquet multipliers will be based in part on a suitable representation of the eigenfunctions of the monodromy operator as infinite series with good

convergence properties. Unfortunately, the problem of computing the Floquet multipliers for the fully general periodic system (7)–(8) seems not very amenable to this approach, even if we assume A and B are analytic. The following proposition and its associated proof should demonstrate the main problem.

Proposition 2.3.1 *Let ϕ be an eigenfunction of the monodromy operator M associated to the scalar impulsive delay differential equation*

$$\begin{aligned} \dot{y} &= \alpha y(t - \tau), & t \neq k \in \mathbb{Z}, \\ \Delta y &= \beta y(t^-), & t = k \in \mathbb{Z}, \end{aligned}$$

for $\alpha \neq 0$, $\beta \neq -1$ and $\tau \in \mathbb{R} \setminus \mathbb{Q}$ irrational. Let $(a, b) \subset [-\tau, 0]$. There exists $q > 0$ such that $\phi|_{(a,b)}$ is at most q times differentiable.

Proof $t \mapsto y(t; 0, \phi)$ is a solution that can be represented in the form $e^{t\lambda} p(t)$ for p periodic with period one and differentiable from the right. Substituting this ansatz into the IDDE and simplifying, it follows that p is a 1-periodic solution of

$$\begin{aligned} \dot{p} &= -\lambda p(t) + \alpha e^{-\lambda\tau} p(t - \tau), & t \neq k \\ \Delta p &= \beta p(t^-), & t = k. \end{aligned}$$

We first prove that p is discontinuous at each integer $k \in \mathbb{Z}$. Suppose not, then we must have $p(k) = 0$ since $\beta \neq -1$. p is therefore a 1-periodic solution of the DDE

$$\dot{p} = -\lambda p(t) + \alpha e^{-\lambda\tau} p(t - \tau)$$

with $p(0) = 0$. The phase space of the above DDE decomposes $\mathcal{C} = \mathcal{C}([-\tau, 0], \mathbb{R})$ as

$$\mathcal{C} = R \oplus S \oplus N \oplus U,$$

where S, N and U are the stable, centre and unstable subspaces respectively, while R generates those solutions that have superexponential decay: $\psi \in R$ if and only if

$$\lim_{t \rightarrow \infty} p(t, 0, \psi)e^{rt} = 0, \quad \forall r > 0.$$

Consequently, any periodic solution must be generated by an element of the centre subspace and is therefore of the form

$$p(t) = c_1 e^{i\omega t} + c_2 e^{-i\omega t}$$

for some $\omega > 0$. Since p must be 1-periodic, we get $\omega = 2\pi$. The condition $p(0) = 0$ implies $p(t) = c \sin(2\pi t)$ for a constant c , with $c \neq 0$ because ϕ is an eigenfunction. Substituting this ansatz into the delay differential equation, performing some algebraic simplifications and recalling that $\alpha \neq 0$, we can derive the equation

$$\left(\frac{e^{\lambda\tau}(2\pi + \lambda)}{\alpha} - \cos(2\pi\tau) \right) \sin(2\pi t) + \sin(2\pi\tau) \cos(2\pi t) = 0.$$

From the linear independence of sine and cosine, τ must be rational, which contradicts our assumption of τ being irrational. We conclude that p must be discontinuous at the integers.

Next, we prove that if p is infinitely many-times differentiable at some $t \in \mathbb{R}$, then $t - k\tau \notin \mathbb{Z}$ for all integers $k \geq 0$. We prove this by strong induction on k . We already know that p is discontinuous on the integers, so we must have $t \notin \mathbb{Z}$ for p to be differentiable

at t . Suppose now that p is infinitely many-times differentiable and that $t - j\tau \notin \mathbb{Z}$ for $j = 0, \dots, k$ for some $k \geq 0$. We have

$$p^{(k+1)}(t) = -\lambda p^{(k)}(t) + \alpha e^{-\lambda\tau} p^{(k)}(t - \tau). \tag{9}$$

If p is indeed infinitely many-times differentiable at t , then the right-hand side must be continuous at t . A straightforward inductive proof shows that each of $p^{(k)}$ and $p^{(k)}(t - \tau)$ can be written as a finite linear combination of the terms $p(t - j\tau)$ for $j = 0, \dots, k + 1$, and in particular the right-hand side of (9) written in terms of these has a nonzero coefficient on $p(t - (k + 1)\tau)$. By the strong induction hypothesis, $t - j\tau \notin \mathbb{Z}$ for $j = 0, \dots, k$. If the right-hand side of (9) is indeed continuous at t , then we must also have $t - (k + 1)\tau \notin \mathbb{Z}$. This completes the inductive proof, and it follows that $t - j\tau \notin \mathbb{Z}$ for all $j \geq 0$.

Finally, let $(a, b) \subset [-\tau, 0]$. The restriction $\phi|_{(a,b)}$ is C^∞ if and only if $p|_{(a,b)}$ is also C^∞ . Consider the sequences

$$p_n = n\tau, \quad c_n = [p_n]_1,$$

where $[x]_1 = x - [x]$. c_n is dense in $[0, 1]$, from which it follows that there exist integers $k, j \geq 0$ such that $p_k \in (a + j, b + j)$. Define $c = k\tau - j \in (a, b)$. From previous analysis, p is not infinitely many-times differentiable at c since $c - k\tau = -j \in \mathbb{Z}$. □

When the delay and the period are non-commensurate, it should be expected that the eigenfunctions of a linear periodic IDDE will have a lower order of smoothness in any subinterval of their domain. In particular, the set of points where an eigenfunction fails to be infinitely many times differentiable is dense in its domain.

2.4 Regularity of the eigenfunctions under commensurate delay and period

With the observations of the previous section in mind, we will need to make the following additional assumption on the structure of (7)–(8) in order to have a chance of eigenfunctions with appropriate series representations. The following definition will be used fairly often.

Definition 2.4.1 Let X be a complex Banach space and let (a_k, b_k) be a (finite, infinite or bi-infinite) sequence of nondegenerate open intervals with $b_k = a_{k+1}$. A function $f : I \subset \mathbb{R} \rightarrow X$ (possibly real-valued) for an interval I is *piecewise-analytic with respect to (a_k, b_k)* if:

- f is continuous from the right and locally bounded,
- for each k , there exists an open neighbourhood U_k of $[a_k, b_k]$ in \mathbb{C} such that $f|_{(a_k, b_k) \cap I} = \tilde{f}_k|_{(a_k, b_k) \cap I}$ for some analytic function $\tilde{f}_k : U_k \rightarrow X$.

Given such a function f , the sequence \tilde{f}_k will denote the analytic extensions from (a_k, b_k) .

Assumption 0 The following conditions are satisfied.

- A0.1 The sequence t_k satisfies $t_{k+1} = t_k + T$ and, additionally, $C_1(k)$ and $C_2(k)$ are constant.
- A0.2 There exist $p, q \in \mathbb{N}$ such that $qT - p\tau = 0$.
- A0.3 The T -periodic functions $t \mapsto A(t)$ and $t \mapsto B(t)$ are piecewise-analytic with respect to the open intervals $I_k := \left(t_0 + \frac{kT}{p}, t_0 + \frac{(k + 1)T}{p} \right)$ for $k \in \mathbb{Z}$.

We refer to the above as **Assumption 0** because we will shortly perform a change of variables that will make its characterization a bit nicer. Under this assumption, we make the change of variables

$$t - t_0 = \frac{\tau}{q} s$$

for s a new rescaled time. Defining $z(s) = y(t(s))$ and observing that $\frac{\tau}{q} = \frac{T}{p}$, we get the IDDE

$$\begin{aligned} \frac{dz}{ds} &= \frac{T}{p} A\left(t_0 + \frac{T}{p}s\right) z(s) + \frac{T}{p} B\left(t_0 + \frac{T}{p}s\right) z(s - q), & s \notin p\mathbb{Z} \\ \Delta z &= C_1 z(s^-) + C_2 z(s - q), & s \in p\mathbb{Z}. \end{aligned}$$

Observe that the matrix-valued functions $s \mapsto \tilde{A}(s) = \frac{T}{p} A(t_0 + \frac{T}{p}s)$ and $s \mapsto \tilde{B}(s) = \frac{T}{p} B(t_0 + \frac{T}{p}s)$ are now periodic functions with period p and are analytic on the intervals $(k, k + 1)$ for $k \in \mathbb{Z}$, while the restriction to each such interval is the itself the restriction of some analytic function. Dropping the tildes and relabeling the variables, we can therefore consider without loss of generality IDDEs of the form

$$\dot{y} = A(t)y(t) + B(t)y(t - q), \quad t \notin p\mathbb{Z} \tag{10}$$

$$\Delta y = C_1 y(t^-) + C_2 y(t - q), \quad t \in p\mathbb{Z}, \tag{11}$$

with $p, q \in \mathbb{N}$ and p -periodic functions A and B that are piecewise-analytic with respect to the open intervals $(k, k + 1)$ for $k \in \mathbb{Z}$.

Remark 2.4.1 If the linear system (7)–(8) is actually the linearization (4)–(5) at a periodic solution from a nonlinear periodic IDDE such as (1)–(2), the piecewise-analytic condition of A0.3 will be satisfied provided f is analytic, γ is piecewise-analytic with respect to the intervals I_k , and both A0.1 and A0.2 are satisfied. The piecewise-analyticity of periodic solutions γ w.r.t. these intervals is a technical detail, but it can be proven with similar arguments as those used in proving Proposition 2.4.1. For our examples, however, we will be taking γ to be a constant solution or an explicitly computable periodic solution, so this detail is unimportant.

The following result will be of fundamental importance once we move onto the representation of eigenfunctions. It states that the eigenfunctions of (10)–(11) with A and B piecewise-analytic with respect to $(k, k + 1)$ are also piecewise-analytic with respect to the same intervals.

Proposition 2.4.1 *Suppose the matrix-valued functions A and B in (10)–(11) are p -periodic and piecewise-analytic with respect to $(k, k + 1)$ for $k \in \mathbb{Z}$. Every eigenfunction of the monodromy operator M with nonzero eigenvalue is piecewise-analytic with respect to the same intervals.*

Proof From the Floquet theory of IDDE [11], ϕ is an eigenfunction of M with eigenvalue $\mu \neq 0$ if and only if there exists a p -periodic function $z : \mathbb{R} \rightarrow \mathbb{C}^d$ and $\lambda \in \mathbb{C}$ such that $y(t, 0, \phi) = e^{\lambda t} z(t)$ is a solution of (10)–(11), and $\mu = e^{\lambda p}$. In particular, $\phi(\theta) = e^{\lambda \theta} z(\theta)$. It follows that z is a complex-valued p -periodic solution of the IDDE

$$\begin{aligned} \dot{z} &= (A(t) - \lambda I)z(t) + B(t)e^{-\lambda q} z(t - q), & t \notin p\mathbb{Z} \\ \Delta z &= C_1 z(t^-) + C_2 e^{-\lambda q} z(t - q), & t \in p\mathbb{Z}. \end{aligned}$$

Define the translates $z_i(t) = z(t - i)$ for $i = 0, 1, \dots, q - 1$ and let $[j]_p$ denote the remainder of j modulo p —that is, $[j]_p \in [0, \dots, p - 1]$ is the unique integer such that $j = [j]_p + rp$ for some $r \in \mathbb{Z}$. It suffices to prove that the z_i are piecewise-analytic with respect to $(k, k + 1)$, and then to establish the analogous analytic continuation. By construction, (z_1, \dots, z_{q-1}) is a p -periodic solution of

$$\begin{aligned} \dot{z}_i &= (A(t - i) - \lambda I)z_i(t) + B(t - i)e^{-\lambda q}z_{[i-q]_p}(t), & t \notin i + p\mathbb{Z} \\ \Delta z_i &= C_1 z_i(t^-) + C_2 e^{-\lambda q}z_{[i-q]_p}(t), & t \in i + p\mathbb{Z}. \end{aligned}$$

Since each of $t \mapsto A(t - i)$ and $t \mapsto B(t - i)$ is piecewise-analytic with respect to $(k, k + 1)$ for $k \in \mathbb{Z}$, each z_i is also piecewise-analytic w.r.t these intervals since it can be identified with the solution of a Cauchy problem of a linear system of ordinary differential equations with analytic coefficients on each interval $[k, k + 1]$. It follows that z is piecewise-analytic with respect to the same intervals. □

The following proposition strengthens the analyticity of the solution by assuming a more precise form of the domain of analytic extensions \tilde{A}_k and \tilde{B}_k of $A|_{(k, k+1)}$ and $B|_{(k, k+1)}$. Its proof is a consequence of the monodromy theorem of complex analysis, which states sufficient conditions under which analytic continuation can be accomplished. The proof is omitted.

Proposition 2.4.2 *Let E_ν denote the Bernstein ν -ellipse in \mathbb{C} ; for background see [31]. Let $s_k(\omega) = k + \frac{1}{2}(s + 1)$ and suppose $\tilde{A}_k \circ s_k$ and $\tilde{B}_k \circ s_k$ are analytic on E_ν . Then every eigenfunction ϕ of M has $\tilde{\phi}_k \circ s_k : E_\nu \rightarrow \mathbb{C}^d$ analytic.*

With these propositions in mind, the following definition and corollary are appropriate.

Definition 2.4.2 The space of piecewise-analytic functions $\phi : [-q, 0] \rightarrow \mathbb{C}^d$ with respect to $(k, k + 1)$ for $k \in \mathbb{Z}$ will be denoted $\mathcal{P}([-q, 0], \mathbb{C}^d)$. When no confusion arises, we will write it simply as \mathcal{P} .

Corollary 2.4.1 *Let $\tilde{M} : \mathcal{P} \rightarrow \mathcal{RCR}$ denote the restriction of M to \mathcal{P} . Then $\sigma(\tilde{M}) \subseteq \sigma(M)$ and if $M\phi = \lambda\phi$ for $\lambda \neq 0$, then $\phi \in \mathcal{P}$. Moreover, \tilde{M} has range in \mathcal{P} .*

Proof The properties of the spectrum are straightforward given Proposition 2.4.1. Given a piecewise-analytic initial condition ϕ , the solution $y(t)$ of (10)–(11) with $y_0 = \phi$ is determined, on each interval $[k, k + 1]$ with $0 \leq k < \min\{p, q\}$, is the solution of an ordinary differential equation (with analytic coefficients) via the method of steps. The resulting solution is therefore piecewise-analytic at least on $[0, \min\{p, q\}]$. Successively stepping forward, $y : [0, p] \rightarrow \mathbb{C}^d$ is piecewise-analytic with respect to $[k, k + 1]$, from which it follows that \tilde{M} has range in \mathcal{P} . □

Note that \mathcal{P} is not complete (and hence not a Banach space) with respect to the supremum norm inherited from \mathcal{RCR} , but \tilde{M} is still compact. In future, we will drop the tildes and identify M with the restricted operator \tilde{M} .

There is a natural isomorphism between \mathcal{P} and a particular product space; see Fig. 1 for a visual aid. This isomorphism will be useful later, and since we are currently discussing M and the structure of \mathcal{P} , it is worth defining it now.

Proposition 2.4.3 *Introduce the spaces*

$$\mathcal{A}_0 = \{f : [-1, 0] \rightarrow \mathbb{C}^d : f = \tilde{f}|_{[-1, 0]} \text{ for some } \tilde{f} \text{ analytic}\},$$

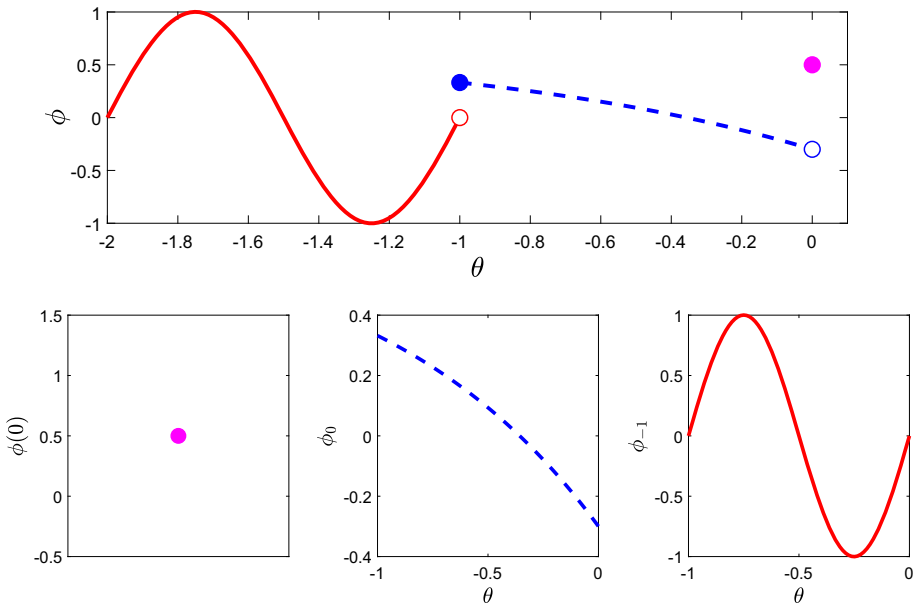


Fig. 1 Top: a typical element of $\mathcal{P}([-2, 0], \mathbb{R})$. Hollow circles denote left limits, while filled circles denote function value at the discontinuity. Bottom: the corresponding element of $\mathcal{S} = \mathbb{R} \times \mathcal{A}^2$ under the isomorphism m in order from left to right

$$\mathcal{A} = \{f|_{[-1,0)} : f \in \mathcal{A}_0\}.$$

Let $j : \mathcal{A}_0 \rightarrow \mathcal{A}$ be the restriction map: $j(f) = f|_{[-1,0)}$. Let $\pi_x : [-1, 0) \rightarrow [-1 + x, x)$ be the translation defined by $\pi_x(y) = x + y$. The following are true.

- When \mathcal{A}_0 and \mathcal{A} are equipped with the supremum norm, j is an isometric isomorphism.
- The function $m : \mathcal{P} \rightarrow \mathbb{C}^d \times \mathcal{A}^q$ defined by

$$m(\phi) = (\phi(0), \phi|_{[-1,0)}, \phi|_{[-2,-1)} \circ \pi_{-1}, \dots, \phi|_{[-q,0)} \circ \pi_{1-q})$$

is an isomorphism.

Definition 2.4.3 The space $\mathcal{S} = \mathbb{C}^d \times \mathcal{A}^q$ will be referred to as the space of *piecewise-analytic segments of length q* .

Corollary 2.4.2 The map $M^{\mathcal{S}} : \mathcal{S} \rightarrow \mathcal{S}$ with $M^{\mathcal{S}} = m \circ M \circ m^{-1}$ is well-defined and $\sigma(M) \setminus \{0\} = \sigma(M^{\mathcal{S}}) \setminus \{0\}$.

Corollary 2.4.3 Let E_ν denote the Bernstein ν -ellipse in \mathbb{C} and denote $s_k(\omega) = k + \frac{1}{2}(s + 1)$. Suppose $\tilde{A}_k \circ s_k$ and $\tilde{B}_k \circ s_k$ are analytic on E_ν . Define $\theta : [-1, 0] \rightarrow [-1, 1]$ by $\theta(s) = \frac{1}{2}(s - 1)$. Let $\phi = (\phi(0), \phi_0, \dots, \phi_{1-p}) \in \sigma(M^{\mathcal{S}})$. Then, $\phi_j \circ \theta : [-1, 1] \rightarrow \mathbb{C}^d$ has an analytic continuation to E_ν for $j = 0, \dots, 1 - p$.

$M^{\mathcal{S}} : \mathcal{S} \rightarrow \mathcal{S}$ is the representation of M on the space of piecewise-analytic segments of length q . As we will see, it is very natural to work with the space of piecewise-analytic segments as opposed to the full space \mathcal{P} when attempting to represent the monodromy operator.

3 Segment decomposition and representation of the monodromy operator

Following the analysis of Sect. 2.4 on the regularity of eigenfunctions, we will from this point on restrict our attention to linear systems

$$\dot{y} = A(t)y(t) + B(t)y(t - q), \quad t \notin p\mathbb{Z} \tag{12}$$

$$\Delta y = C_1y(t^-) + C_2y(t - q), \quad t \in p\mathbb{Z}, \tag{13}$$

with the following assumptions: The linear system (12)–(13) satisfies:

A1.1 $p \leq q$ (but see later Sect. 7.2).

A1.2 A and B are p -periodic and piecewise-analytic with respect to the intervals $(k, k + 1)$ for $k \in \mathbb{Z}$.

For the purposes of developing a numerical method with guaranteed convergence, assumption A1.1 is not too strong (see Sect. 7.2). Given Proposition 2.4.1, we know that the eigenfunctions associated to the monodromy operator M of this linear system are in \mathcal{P} —that is, piecewise-analytic with respect to the intervals $(k, k + 1)$. The identification of M with the operator on piecewise-analytic segments of length q , $M^S : \mathcal{S} \rightarrow \mathcal{S}$, is designed to reflect this. Our goal in this section will be to represent M^S in terms of concrete integral operators.

Remark 3.0.1 In the following four sections, we will be defining some linear operators E and W that will be used to represent M^S . The definitions of these operators depend on the relationship between p and q . This should not cause confusion.

3.1 Intuition and diagrams: the example of $p = 1, q = 2$

For arbitrary natural numbers $p \leq q$, the representation of M^S ends up being fairly cumbersome and does not provide good intuition. To simplify the exposition we will derive the representation for one of the simplest cases—the pair $(p, q) = (1, 2)$ —before presenting the construction in full generality.

It is best to begin with $M : \mathcal{P} \rightarrow \mathcal{P}$ and then to construct M^S using the isomorphism. When $p = 2$, the monodromy operator is a map $M : \mathcal{P}([-2, 0], \mathbb{C}^d) \rightarrow \mathcal{P}([-2, 0], \mathbb{C}^d)$. Formally,

$$M\phi(\theta) = y(1 + \theta, \phi)$$

where $t \mapsto y(t, \phi)$ is the solution of the IDDE (12)–(13) satisfying the initial condition $y_0(\cdot, \phi) = \phi$. For $t \in [0, 1]$, we can write

$$y(t, \phi) = \begin{cases} (I + C_1) \left[\phi(0) + \int_0^1 A(s)y(s) + B(s)\phi(s - 2)ds \right] + C_2\phi(0), & t = 1 \\ \phi(0) + \int_0^t A(s)y(s) + B(s)\phi(s - 2)ds, & 0 \leq t < 1. \end{cases}$$

We can write this in a slightly more suggestive fashion. Define for $\theta \in [-1, 0)$ the functions

$$y_1(\theta) = y(1 + \theta), \quad \phi_0(\theta) = \phi(\theta), \quad \phi_{-1}(\theta) = \phi(-1 + \theta).$$

Also define $y_1(0) = y(1)$. See Fig. 2 for a schematic diagram.

Performing a few changes of variables, we can write y_1 as follows:

$$y_1(0) = (I + C_1) \left[\phi(0) + \int_{-1}^0 A_1(s)y_1(s) + B_1(s)\phi_{-1}(s)ds \right] + C_2\phi(0), \quad \theta = 0$$

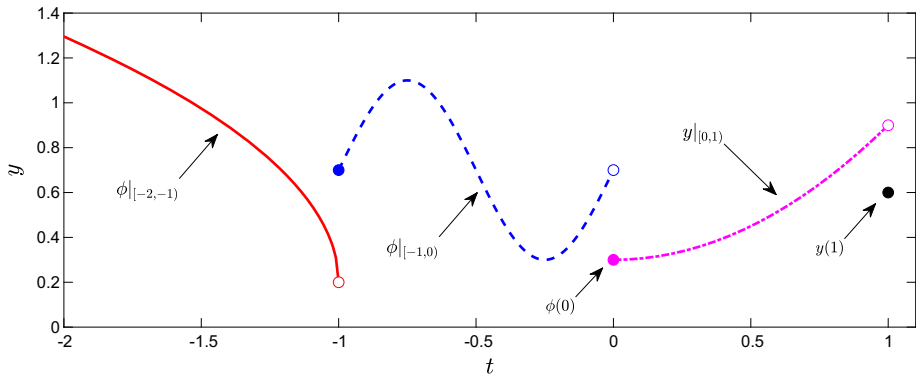


Fig. 2 After translating onto the interval $[-1, 0)$, the functions $\phi|_{[-2,-1)}$ (red solid curve) and $\phi|_{[-1,0)}$ (blue dashed curve) together with $\phi(0)$ (magenta dot) are sufficient to specify the analytic initial condition ϕ . Up to translation, M^S acts on this data by $M^S : (\text{magenta dot, blue curve, red curve}) \mapsto (\text{black dot, magenta curve, blue curve})$. Curves are for illustrative purposes only (e.g. the red solid curve one does not appear to represent an analytic function since it has a pole approaching the right endpoint) (Color figure online)

$$:= (I + C_1 + C_2)\phi(0) + (I + C_1)L_1[y_1](0^-) + (I + C_1)L_2[\phi_{-1}](0^-) \tag{14}$$

$$y_1(\theta) = \phi(0) + \int_{-1}^{\theta} A_1(s)y_1(s) + B_1(s)\phi_{-1}(s)ds, \tag{15}$$

$\theta < 0$

$$:= \phi(0) + L_1[y_1] + L_2[\phi_{-1}] \tag{15}$$

where $A_1(s) = A(1 + s)$, $B_1(s) = B(1 + s)$, and $L_1[f](\theta) = \int_{-1}^{\theta} A_1(s)f(s)ds$ and $L_2[f](\theta) = \int_{-1}^{\theta} B_1(s)f(s)ds$ are defined for $\theta \in [-1, 0)$. Note that L_1 and L_2 define bounded linear operators on \mathcal{A} and also on \mathcal{A}_0 . From (14)–(15), it is clear that each of y_1 and $y_1(0)$ can be expressed implicitly in terms of y_1 and ϕ_{-1} . This will be helpful later.

We can now very suggestively write $M\phi$ as follows:

$$\begin{aligned} M\phi(\theta) &= \mathbb{1}_{\{0\}}(\theta)y_1(0) + \mathbb{1}_{[-1,0)}(\theta)y_1(\theta) + \mathbb{1}_{[-2,-1)}(\theta)\phi_0(1 + \theta) \\ &= \mathbb{1}_{\{0\}}(\theta) [(I + C_1 + C_2)\phi(0) + (I + C_1)(L_1[y_1](0^-) + L_2[\phi_{-1}](0^-))] \\ &\quad + \mathbb{1}_{[-1,0)}(\theta) [\phi(0) + L_1[y_1](\theta) + L_2[\phi_{-1}](\theta)] + \mathbb{1}_{[-2,-1)}(\theta)\phi_0(1 + \theta) \end{aligned}$$

From here, we can make use of the isomorphism $m : \mathcal{P} \rightarrow \mathcal{S} = \mathbb{C}^d \times \mathcal{A}^2$ so that we may instead work with the piecewise-analytic segments of length 2. To do this, we first write

$$M^S(\phi) = M^S(\phi(0), \phi_0, \phi_{-1}) = \begin{pmatrix} y(1) \\ y_1 \\ \phi_0 \end{pmatrix}$$

where we have abused notation and identified $\phi \in \mathcal{P}$ with $(\phi(0), \phi_0, \phi_{-1}) \in \mathcal{S}$. By definition of the monodromy operator, $y_1 = e_2^T M^S(\phi)$ where e_2^T denotes projection onto the second factor. From our previous derivation, it follows that $M^S(\phi)$ satisfies the implicit equation

$$M^S(\phi) = \begin{pmatrix} (I + C_1 + C_2)\phi(0) + (I + C_1)(L_1[e_2^T M^S(\phi)](0^-) + L_2[\phi_{-1}](0^-)) \\ \phi(0) + L_1[e_2^T M^S(\phi)] + L_2[\phi_{-1}] \\ \phi_0 \end{pmatrix}.$$

This can be further factored as the sum of two linear maps: $E : \mathcal{S} \rightarrow \mathcal{S}$ that only involves the initial condition, and the other one $W : \mathcal{S} \rightarrow \mathcal{S}$ taking $M^{\mathcal{S}}(\phi)$ as its input.

$$M^{\mathcal{S}}(\phi) = E(\phi) + W(M^{\mathcal{S}}(\phi)), \quad E(\phi) = \begin{pmatrix} (I + C_1 + C_2)\phi(0) + (I + C_1)L_2[\phi_{-1}](0^-) \\ \phi(0) + L_2[\phi_{-1}] \\ \phi_0 \end{pmatrix}$$

$$W(\psi) = \begin{pmatrix} (I + C_1)L_1[e_2^T \psi](0^-) \\ L_1[e_2^T \psi] \\ 0 \end{pmatrix}.$$

In this sense, we can think of E as the *explicit part* of the monodromy operator, and W as the *implicit part*. If $(I - W) : \mathcal{S} \rightarrow \mathcal{S}$ is an isomorphism, we can write

$$M^{\mathcal{S}} = (I - W)^{-1}E.$$

Indeed, it turns out that $(I - W) : \mathcal{S} \rightarrow \mathcal{S}$ is an isomorphism and the inverse $(I - W)^{-1}$ is bounded. We will not prove this now, since we will prove a more general result in the following section.

3.2 Segment representation of monodromy operator: the case $p < q$

First, identify $\phi \in \mathcal{P}$ with $(\phi(0), \phi_0, \dots, \phi_{1-q}) \in \mathcal{S}$ through the isomorphism m . Let $t \mapsto y(t)$ denote the solution of (12)–(13) satisfying the initial condition $y_0(\cdot) = \phi$. Define a finite sequence in \mathcal{A} as follows:

$$z_k = \begin{cases} y_k|_{[-1,0)}, & 0 < k \leq p \\ \phi_k & -q < k \leq 0. \end{cases}$$

By definition, we can reconstruct y from the sequence z_k for $t \in [-q, p)$ via

$$y(t) = \sum_{k=1-q}^p \mathbb{1}_{[k-1,k)}(t)y_k(t - k),$$

so, we may identify $y|_{[-q,p)}$ with this sequence. For $t \in [k - 1, k)$ for $k = 1, \dots, p$, the function y satisfies the integral equation

$$y(t) = y(k - 1) + \int_{k-1}^t A(s)y(s) + B(s)y(s - 1)ds.$$

We can make use of the sequence z and a change of variables to write this equivalently in the form

$$z_k(\theta) = \begin{cases} \phi(0) + \int_{-1}^{\theta} A_k(s)z_k(s) + B_k(s)z_{k-q}(s)ds, & k = 1 \\ z_{k-1}(0^-) + \int_{-1}^{\theta} A_k(s)z_k(s) + B_k(s)z_{k-q}(s)ds, & k \neq 1. \end{cases} \tag{16}$$

Remark that for $1 \neq k \leq p$, we have

$$z_{k-1}(0^-) = \lim_{t \rightarrow (k-1)^-} y(t) = y(k - 1)$$

because $k - 1 \notin p\mathbb{Z}$, so y is continuous at $t = k - 1$. This justifies the use of the left limit above. Since $p < q$, each of the terms z_{k-q} in (16) can be replaced with ϕ_{k-q} . The result is

$$z_k(\theta) = \begin{cases} \phi(0) + \int_{-1}^{\theta} A_k(s)z_k(s) + B_k(s)\phi_{k-q}(s)ds, & k = 1 \\ z_{k-1}(0^-) + \int_{-1}^{\theta} A_k(s)z_k(s) + B_k(s)\phi_{k-q}(s)ds, & k \neq 1. \end{cases} \tag{17}$$

Also, $y(p)$ is given as follows:

$$y(p) = \begin{cases} (I + C_1) \left[z_{p-1}(0^-) + \int_{-1}^0 A_p(s)z_p(s) + B_p(s)z_{p-q}(s)ds \right] + C_2y(p - q), & p \neq 1 \\ (I + C_1) \left[\phi(0) + \int_{-1}^0 A_p(s)z_p(s) + B_p(s)z_{p-q}(s)ds \right] + C_2y(p - q), & p = 1. \end{cases} \tag{18}$$

Once again, $z_{p-q} = \phi_{p-q}$. Similarly, $p < q$ implies $z(p - q) = \phi_{p-q+1}(-1)$. We can therefore equivalently express (18) as

$$y(p) = \begin{cases} (I + C_1) \left[z_{p-1}(0^-) + \int_{-1}^0 A_p(s)z_p(s) + B_p(s)\phi_{p-q}(s)ds \right] + C_2\phi_{p-q+1}(-1), & p \neq 1 \\ (I + C_1) \left[\phi(0) + \int_{-1}^0 A_p(s)z_p(s) + B_p(s)\phi_{p-q}(s)ds \right] + C_2\phi_{p-q+1}(-1), & p = 1. \end{cases} \tag{19}$$

In the space $S = \mathbb{C}^d \times \mathcal{A}^q$ we have the representation

$$M^S(\phi) = \left(y(p), z_p, z_{p-1}, \dots, z_1 \right). \tag{20}$$

of the action of the monodromy operator on the element ϕ .

Let us define some linear maps to make the expressions (17) and (19) a bit more compact. Define for $k = 1, \dots, p$ the maps $E_k : S \rightarrow \mathcal{A}$, $E_p^0 : S \rightarrow \mathbb{C}^d$, $W_k : S \rightarrow \mathcal{A}$, $W_p^0 : S \rightarrow \mathbb{C}^d$ as follows. For $f = (f(0), f_0, \dots, f_{1-q}) \in S$,

$$E_k[f](\theta) = \begin{cases} f(0) + \int_{-1}^\theta B_k(s)fk_{-q}(s)ds, & k = 1 \\ \int_{-1}^\theta B_k(s)fk_{-q}(s)ds, & k \neq 1 \end{cases} \tag{21}$$

$$E_p^0[f] = \begin{cases} (I + C_1) \int_{-1}^0 B_p(s)f_{p-q}(s)ds + C_2f_{p-q+1}(-1), & p \neq 1, q \neq p \\ (I + C_1) \left[f(0) + \int_{-1}^0 B_p(s)f_{p-q}(s)ds \right] + C_2f_{p-q+1}(-1), & p = 1, q \neq p \\ (I + C_1) \left[f(0) + \int_{-1}^0 B_p(s)f_0(s)ds \right] + C_2f(0), & q = p \end{cases} \tag{22}$$

$$W_k[f](\theta) = \begin{cases} \int_{-1}^\theta A_k(s)fk_{-p}(s)ds, & k = 1 \\ f_{k-p-1}(0^-) + \int_{-1}^\theta A_k(s)fk_{-p}(s)ds, & k \neq 1 \end{cases} \tag{23}$$

$$W_p^0[f] = \begin{cases} (I + C_1) \left[f_{-1}(0^-) + \int_{-1}^0 A_p(s)f_0(s)ds \right], & p \neq 1 \\ (I + C_1) \int_{-1}^0 A_p(s)f_0(s)ds, & p = 1. \end{cases} \tag{24}$$

Remark 3.2.1 Observe that if $k = p = 1$ then $W_k[f](\theta)$ is defined by the first line of (23), so it is of no consequence that $f = (f(0), f_0)$ does not contain the element $f_{k-p-1} = f_{-1}$ needed to define the second line. We have also taken the liberty to define E_p^0 when $q = p$ at this time as well; the main difference is that when $p = q$, we have $z(p - q) = z(0) = \phi(0)$ and the latter can not be identified with $\phi_{p-q+1}(-1) = \phi_1(-1)$ since this is not part of the initial condition vector $(\phi(0), \phi_0, \dots, \phi_{1-q})$.

Remark 3.2.2 $E_p^0[f]$ and $W_p^0[f]$ can be written more succinctly as

$$\begin{aligned} E_p^0[f] &= (I + C_1)E_p[f](0) + C_2\mathbf{f} \\ W_p^0[f] &= (I + C_1)W_p[f](0), \end{aligned}$$

where \mathbf{f} is one of $f_{p-q+1}(-1)$ or $f(0)$, depending on whether or not $p = q$.

With these maps defined, we can write

$$\begin{aligned} z_k &= E_k[\phi] + W_k[(y(p), z_p, z_{p-1}, \dots, z_{p-q+1})], \\ z(p) &= E_p^0[\phi] + W_p^0[(y(p), z_p, z_{p-1}, \dots, z_{p-q+1})] \end{aligned} \tag{25}$$

for $k = 1, \dots, p$. In view of (20), it makes sense to define a pair of operators $E : \mathcal{S} \rightarrow \mathcal{S}$ and $W : \mathcal{S} \rightarrow \mathcal{S}$ as follows:

$$\begin{aligned} Ef &= (E_p^0[f], E_p[f], \dots, E_1[f], f_0, \dots, f_{1-(q-p)}), \\ Wf &= (W_p^0[f], W_p[f], \dots, W_k[f], \dots, W_1[f], 0, \dots, 0), \end{aligned} \tag{26}$$

where there are $q - p$ zeroes at the end of Wf . Finally, using (20), (25) and (26), we can write the monodromy operator on the piecewise-analytic segments of length q in the explicit-implicit form

$$M^{\mathcal{S}}\phi = E(\phi) + W(M^{\mathcal{S}}\phi). \tag{27}$$

We will now characterize the invertibility of the bounded linear operator $(I - W) : \mathcal{S} \rightarrow \mathcal{S}$ with the goal of providing a more explicit representation of $M^{\mathcal{S}}$. The main result is Theorem 3.2.1. It is preceded by three short lemmas, the first of which is straightforward and will not be proven.

Lemma 3.2.1 Denote $X = \{\phi : [-1, 0) \rightarrow \mathbb{C}^d \text{ continuous, such that } \lim_{t \rightarrow 0^-} \phi(t) \text{ exists}\}$, and let $\tilde{\mathcal{S}} = \mathbb{C}^d \times X^q$. The operator $W : \mathcal{S} \rightarrow \mathcal{S}$ is the restriction of $\tilde{W} : \tilde{\mathcal{S}} \rightarrow \tilde{\mathcal{S}}$ to \mathcal{S} , with

$$\tilde{W}(f) = (W_p^0[f], W_p[f], \dots, W_1[f], 0, \dots, 0)$$

where each of W_k and W_p^0 are defined as in (23) and (24). $\tilde{\mathcal{S}}$ is a Banach space with norm $\|(f(0), f_0, \dots, f_{1-q})\|_{\tilde{\mathcal{S}}} = \max\{\|f(0)\|, \|f_0\|, \dots, \|f_{1-q}\|\}$, and $\|\cdot\|$ either denotes some norm on \mathbb{C}^d or the induced supremum norm.

Lemma 3.2.2 $(I - \tilde{W}) : \tilde{\mathcal{S}} \rightarrow \tilde{\mathcal{S}}$ is injective. Also, $(I - W) : \mathcal{S} \rightarrow \mathcal{S}$ is injective.

Proof Let $f \in \tilde{\mathcal{S}}$ and suppose $(I - \tilde{W})f = 0$. Since the trailing $q - p$ elements of $\tilde{W}(f)$ are zero, it follows that $(f_{-p}, \dots, f_{1-q}) = 0$. We will prove now that $f_{-p+k} = 0$ for $k = 0, \dots, p$ by way of induction. The base case already proven, suppose $f_{-p+k} = 0$ for some $k \in \{0, \dots, p\}$. Then, $h = f_{-p+k+1}$ satisfies

$$h(\theta) = W_{k+1}[f](\theta) = \int_{-1}^{\theta} A_{k+1}(s)h(s)ds$$

for $\theta \in [-1, 0)$. By Gronwall’s inequality, $h \equiv 0$. By induction, we have $f_0 = f_{-1} = \dots = f_{1-p} = 0$. Since $f(0) = W_p^0[(f(0), 0, \dots, 0)] = 0$, we conclude that $f = 0$, so $(I - \tilde{W})$ is injective. The same argument proves that $(I - W)$ is injective. \square

Lemma 3.2.3 $(I - \tilde{W}) : \tilde{\mathcal{S}} \rightarrow \tilde{\mathcal{S}}$ is surjective. Also, $(I - W) : \mathcal{S} \rightarrow \mathcal{S}$ is surjective.

Proof Let $\psi \in \tilde{\mathcal{S}}$. We will construct $f \in \tilde{\mathcal{S}}$ such that $(I - \tilde{W})f = \psi$. To begin, set $(f_{-p}, \dots, f_{1-q}) = (\psi_{-p}, \dots, \psi_{1-q})$. Next, given f_{-p+k} for $k \in \{0, \dots, p - 1\}$, let $h = f_{-p+k+1} \in X$ denote the solution of the Volterra integral equation

$$h(\theta) = \psi_{-p+k+1}(\theta) + \begin{cases} \int_{-1}^{\theta} A_{k+1}(s)h(s)ds, & k = 0 \\ \psi_{-p+k}(0^-) + \int_{-1}^{\theta} A_{k+1}(s)g_1(s)ds, & k \neq 0. \end{cases}$$

A straightforward inductive argument demonstrates that each of f_{-p+1}, \dots, f_0 exists, is unique and is an element of X . Finally, set $f(0) = W_p^0(0, f_0, \dots, f_{1-q}) - \psi(0)$. By construction, $(I - \tilde{W})f = \psi$. If $\psi \in \mathcal{S}$, a small modification of this proof shows that $h \in \mathcal{A}$ and, consequently, $f \in \mathcal{S}$, thereby proving $(I - W)$ is surjective. \square

Theorem 3.2.1 *With E and W defined by (26), $(I - W) : \mathcal{S} \rightarrow \mathcal{S}$ is an isomorphism, $(I - W)^{-1}$ is bounded, and $M^{\mathcal{S}} = (I - W)^{-1}E$. We refer to E as the explicit part and W the implicit part of $M^{\mathcal{S}}$.*

Proof By Lemmas 3.2.2 and 3.2.3, $(I - \tilde{W}) : \tilde{\mathcal{S}} \rightarrow \tilde{\mathcal{S}}$ is a bijection. $(I - \tilde{W})$ is clearly bounded, and as $\tilde{\mathcal{S}}$ is a Banach space the bounded inverse theorem guarantees $(I - \tilde{W})^{-1}$ exists and is bounded. Similarly, $(I - W)^{-1}$ exists, and by Lemma 3.2.1, W is the restriction of \tilde{W} , from which it follows that $(I - W)^{-1}$ is also bounded. Solving for $M^{\mathcal{S}}$ in (27), the theorem is proven. \square

3.3 Segment representation of monodromy operator: the boundary case $p = q$

First suppose $p = q = 1$; we will deal with the other case later. With the same notation as the previous section, we have $M^{\mathcal{S}}(\phi) = (y(1), z_1)$ with

$$z_1(\theta) = \phi(0) + \int_{-1}^{\theta} A_1(s)z_1(s) + B_1(s)\phi(s)ds, \tag{28}$$

$$y(1) = (I + C_1) \left[\phi(0) + \int_{-1}^0 A_1(s)z_1(s) + B_1(s)\phi(s)ds \right] + C_2\phi(0). \tag{29}$$

We can perform an analogous decomposition. With the same definitions of E_1, E_1^0, W_1 and W_1^0 from (21)–(24), we can write $M^{\mathcal{S}}(\phi) = E(\phi) + W(M^{\mathcal{S}}\phi)$ with

$$Ef = (E_1^0[f], E_1[f]), \quad Wf = (W_1^0[f], W_1[f]). \tag{30}$$

Theorem 3.2.1 then holds verbatim with the appropriate definitions of E and W . The proof is omitted.

Theorem 3.3.1 *With E and W defined by (30), $(I - W) : \mathcal{S} \rightarrow \mathcal{S}$ is an isomorphism, $(I - W)^{-1}$ is bounded, and $M^{\mathcal{S}} = (I - W)^{-1}E$. We refer to E as the explicit part and W the implicit part of $M^{\mathcal{S}}$.*

Remark 3.3.1 If $p = q \neq 1$, the changes in the definition of the operators E and W are not dramatic. We get instead

$$Ef = (E_p^0[f], E_p[f], \dots, E_2[f], E_1[f]),$$

$$Wf = (W_p^0[f], W_p[f], W_{p-1}[f], \dots, W_2[f], W_1[f]).$$

4 Chebyshev series and validated numerics framework for the monodromy operator

In Sect. 3 we represented the monodromy operator on the space \mathcal{S} of piecewise-analytic segments of length q in terms of integral operators that we referred to as the explicit and implicit part(s) of $M^{\mathcal{S}}$. The next step is to replace the abstract space \mathcal{S} with a concrete space that is more amenable to numerical computation and determine how $M^{\mathcal{S}}$ acts on this space.

4.1 Banach spaces of infinite sequences and Chebyshev series

Let $\|\cdot\|$ be a norm on \mathbb{C}^d . Let $v > 1$. For a sequence $a = \{a_n : n \in \mathbb{N}\} \subset \mathbb{C}^d$, define a weighted norm $\|\cdot\|_v$ by

$$\|a\|_v = \sum_{n=0}^{\infty} v^n \|a_n\|.$$

We then define the space ℓ_v^1 by

$$\ell_v^1 = \{a = \{a_n : n \in \mathbb{N}\} \subset \mathbb{C}^d : \|a\|_v < \infty\}.$$

Equipped with the norm $\|\cdot\|_v$, ℓ_v^1 is a Banach space. Next, define $X_v = \mathbb{C}^d \times (\ell_v^1)^q$ and let it be equipped with the norm $\|\cdot\|$ defined by

$$\|(f(0), f_0, \dots, f_{1-q})\| = \max \{ \|f(0)\|, \|f_0\|_v, \dots, \|f_{1-q}\|_v \}.$$

Then, $(X_v, \|\cdot\|)$ is a Banach space. Define also

$$\ell_v^1(\mathbb{C}^{d \times d}) = \{A = \{A_n : n \in \mathbb{N}\} \subset \mathbb{C}^{d \times d} : \|A\|_v < \infty\},$$

where $\|A\|_v = \sum_{n \geq 0} \|A_n\|_v^n$ and the norm inside the summation is the operator norm on $\mathbb{C}^{d \times d}$ induced by $\|\cdot\|$. Finally, to the space $B(X_v)$ of bounded linear operators on X_v , we let $\|\cdot\|_{B(X_v)}$ denote the induced operator norm.

The following result will be helpful later; its proof is simple and omitted.

Proposition 4.1.1 For $x \in \ell_v^1$ and $Y \in \ell_v^1(\mathbb{C}^{d \times d})$, define the sequence $\{(Y * x)_n\}_{n \geq 0}$ by

$$(Y * x)_n = \sum_{k=-\infty}^{\infty} Y_{|n-k|} x_{|k|}.$$

Then $Y * x \in \ell_v^1$ and $\|Y * x\|_v \leq (2\|Y\|_v - \|Y_0\|)(2\|x\|_v - \|x_0\|) \leq 4\|Y\|_v \|x\|_v$.

The following lemma and corollary follow from Propositions 2.4.1, 2.4.2, Corollary 2.4.2, and the linear scaling $\theta \in [-1, 0] \rightarrow [-1, 1]$ via $\theta = \frac{1}{2}(\omega - 1)$. The proof is simple and omitted.

Lemma 4.1.1 Let $v > 1$. For $g_j = \{g_{j,n}\}_{n \geq 0}$, denote $\mathcal{E}_v(x, g_0, \dots, g_{1-q}) = (x, f_0, \dots, f_{1-q})$ with

$$f_j(\theta) = g_{j,0} + 2 \sum_{n \geq 1} g_{j,n} T_n(1 + 2\theta), \quad \theta \in [-1, 0],$$

and T_n the n th Chebyshev polynomial of the first kind. This expression induces a well-defined, bounded linear map $\mathcal{E}_v : X_v \rightarrow S$. This map is one-to-one onto its range, and so denoting $S_v = \mathcal{E}(X_v)$, the map $\mathcal{E}_v : X_v \rightarrow S_v$ is an isomorphism.

Corollary 4.1.1 There exists some $v^* > 1$ such that if ϕ is an eigenvector of M^S with nonzero eigenvalue, then $\phi \in S_v$ for all $v \in (1, v^*)$. More precisely, let $\theta(\omega) = \frac{1}{2}(\omega - 1)$ and write $\omega \mapsto Y_k(\theta(\omega))$ for $Y \in \{A, B\}$ as a Chebyshev series

$$Y_k(\omega) = Y_{k,0} + 2 \sum_{n \geq 1} Y_{k,n} T_n(\omega),$$

for matrix sequences $\{Y_{k,n}\}_{n \geq 0} \subset \mathbb{R}^{d \times d}$, where $Y_k(s) := Y(k + s)$ for $s \in [-1, 0]$. Then

$$v^* = \sup\{v > 1 : \forall k \in \mathbb{Z}, Y_k \in \ell_v^1(\mathbb{C}^{d \times d}), Y \in \{A, B\}\}.$$

Remark 4.1.1 Under Assumption A1.2, the Chebyshev series of A_k have coefficients in $\ell_v^1(\mathbb{R}^{d \times d})$ for some $v = v_k^A > 1$ for each k , and those of B_k are in $\ell_v^1(\mathbb{R}^{d \times d})$ for some $v = v_k^B > 1$. By the periodicity Assumption A.1, we have $v^* = \min\{v_0^A, \dots, v_{p-1}^A, v_0^B, \dots, v_{p-1}^B\}$.

From the above lemma and corollary, it makes sense to consider the (formal) linear operator $M^v : X_v \rightarrow X_v$ defined by

$$M^v = \mathcal{E}_v^{-1} \circ M^S \circ \mathcal{E}_v. \tag{31}$$

If $M^S(\mathcal{S}_v) \subseteq \mathcal{S}_v$, this expression is well-defined and, in particular, we will immediately have from Corollaries 2.4.2, 2.4.3 and Corollary 4.1.1 the spectral equivalence $\sigma(M^v) \setminus \{0\} = \sigma(M^S) \setminus \{0\}$. Since M^v is an operator on sequence spaces, it is amenable to approximation, truncation and other constructs. In the following section we will show that this operator is indeed well-defined.

4.2 Representation of M^v on Chebyshev series in X_v coefficients

To represent M^v on the space X_v , we will need to settle on a convention for the Chebyshev series coefficients of the matrix-valued functions A_k and B_k needed to define the explicit and implicit parts of M^S —for example, in equations (21)–(24). A brief reminder: $A_k(\theta) = A(k + \theta)$ and $B_k(\theta) = B(k + \theta)$. Recall that by Assumption 1, A and B are piecewise-analytic with respect to $(k, k + 1)$ for the integers k . This means for each integer k there exists $\tilde{A}_k : U_k^A \rightarrow \mathbb{C}^{d \times d}$ and $\tilde{B}_k : U_k^B \rightarrow \mathbb{C}^{d \times d}$ analytic such that $A_k = \tilde{A}_k|_{[-1, 0]}$ and $B_k = \tilde{B}_k|_{[-1, 0]}$, for some open neighbourhoods U_k^A and U_k^B of $[-1, 0]$. For $\omega \in [-1, 1]$, define

$$\hat{A}_k(\omega) = \tilde{A}_k\left(\frac{1}{2}(\omega - 1)\right), \quad \hat{B}_k(\omega) = \tilde{B}_k\left(\frac{1}{2}(\omega - 1)\right).$$

We will write our (uniformly convergent) Chebyshev series for \hat{A}_k and \hat{B}_k as follows:

$$\begin{aligned} \hat{A}_k(\omega) &= \hat{A}_{k,0} + 2 \sum_{n \geq 1} \hat{A}_{k,n} T_n(\omega), \quad \hat{A}_{k,n} \in \mathbb{R}^{d \times d} \\ \hat{B}_k(\omega) &= \hat{B}_{k,0} + 2 \sum_{n \geq 1} \hat{B}_{k,n} T_n(\omega), \quad \hat{B}_{k,n} \in \mathbb{R}^{d \times d}. \end{aligned}$$

By construction, the entries of the matrix sequences $\{\hat{A}_{k,n}\}_{n \geq 0}$ and $\{\hat{B}_{k,n}\}_{n \geq 0}$ are elements of $\ell_v^1(\mathbb{C}^{d \times d})$ for any $v \in (1, v^*)$, where v^* is the constant guaranteed by Corollary 4.1.1 (or more concretely from Remark 4.1.1). Similarly, if $\hat{f}_k(\omega) = f_k\left(\frac{1}{2}(\omega - 1)\right)$ for $f_k : [-1, 0] \rightarrow \mathbb{C}^d$ and some $k \in \{1 - q, \dots, -1, 0\}$, we will write

$$\hat{f}_k(\omega) = \hat{f}_{k,0} + 2 \sum_{n \geq 1} \hat{f}_{k,n} T_n(\omega), \quad \hat{f}_{k,n} \in \mathbb{C}^d. \tag{32}$$

Remark 4.2.1 From this point onward, unless explicitly stated, it will be assumed that $v \in (1, v^*)$.

Recall that if $u_k(t) = u_{k,0} + 2 \sum_{n \geq 1} u_{k,n} T_n(t)$ for $k = 1, 2$ are two Chebyshev series such that the product $u_1(t)u_2(t)$ is well-defined (i.e. u_1 is a $a \times b$ matrix and u_2 is a $b \times c$

matrix), then their product has the Chebyshev series

$$u_1(t)u_2(t) = \left(\sum_{j_1+j_2=0} u_{1,j_1}u_{2,j_2} \right) + 2 \sum_{n \geq 1} \left(\sum_{k_1+k_2=n} u_{1,k_1}u_{2,k_2} \right) T_n(t)$$

with $u_{k,-m} = u_{k,m}$. These can therefore be written in terms of the convolution:

$$u_1(t)u_2(t) = (u_1 * u_2)_0 + 2 \sum_{n \geq 1} (u_1 * u_2)_n T_n(t),$$

where here the interpretation is we are identifying u_k with its sequence of Chebyshev coefficients. Using this property and the fact that $T_0 = 1$, the equations

$$T_1(t) = \frac{d}{dt} \left(\frac{T_0(t) + T_2(t)}{4} \right)$$

$$2T_n(s) = \frac{d}{dt} \left(\frac{T_{n+1}(s)}{n+1} - \frac{T_{n-1}(s)}{n-1} \right), \quad n \geq 2,$$

in addition to $T_n(-1) = (-1)^n$, we can derive formulas for the action of the explicit and implicit parts of M^ν in the space X^ν , as follows. Let $f = (f(0), f_0, \dots, f_{1-q}) \in \mathcal{S}_\nu$, so we can write each \hat{f}_k as in (32). This also ensures that $f = \mathcal{E}_\nu(f(0), \{\hat{f}_{0,n}\}_{n \geq 0}, \dots, \{\hat{f}_{1-q,n}\}_{n \geq 0})$. Then, for $k \neq 1$,

$$\begin{aligned} E_k[f](\theta) &= \int_{-1}^\theta B_k(s) f_{k-q}(s) ds = \frac{1}{2} \int_{-1}^\omega \hat{B}_k(s) \hat{f}_{k-q}(s) ds \\ &= \frac{1}{2} \int_{-1}^\omega (\hat{B}_k * \hat{f}_{k-q})_0 + 2 \sum_{n \geq 1} (\hat{B}_k * \hat{f}_{k-q})_n T_n(s) ds \\ &= \frac{1}{2} (\hat{B}_k * \hat{f}_{k-q})_0 (\omega + 1) + (\hat{B}_k * \hat{f}_{k-q})_1 \left(\frac{T_2(\omega) + T_0(\omega)}{4} - \frac{1}{2} \right) \\ &\quad + \frac{1}{2} \sum_{n \geq 2} (\hat{B}_k * \hat{f}_{k-q})_n \left(\frac{T_{n+1}(\omega)}{n+1} - \frac{T_{n-1}(\omega)}{n-1} - \frac{2(-1)^n}{n^2-1} \right) \\ &= \frac{(\hat{B}_k * \hat{f}_{k-q})_0}{2} (T_1(\omega) + T_0(\omega)) + \frac{(\hat{B}_k * \hat{f}_{k-q})_1}{4} (T_2(\omega) - T_0(\omega)) \\ &\quad - \sum_{j \geq 2} \frac{(-1)^j (\hat{B}_k * \hat{f}_{k-q})_j}{j^2-1} T_0(t) \\ &\quad + \frac{1}{2} \sum_{n \geq 3} \frac{(\hat{B}_k * \hat{f}_{k-q})_{n-1}}{n} T_n(\omega) - \frac{1}{2} \sum_{m \geq 1} \frac{(\hat{B}_k * \hat{f}_{k-q})_{m+1}}{m} T_m(\omega) \\ &= \left(\frac{1}{2} (\hat{B}_k * \hat{f}_{k-q})_0 - \frac{1}{4} (\hat{B}_k * \hat{f}_{k-q})_1 - \sum_{j \geq 2} \frac{(-1)^j}{j^2-1} (\hat{B}_k * \hat{f}_{k-q})_j \right) T_0(\omega) \\ &\quad + 2 \sum_{n \geq 1} \frac{1}{4n} \left((\hat{B}_k * \hat{f}_{k-q})_{n-1} - (\hat{B}_k * \hat{f}_{k-q})_{n+1} \right) T_n(\omega), \end{aligned}$$

where $\theta = \frac{1}{2}(\omega - 1)$. When $k = 1$, we need to add $f(0)$ to the right-hand side of the above. Since $\hat{f}(0) = f(0)T_0(\omega)$, the modification is straightforward. The induced map

$\hat{E}_k : X_v \rightarrow \ell_v^1$ obtained by applying \mathcal{E}_v^{-1} to the above is then given in indexed form as follows:

$$\hat{E}_k[\hat{f}]_n = \begin{cases} \mathbb{1}_0(k-1)f(0) + \frac{1}{2}(\hat{B}_k * \hat{f}_{k-q})_0 - \frac{1}{4}(\hat{B}_k * \hat{f}_{k-q})_1 - \sum_{j \geq 2} \frac{(-1)^j}{j^2 - 1} (\hat{B}_k * \hat{f}_{k-q})_j, & n = 0 \\ \frac{1}{4n} \left((\hat{B}_k * \hat{f}_{k-q})_{n-1} - (\hat{B}_k * \hat{f}_{k-q})_{n+1} \right), & n > 0, \end{cases} \tag{33}$$

for $\hat{f} = (f(0), \{\hat{f}_{0,k}\}_{k \geq 0}, \dots, \{\hat{f}_{1-q,k}\}_{k \geq 0}) \in X_v$. Notice that we have incorporated the inclusion of $f(0)T_0(\omega)$ when $k = 1$ by way of the indicator function: $\mathbb{1}_0(t) = 1$ if and only if $t = 0$, otherwise it is zero. Making use of Proposition 4.1.1, we see that \hat{E}_k is well-defined as a map $\hat{E}_k : X_v \rightarrow \ell_v^1$.

We can perform a similar derivation for the map $E_p^0 : \mathcal{S} \rightarrow \mathbb{C}^d$. Since $E_p^0[f] = (I + C_1)E_p[f](0) + C_2\mathbf{f}$ —see Remark 3.2.2—the observation that $\theta = 0$ precisely when $\omega = 1$ gives

$$\begin{aligned} \hat{E}_p^0[\hat{f}] &= (I + C_1) \left(\mathbb{1}_0(p-1)f(0) + \frac{1}{2}(\hat{B}_p * \hat{f}_{p-q})_0 \right. \\ &\quad \left. - \frac{1}{4}(\hat{B}_p * \hat{f}_{p-q})_1 - \sum_{j \geq 2} \frac{(-1)^j}{j^2 - 1} (\hat{B}_p * \hat{f}_{p-q})_j \right. \\ &\quad \left. + \sum_{n \geq 1} \frac{1}{2n} \left((\hat{B}_p * \hat{f}_{p-q})_{n-1} - (\hat{B}_p * \hat{f}_{p-q})_{n+1} \right) \right) + \mathbb{1}_0(p-q)C_2\hat{f}(0) \\ &\quad + (1 - \mathbb{1}_0(p-q))C_2 \left(f_{p-q+1,0} + 2 \sum_{n \geq 1} (-1)^n \hat{f}_{p-q+1,n} \right). \end{aligned} \tag{34}$$

for the (well-defined) linear map $\hat{E}_p^0 : X_v \rightarrow \mathbb{C}^d$. Note that we have used the identities $T_n(-1) = (-1)^n$ and $T_n(1) = 1$.

The differences between the implicit parts W_k and W_p^0 and the explicit parts E_k and E_p^0 are mostly symbolic (the main difference being the appearance of $f_{k-p-1}(0^-)$ rather than $f(0)$, the former which is easily managed at the Chebyshev level), and the derivation of the induced maps $\hat{W}_k : X_v \rightarrow \ell_v^1$ and $\hat{W}_p^0 : X_v \rightarrow \mathbb{C}^d$ are nearly identical. They are well-defined and can be expressed as

$$\hat{W}_k[\hat{f}]_n = \begin{cases} (1 - \mathbb{1}_0(k-1)) \left(\hat{f}_{k-p-1,0} + 2 \sum_{n \geq 1} \hat{f}_{k-p-1,n} \right) + \frac{1}{2}(\hat{A}_k * \hat{f}_{k-p})_0 & n = 0 \\ -\frac{1}{4}(\hat{A}_k * \hat{f}_{k-p})_1 - \sum_{j \geq 2} \frac{(-1)^j}{j^2 - 1} (\hat{A}_k * \hat{f}_{k-p})_j, & \\ \frac{1}{4n} \left((\hat{A}_k * \hat{f}_{k-p})_{n-1} - (\hat{A}_k * \hat{f}_{k-p})_{n+1} \right), & n > 0, \end{cases} \tag{35}$$

$$\begin{aligned} \hat{W}_p^0[\hat{f}] &= (I + C_1) \left((1 - \mathbb{1}_0(p-1)) \left(\hat{f}_{-1,0} + 2 \sum_{n \geq 1} \hat{f}_{-1,n} \right) \right. \\ &\quad \left. + \frac{1}{2}(\hat{A}_p * \hat{f}_0)_0 - \frac{1}{4}(\hat{A}_p * \hat{f}_0)_1 \right) \end{aligned} \tag{36}$$

$$-\sum_{j \geq 2} \frac{(-1)^j}{j^2 - 1} (\hat{A}_p * \hat{f}_0)_j + \sum_{n \geq 1} \frac{1}{2n} \left((\hat{A}_p * \hat{f}_0)_{n-1} - (\hat{A}_p * \hat{f}_0)_{n+1} \right). \tag{37}$$

Next, we need to form the implicit and explicit part functions acting on X_ν . This is accomplished by replacing each of the relevant maps E_k, E_p^0, W_k and W_p^0 on \mathcal{S} with their associated “hat” counterparts on X_ν . To spell this out explicitly, it is best to separate the two relevant cases.

4.2.1 $p < q$

Define $\hat{E} : X_\nu \rightarrow X_\nu$ and $\hat{W} : X_\nu \rightarrow X_\nu$ by

$$\begin{aligned} \hat{E} \hat{f} &= (\hat{E}_p^0[\hat{f}], \hat{E}_p[\hat{f}], \dots, \hat{E}_1[\hat{f}], \hat{f}_0, \dots, \hat{f}_{1-(q-p)}) \\ \hat{W} \hat{f} &= (\hat{W}_p^0[\hat{f}], \hat{W}_p[\hat{f}], \dots, \hat{W}_1[\hat{f}], 0, \dots, 0), \end{aligned} \tag{38}$$

where there are $q - p$ zeroes at the end of $\hat{W} \hat{f}$. Then $(I - \hat{W}) : X_\nu \rightarrow X_\nu$ is invertible and $M^\nu = (I - \hat{W})^{-1} \hat{E}$ is the representation of the restriction of M^S to \mathcal{S}_ν in the space X_ν .

4.2.2 $p = q$

If $p = q = 1$, define $\hat{E} : X_\nu \rightarrow X_\nu$ and $\hat{W} : X_\nu \rightarrow X_\nu$ by

$$\hat{E} \hat{f} = (\hat{E}_1^0[\hat{f}], \hat{E}_1[\hat{f}]), \quad \hat{W} \hat{f} = (\hat{W}_1^0[\hat{f}], \hat{W}_1[\hat{f}]). \tag{39}$$

$(I - \hat{W}) : X_\nu \rightarrow X_\nu$ is invertible and $M^\nu = (I - \hat{W})^{-1} \hat{E}$ is the representation of the restriction of M^S to \mathcal{S}_ν in the space X_ν .

Remark 4.2.2 If $p = q \neq 1$, Remark 3.3.1 extends analogously to the operator \hat{E} and \hat{W} .

4.3 The validated numerics setup

At this stage we will drop all of the hats and identify the maps E_k, W_k, E_p^0 and W_p^0 with their representations on X_ν . The same thing will be done with the matrix-valued functions A_k and B_k . Moreover, we will identify each of A_k and B_k with their associated sequence of Chebyshev coefficients. This should not provide too much confusion. Finally, we will drop the superscripts of ν on M .

In view of applications, we should always keep in mind that not all Chebyshev modes of A_k and B_k might be known, and they may be subject to error. This could be the case if, for example, they are the matrices associated to a linearization at a periodic solution, the latter which is obtained by a computer-assisted proof. Additionally, any computations that are done on a computer and make use of specific Chebyshev modes will need to take into account some truncation even if the coefficients of every mode are available analytically. To this end, given a matrix sequence $Y \in \ell^1_\nu(\mathbb{R}^{d \times d})$, define the N_1 -mode truncation Y^{N_1} as follows:

$$[Y^{N_1}]_n = \begin{cases} Y_n, & 0 \leq n \leq N_1 \\ 0 & n \geq N_1 + 1 \end{cases}$$

Then, define $M_{N_1} : X_\nu \rightarrow X_\nu$ to be the operator M^ν as defined in Sect. 4.2, except that A_k and B_k for $k = 1, \dots, p$ are replaced with the N_1 -mode truncations $A_k^{N_1}$ and $B_k^{N_1}$.

The next level of approximation comes from the need to represent M_{N_1} as a finite matrix operator. As we will see, the specific way this is done will depend somewhat on the relationship between p and q . In the simplest case ($p = q = 1$), we will truncate the domain and range of each of the implicit and explicit parts at some prescribed number N_2 of modes, and use these to define a mode-truncated version of M_{N_1} that can be represented by a matrix up to an appropriate embedding. In all cases, the symbol M_{N_1, N_2} will be used to refer to the truncation and this operator will always be compact (or eventually compact).

To state some technical requirements concerning the truncated operator M_{N_1, N_2} , we will need to specify two subspaces of X_v . Define

$$X_v^{N_2} = \{(\phi(0), \phi_0, \dots, \phi_{1-q}) \in X_v : \phi_{j,k} = 0, \quad k > N_2\},$$

$$X_v^\infty = \{(\phi(0), \phi_0, \dots, \phi_{1-q}) \in X_v : \phi(0) = 0, \quad \phi_{j,k} = 0, \quad k \leq N_2\}.$$

X_v can be expressed as the internal direct sum $X_v = X_v^{N_2} \oplus X_v^\infty$ for any $N_2 \geq 0$.

Our objective is to use information concerning the eigenvalues of M_{N_1, N_2} to infer properties of the eigenvalues of $M : X_v \rightarrow X_v$, the representation of the monodromy operator on X_v . With a view toward stability and so-called generalized Morse indices, we adapt a result attributed to Lessard and Mireles-James [21]. The main idea is captured by the following lemma.

Lemma 4.3.1 (Generalized Morse index validation) *Let $r > 0$ and let M_{N_1, N_2} be a bounded operator on X_v with with the following properties.*

- M_{N_1, N_2} has only finitely many eigenvalues in the complement of the closed disc D_r in the \mathbb{C} .
- M_{N_1, N_2} has no eigenvalues on the circle of radius r in \mathbb{C} .
- Each of $X_v^{N_2}$ and X_v^∞ are invariant subspaces of M_{N_1, N_2} : that is, $M_{N_1, N_2}(X_v^{N_2}) \subseteq X_v^{N_2}$ and $M_{N_1, N_2}(X_v^\infty) \subseteq X_v^\infty$.

Suppose there are positive constants c_1, c_2 and c_3 such that

$$\max \left(\sup_{\theta \in [0, 2\pi]} \|(M_{N_1, N_2} - re^{i\theta} I)^{-1}\|_{B(X_v^{N_2})}, \sup_{\theta \in [0, 2\pi]} \|(M_{N_1, N_2} - re^{i\theta} I)^{-1}\|_{B(X_v^\infty)} \right) \leq c_1$$

$$\|(I - W)^{-1}\|_{B(X_v)} \leq c_2$$

$$\|(I - W)M_{N_1, N_2} - E\|_{B(X_v)} \leq c_3,$$

and $c_1 c_2 c_3 < 1$. Then, M_{N_1, N_2} and M have the same number of eigenvalues in the complement of the open ball of radius r .

Proof By construction, M_{N_1, N_2} has only finitely many non-zero eigenvalues in the complement of D_r . Since the monodromy operator is eventually compact, the representation $M \in B(X_v)$ has only finitely-many eigenvalues in the complement of D_r . Consider the straight-line homotopy

$$H(s) = (1 - s)M_{N_1, N_2} + sM. \tag{40}$$

Since $H : [0, 1] \rightarrow B(X_v)$ is continuous, M and M_{N_1, N_2} can only have a different number of eigenvalues in the complement of D_r if there is some $s \in [0, 1]$ and $\theta \in [0, 2\pi]$ such that $re^{i\theta}$ is an eigenvalue of $H(s)$. This follows by the continuity of a finite eigensystem of a continuous family of bounded linear operators [19]. It suffices to show $H(s) - re^{i\theta} I$ is boundedly invertible for all $s \in [0, 1]$ and $\theta \in [0, 2\pi]$.

Define $N(\theta) = M_{N_1, N_2} - r e^{i\theta} I$. From the assumptions of the lemma, $N(\theta)$ satisfies the estimate $\|N(\theta)^{-1}\|_{B(X_v)} \leq c_1$.

Next, observe that

$$H(s) - r e^{i\theta} I = N(\theta)\{I - sN(\theta)^{-1}(M_{N_1, N_2} - M)\}. \tag{41}$$

From the previous result, it remains to show that the term in curly braces boundedly is invertible. To accomplish this, observe that

$$M_{N_1, N_2} - M = (I - W)^{-1}(I - W)(M_{N_1, N_2} - M) = (I - W)^{-1}[(I - W)M_{N_1, N_2} - E],$$

from which it follows that $\|M_{N_1, N_2} - M\|_{B(X_v)} \leq c_2 c_3$. Thus, $\|sN(\theta)^{-1}(M_{N_1, N_2} - M)\|_{B(X_v)} \leq c_1 c_2 c_3 < 1$, so by the Neumann series theorem, the term in the curly braces is invertible. It follows that $H(s) - r e^{i\theta} I$ is invertible with inverse satisfying

$$\|(H(s) - r e^{i\theta} I)^{-1}\|_{B(X_v)} \leq \frac{c_1}{1 - c_1 c_2 c_3}.$$

This would complete the proof if we were only interested in the eigenvalues in the complement of the *closed disc* of radius r . To extend to the complement of the *open ball* of radius r , observe that the inequality $\|sN(\theta)^{-1}(M_{N_1, N_2} - M)\|_{B(X_v)} \leq c_1 c_2 c_3 < 1$ is strict, implying that the conclusion is robust with respect to the radius. □

The previous lemma exploits the fact that each of M and (by assumption) M_{N_1, N_2} have only finitely many eigenvalues in the complement of D_r for any finite $r > 0$. However, this is not the only set in which the number of eigenvalues of M must be finite. In fact, this is true for any set—open or closed—that is bounded away from zero, since M is compact (or eventually compact). If the goal is to validate a *specific* eigenvalue of M_{N_1, N_2} rather than a generalized Morse index, one can accomplish this using a very similar setup.

Lemma 4.3.2 (Compact eigenvalue validation) *Let $U \subset \mathbb{C}$ be compact, bounded away from zero, path-connected and have a continuous boundary. Let M_{N_1, N_2} be a bounded operator on X_v with with the following properties.*

- M_{N_1, N_2} has only finitely many eigenvalues in U .
- M_{N_1, N_2} has no eigenvalues on the boundary of U (denoted ∂U).
- Each of $X_v^{N_2}$ and X_v^∞ are invariant subspaces of M_{N_1, N_2} .

Suppose there are positive constants c_1, c_2 and c_3 such that

$$\begin{aligned} & \max \left(\sup_{z \in \partial U} \|(M_{N_1, N_2} - zI)^{-1}\|_{B(X_v^{N_2})}, \sup_{z \in \partial U} \|(M_{N_1, N_2} - zI)^{-1}\|_{B(X_v^\infty)} \right) \leq c_1 \\ & \|(I - W)^{-1}\|_{B(X_v)} \leq c_2 \\ & \|(I - W)M_{N_1, N_2} - E\|_{B(X_v)} \leq c_3, \end{aligned}$$

and $c_1 c_2 c_3 < 1$. Then, M_{N_1, N_2} and M have the same number of eigenvalues in U .

Proof By assumption, M_{N_1, N_2} has only finitely-many eigenvalues in U , and the same is true of M due to compactness (or eventual compactness) and the assumption U is bounded away from zero. Let $z : [0, 1] \rightarrow \partial U$ be a parameterization of the boundary. If H is denotes the straight-line homotopy (40), to prove the theorem it suffices to show that $H(s) - z(t)I$ is boundedly invertible for all $(s, t) \in [0, 1] \times [0, 1]$, for then no eigenvalue of $H(s)$ crosses the boundary ∂U and the continuity of a finite eigensystem of a family of bounded linear operators implies that M and M_{N_1, N_2} must have the same number of eigenvalues inside U .

Define $N(t) = M_{N_1, N_2} - z(t)I$. By assumption, $\|N(t)^{-1}\|_{B(X_v)} \leq c_1$. Also,

$$H(s) - z(t)I = N(t)\{I - sN(t)^{-1}(M_{N_1, N_2} - M)\}.$$

It remains to show that the term in the curly braces is boundedly invertible. By the same argument as in the proof of Lemma 4.3.1, we know that $\|M_{N_1, N_2} - M\| \leq c_2c_3$, so $\|sN(t)^{-1}(M_{N_1, N_2} - M)\|_{B(X_v)} \leq c_1c_2c_3 < 1$ for all $(s, t) \in [0, 1]^2$. It follows that the term in curly braces is boundedly invertible. This completes the proof. \square

4.3.1 Interpretation of the bounds c_1, c_2 and c_3

c_1 is an upper bound for $\sup_{z \in \partial U} \|(M_{N_1, N_2} - zI)^{-1}\|_{B(X_v)}$. If $M_{N_1, N_2} \rightarrow M$ as $(N_1, N_2) \rightarrow \infty$, it can be interpreted as an asymptotic proxy for the distance between the spectrum of M and the boundary of the set U , whatever this happens to be. c_3 is a proxy for numerical defect: if $\Delta M := M_{N_1, N_2} - M$ satisfies $\|\Delta M\|_{B(X_v)} = \epsilon$, then

$$\begin{aligned} \|(I - W)M_{N_1, N_2} - E\|_{B(X_v)} &= \|(I - W)(M + \Delta M) - E\|_{B(X_v)} \\ &= \|(I - W)\Delta M\|_{B(X_v)} \\ &\leq \epsilon\|I - W\|_{B(X_v)} \end{aligned}$$

As for c_2 , it is a technical bound on the inverse $(I - W)^{-1}$ and does not lend itself to interpretation relative to the discretization M_{N_1, N_2} . The only connection it has is that we always have the estimate

$$\|M_{N_1, N_2} - M\|_{B(X_v)} \leq c_2c_3, \tag{42}$$

so c_2 contributes to the upper bound of the discretization error $\|\Delta M\|_{B(X_v)}$.

4.3.2 Candidates sets for compact eigenvalue validation

There are two fairly natural candidates for compact sets on which one might want to validate eigenvalues. The most obvious is simply a closed ball $D_r(\lambda) := \overline{B_r(\lambda)}$ centered at an approximate eigenvalue λ with radius $r \in (0, |\lambda|)$. We have $b(\cdot, \lambda, r) : [0, 2\pi] \rightarrow \partial D_r(\lambda)$ defined by

$$b(t, \lambda, r) = \lambda + re^{it} \tag{43}$$

is a continuous parameterization of the boundary. An alternative to such a closed ball is the following.

Definition 4.3.1 (Radial sector) Let $\lambda \in \mathbb{C}$. The *radial sector centered at λ with width $r \in (0, |\lambda|)$ and sweep $\omega \in (0, \pi)$* is the set

$$R_\lambda(r, \omega) = \{z \in \mathbb{C} : z = \lambda + \mu e^{i(\arg \lambda + \theta)}, \quad |\mu| \leq r, \quad |\theta| \leq \omega\}.$$

We will refer to such a set without qualification as being a *radial sector centered at λ* .

A radial sector is simply a translated rectangle in polar coordinates, parameterized by its half-width and half-length. Having two parameters (width and sweep, versus only a radius) allows for a finer level of control. Additionally, as we will see later (see Remark 6.1.2), the tail bounds (i.e. on $B(X_v^\infty)$) for c_1 are generally tighter for a radial sector (of width r) than they are for a closed ball (of radius r) centered at a given λ . Also, though the associated boundary parameterization is only piecewise continuous, it is smooth on each

piece and this poses no problem for the c_1 bound computation; see Sect. 7.1. The function $z(\cdot, \lambda, r, \omega) : [0, 4] \rightarrow \partial R_\lambda(r, \omega)$ given by

$$z(t; \lambda, r, \omega) = \begin{cases} (|\lambda| - r)e^{i(\arg \lambda + \omega(1-2t))}, & 0 \leq t < 1 \\ (|\lambda| + (2t - 3)r)e^{i(\arg \lambda - \omega)}, & 1 \leq t < 2 \\ (|\lambda| + r)e^{i(\arg \lambda + (2t-5)\omega)}, & 2 \leq t < 3 \\ (|\lambda| + r(7 - 2t))e^{i(\arg \lambda + \omega)}, & 3 \leq t \leq 4. \end{cases} \tag{44}$$

is a parameterization of the boundary. For the purposes of later validation and enclosure, the following proposition concerning inclusions of balls inside radial sectors as well as inclusion characterizations of two radial sectors will be of use. Its proof is a straightforward geometry exercise.

Proposition 4.3.1 *The ball $B_r(x)$ with $r < |x|$ satisfies $B_r(x) \subset R_x\left(r, 2 \arcsin\left(\frac{r}{2|x|}\right)\right)$. Also, we have $R_{\lambda_1}(r_1, \omega) \subseteq R_{\lambda_2}(r_2, \omega_2)$ if and only if the following are satisfied:*

$$\begin{aligned} |\lambda_2| - r_2 &\leq |\lambda_1| - r_1, & |\lambda_1| + r_1 &\leq |\lambda_2| + r_2, \\ \arg(\lambda_2) - \omega_2 &\leq \arg(\lambda_1) - \omega_1, & \arg(\lambda_1) + \omega_1 &\leq \arg(\lambda_2) + \omega_2. \end{aligned}$$

4.4 Infinite matrix representation of implicit and explicit part maps

Each of the maps E_k, W_k, E_p^0 and W_p^0 with their representations on X_ν are linear with respect to two pieces of datum: the input $f = (f(0), f_0, \dots, f_{1-q})$ and a convolution term $\mathbf{X}_k * f_m$, where \mathbf{X}_k is one of \hat{A}_k or \hat{B}_k , and $m \in \{0, \dots, 1 - q\}$ is some index. It will be beneficial later to have these maps split into those parts that are linear in f and those that are linear in $\mathbf{X}_k * f_m$. One can verify by inspection that the following representations are valid:

$$W_k f = (1 - \mathbb{1}_0(k - 1))\mathbf{e}_0 S f_{k-p-1} + H_1(A_k * f_{k-p}) \tag{45}$$

$$W_p^0 f = (1 - \mathbb{1}_0(p - 1))(I + C_1)S f_{-1} + (I + C_1)H_2(A_p * f_0) \tag{46}$$

$$E_k f = \mathbb{1}_0(k - 1)\mathbf{e}_0 f(0) + H_1(B_k * f_{k-q}) \tag{47}$$

$$\begin{aligned} E_p^0 f &= (\mathbb{1}_0(p - 1)(I + C_1) + \mathbb{1}_0(p - q)C_2) f(0) \\ &\quad + (1 - \mathbb{1}_0(p - q))C_2 S^* f_{p-q+1} + (I + C_1)H_2(B_p * f_{p-q}), \end{aligned} \tag{48}$$

where H_1 and H_2 are infinite matrices defined inductively by

$$H_1 = \begin{bmatrix} \frac{1}{2}I_d & -\frac{1}{4}I_d & -\frac{1}{3}I_d & \frac{1}{8}I_d & -\frac{1}{15}I_d & \dots & -\frac{(-1)^n}{n^2-1}I_d & \dots & \ddots & \ddots \\ \frac{1}{4}I_d & 0 & -\frac{1}{4}I_d & 0 & 0 & \dots & 0 & \dots & \dots & \dots \\ 0 & \frac{1}{8}I_d & 0 & -\frac{1}{8}I_d & 0 & \dots & 0 & \dots & \dots & \dots \\ 0 & 0 & \ddots & \ddots & \ddots & \ddots & \ddots & \ddots & \ddots & \ddots \\ 0 & 0 & 0 & \dots & 0 & \frac{1}{4n}I_d & 0 & -\frac{1}{4n}I_d & 0 & \ddots \\ \vdots & \vdots & \vdots & \vdots & \vdots & \vdots & \ddots & \ddots & \ddots & \ddots \end{bmatrix} \tag{49}$$

$$H_2 = \left[I_d \quad 0 - \frac{2}{3}I_d \quad 0 \quad \dots \quad -\frac{(-1)^n+1}{n^2-1}I_d \quad \dots \right], \tag{50}$$

and the remaining terms are

$$Sf = f_{\cdot,0} + 2 \sum_{m \geq 1} f_{\cdot,m} \in \mathbb{C}^d \tag{51}$$

$$S^*f = f_{\cdot,0} + 2 \sum_{m \geq 1} (-1)^m f_{\cdot,m} \in \mathbb{C}^d \tag{52}$$

$$e_0y = (y, 0, \dots) \in \ell_v^1, \quad y \in \mathbb{C}^d. \tag{53}$$

Note that in (49), the final (rightmost) displayed column has index n th, the final (bottom) displayed row is index n th as well, and similarly in (50) the final displayed entry has index n th entry, where indexing is from zero so that the first rows and columns have index zero.

For convenience, we will write H_1 as the sum

$$H_1 = H_1^0 + DT, \tag{54}$$

where $(H_1^0x)_0 = (H_1x)_0$ and $(H_1^0x)_j = 0$ for $j > 0$ (i.e. H_1^0 is the first row of H_1 continuously embedded as an operator on ℓ_v^1), T is Toeplitz and D is a diagonal operator defined as follows:

$$T = \begin{bmatrix} 0 & -I & 0 & \dots & & \\ I & 0 & -I & 0 & \dots & \\ 0 & I & 0 & -I & 0 & \dots \\ & & \ddots & & \ddots & \\ & & & & & \ddots \end{bmatrix}, \quad D = \begin{bmatrix} 0 & & & & & \\ & \frac{1}{4}I & & & & \\ & & \frac{1}{8}I & & & \\ & & & \ddots & & \\ & & & & \frac{1}{4n} & \\ & & & & & \ddots \end{bmatrix}, \tag{55}$$

where the $\frac{1}{4n}$ occurs at the (n, n) diagonal index (again with zero-indexing).

We conclude this section with an observation concerning an elementwise product operation. First, concerning the maps H_2 and S . Each of these commute with $d \times d$ matrix multiplication in the following sense. If $M \in \mathbb{C}^{d \times d}$, $h \in \ell_v^1$ and we define $(M \odot h)_n = Mh_n$ to be the “elementwise (block) product”, then

$$MH_2h = H_2(M \odot h), \quad MSh = S(M \odot h). \tag{56}$$

Next, if $Y \in \ell_v^1(\mathbb{C}^{d \times d})$ and $h \in \ell_v^1$, we have the following identity concerning “associativity” of the elementwise product with convolution:

$$M \odot (Y * h) = (M \odot Y) * h. \tag{57}$$

provided we overload the notation and define $(M \odot Y)_n = MY_n$.

5 A dictionary of norm bounds

In the sections that follow, we will be computing formulas for the c_2 and c_3 bounds of Lemma 4.3.1. Especially once we consider the case $1 < p < q$ for the period and delay, the individual linear maps that we need to bound (in norm) to get tight estimates for c_2 and c_3 become quite numerous and the analysis can at times be technical. To facilitate the presentation of later proofs, in this section we will list and prove a collection of norm bounds for such maps. However, as some bounds are used very frequently and it is easier to locate them from a table, we place these bounds (and their proofs) in “Appendix A”.

There are some common elements between the computation of the bounds, so at this stage we introduce some additional notation. For $N > 0$, define $\pi^N : \ell_v^1 \rightarrow \ell_v^1$ by $[\pi^N h]_n = h_n$ if $n \leq N$, and zero otherwise. Then, define $\pi_N^\infty : \ell_v^1 \rightarrow \ell_v^1$ to be the complementary projector $\pi_N^\infty h = h - \pi^N h$. For $h \in \ell_v^1$, the decomposition $h = h^N + h^\infty$ will always mean $h^N = \pi^N h$ and $h^\infty = \pi_N^\infty h$. Analogously, if $\phi \in X_v$, and $N \geq 0$, we will write $\phi = \phi^N + \phi^\infty$ for $\phi^N \in X_v^N$ and $\phi^\infty \in X_v^\infty$. Also, because ℓ_v^1 admits the internal direct sum $\ell_v^1 = \pi^N(\ell_v^1) \oplus \pi_N^\infty(\ell_v^1)$ and $h = h^N + h^\infty$ satisfies $\|h\|_v = \|h^N\|_v + \|h^\infty\|_v$, any linear operator $L : \ell_v^1 \rightarrow \ell_v^1$ satisfies

$$\|L\|_{B(\ell_v^1)} \leq \max \left\{ \sup_{\|h^N\|_v \leq 1} \|Lh^N\|_v, \sup_{\|h^\infty\|_v \leq 1} \|Lh^\infty\|_v \right\}, \tag{58}$$

where the suprema are taken over $h^N \in \pi^N(\ell_v^1)$ and $h^\infty \in \pi_N^\infty(\ell_v^1)$. Similarly, for $L_0 : \ell_v^1 \rightarrow \mathbb{C}^d$ we have

$$\|L_0\|_{L(\ell_v^1, \mathbb{C}^d)} \leq \max \left\{ \sup_{\|h^N\|_v \leq 1} \|L_0 h^N\|, \sup_{\|h^\infty\|_v \leq 1} \|L_0 h^\infty\| \right\}. \tag{59}$$

Analogous bounds hold for a linear operator $\mathcal{L} : X_v \rightarrow X_v$. First, write

$$\begin{aligned} \mathcal{L}(x(0), x_0, \dots, x_{1-q}) &= (L(0)(x(0), x_0, \dots, x_{1-q}), L_0(x(0), x_0, \dots, x_{1-q}), \\ &\dots, L_{1-q}(x(0), x_0, \dots, x_{1-q})). \end{aligned}$$

We can decompose by linearity over the direct sum:

$$\begin{aligned} L(0)(x(0), x_0, \dots, x_{1-q}) &= L(0)(x(0), 0, \dots, 0) + L(0)(0, x_0, 0, \dots, 0) \\ &\quad + \dots + L(0)(0, 0, \dots, x_{1-q}) \\ L_j(x(0), x_0, \dots, x_{1-q}) &= L_j(x(0), 0, \dots, 0) + L_j(0, x_0, 0, \dots, 0) \\ &\quad + \dots + L_j(0, 0, \dots, x_{1-q}), \end{aligned}$$

for $j = 1 - q, \dots, 0$. Then each $L_j : X_v \rightarrow \ell_v^1$ satisfies

$$\|L_j\| \leq \sup_{|x(0)| \leq 1} \|L_j(x(0), 0)\|_v + \sum_{k=1-q}^0 \max \left\{ \sup_{\|x_k^N\|_v \leq 1} \|L_j(0, x_k^N)\|_v, \sup_{\|x_k^\infty\|_v \leq 1} \|L_j(0, x_k^\infty)\|_v \right\},$$

where $L_j(x(0), 0) \equiv L_j(x(0), 0, \dots, 0)$, and $L_j(0, x_k) \equiv L_j(0, \dots, x_k, \dots)$ has zeros except at the k index. It then follows by definition of the norm on X_v that

$$\begin{aligned} \|\mathcal{L}\|_{B(X_v)} &\leq \max \left\{ \sup_{|x(0)| \leq 1} \|L(0)(x(0), 0)\| \right. \\ &\quad + \sum_{k=1-q}^0 \max \left\{ \sup_{\|x_k^N\|_v \leq 1} \|L(0)(0, x_k^N)\|, \sup_{\|x_k^\infty\|_v \leq 1} \|L(0)(0, x_k^\infty)\| \right\}, \\ &\quad \max_{j=1-q, \dots, 0} \left\{ \sup_{|x(0)| \leq 1} \|L_j(x(0), 0)\|_v \right. \\ &\quad \left. + \sum_{k=1-q}^0 \max \left\{ \sup_{\|x_k^N\|_v \leq 1} \|L_j(0, x_k^N)\|_v, \sup_{\|x_k^\infty\|_v \leq 1} \|L_j(0, x_k^\infty)\|_v \right\} \right\} \tag{60} \end{aligned}$$

Conversely, if the right-hand side of (60) is finite then \mathcal{L} is bounded.

In the following sections we will be playing somewhat fast and loose with the notation involving our convolutions. The primary abuse of notation will be as follows. If $Y \in \ell_v^1(\mathbb{C}^{d \times d})$ and $L \in B(\ell_v^1)$, we define the operator $Y * L \in B(\ell_v^1)$ by $h \mapsto Y * L(h) := Y * (Lh)$. For example, often L will be a projection operator (although there are exceptions). Finally, the following equivalent norm on $\ell_v^1(\mathbb{C}^{d \times d})$ will be beneficial later. For $Y \in \ell_v^1(\mathbb{C}^{d \times d})$, define $\|Y\|_\omega = 2\|Y\|_v - \|Y_0\|$. This implies the convenient formula $\|(Y * h)\|_v \leq 2\|Y\|_\omega \|h\|_v$ whenever $h \in \ell_v^1$; see Proposition 4.1.1.

A brief warning before we proceed. The symbol I will always denote an the identity operator, though on which space it acts will sometimes be left implicit by context. When we wish to make the domain X explicit, we will write I_X .

5.1 The operators Q and \tilde{Q}

Many of the bounds of this section will involve the following pair of linear operators. They appear frequently in the “block operator” representation of implicit part operators. Let $Y \in \ell_v^1(\mathbb{C}^{d \times d})$ and $N_2, N_1 \in \mathbb{N}$.

$$Q(Y) = I_{\ell_v^1} - H_1 Y * I_{\ell_v^1}, \quad \tilde{Q}(Y) = I_{\ell_v^1} - \pi^{N_2} H_1 Y^{N_1} * \pi^{N_2}, \quad \tilde{Q}^{-1}(Y) = (\tilde{Q}(Y))^{-1}. \tag{61}$$

Whenever these symbols appear, N_1 and N_2 will always be fixed a priori so they can be used without ambiguity. We will sometimes also write $\tilde{Q}^{-1}(Y^{N_1})$ whenever we want to make the dependence on N_1 explicit.

Remark 5.1.1 It is a simple consequence of Theorem 3.2.1 that $\tilde{Q}^{-1}(Y)$ exists and is bounded.

Lemma 5.1.1 $\|\tilde{Q}^{-1}(Y)\|_{B(\ell_v^1)} \leq \max\{\|\tilde{Q}^{-1}(Y)\pi^{N_2}\|_{B(\ell_v^1)}, 1\}$.

Proof By construction, \tilde{Q}^{-1} acts as the identity on $\pi_{N_2}^\infty(\ell_v^1)$. The inequality then follows from (58). □

Lemma 5.1.2 $\pi^{N_2} \tilde{Q}^{-1}(Y) = \pi^{N_2} \tilde{Q}^{-1}(Y) \pi^{N_2}$ and $\pi_{N_2}^\infty \tilde{Q}^{-1}(Y) = \pi_{N_2}^\infty$.

Proof Set $\tilde{Q}^{-1} = \tilde{Q}^{-1}(Y)$. If $\tilde{Q}^{-1}x = y$ then $x = y - \pi^{N_2} H_1 Y^{N_1} * \pi^{N_2} y$ and $x^{N_2} = y^{N_2} - \pi^{N_2} H_1 Y^{N_1} * y^{N_2}$. But then

$$y^{N_2} = \pi^{N_2} \tilde{Q}^{-1} x = (I_{\pi^{N_2}(\ell_v^1)} - \pi^{N_2} H_1 Y^{N_1} * I_{\pi^{N_2}(\ell_v^1)})^{-1} x^{N_2},$$

which coincides with $\pi^{N_2} \tilde{Q}^{-1} \pi^{N_2} x$. The other statement is proven by similar arguments. □

Lemma 5.1.3 Let $N_2, N_1 \geq 0$ and given $Y \in \ell_v^1(\mathbb{C}^{d \times d})$, let $Y^{N_1} = (Y_0, \dots, Y_{N_1})$ and $Y^\infty = Y - Y^{N_1}$. Denote $Q = Q(Y)$ and $\tilde{Q}^{-1} = \tilde{Q}^{-1}(Y)$. The linear operators $I_{\ell_v^1} - \tilde{Q}^{-1}Q$ and $I_{\ell_v^1} - Q\tilde{Q}^{-1}$ can be written as follows:

$$\begin{aligned} I_{\ell_v^1} - \tilde{Q}^{-1}Q &= \tilde{Q}^{-1} \pi^{N_2} \left(H_1(Y^\infty * I_{\ell_v^1}) + H_1(Y^{N_1} * \pi_{N_2}^\infty) \right) + \pi_{N_2}^\infty H_1(Y * I_{\ell_v^1}) \\ I_{\ell_v^1} - Q\tilde{Q}^{-1} &= H_1(Y^\infty * \tilde{Q}^{-1}) + \pi^{N_2} (H_1(Y^{N_1} * \pi_{N_2}^\infty)) + \pi_{N_2}^\infty H_1(Y^{N_1} * \tilde{Q}^{-1}). \end{aligned}$$

Proof Keeping track of the projection operators, recalling that each of $\pi^{N_2}(\ell_v^1)$ and $\pi_{N_2}^\infty(\ell_v^1)$ is invariant under \tilde{Q}^{-1} and the latter acts as the identity on $\pi_{N_2}^\infty(\ell_v^1)$, we can equivalent write

$$I_{\ell_v^1} - \tilde{Q}^{-1}Q = I_{\ell_v^1} - \tilde{Q}^{-1}(I_{\ell_v^1} - \pi^{N_2} H_1(Y * I_{\ell_v^1}) - \pi_{N_2}^\infty H_1(Y * I_{\ell_v^1}))$$

$$\begin{aligned}
 &= I_{\ell_v^1} - \tilde{Q}^{-1}(I_{\ell_v^1} - \pi^{N_2} H_1(Y^{N_1} * \pi^{N_2}) - \pi^{N_2} H_1(Y^\infty * I_{\ell_v^1}) \\
 &\quad - \pi^{N_2} H_1(Y^{N_1} * \pi_{N_2}^\infty) - \pi_{N_2}^\infty H_1(Y * I_{\ell_v^1})) \\
 &= I_{\ell_v^1} - \tilde{Q}^{-1}(\tilde{Q} - \pi^{N_2} H_1(Y^\infty * I_{\ell_v^1}) - \pi^{N_2} H_1(Y^{N_1} * \pi_{N_2}^\infty) - \pi_{N_2}^\infty H_1(Y * I_{\ell_v^1})) \\
 &= \tilde{Q}^{-1} \pi^{N_2} (H_1(Y^\infty * I_{\ell_v^1}) + H_1(Y^{N_1} * \pi_{N_2}^\infty)) + \tilde{Q}^{-1} \pi_{N_2}^\infty H_1(Y * I_{\ell_v^1}) \\
 &= \tilde{Q}^{-1} \pi^{N_2} (H_1(Y^\infty * I_{\ell_v^1}) + H_1(Y^{N_1} * \pi_{N_2}^\infty)) + \pi_{N_2}^\infty H_1(Y * I_{\ell_v^1})
 \end{aligned}$$

Similarly, one can verify

$$\begin{aligned}
 I_{\ell_v^1} - Q\tilde{Q}^{-1} &= \pi^{N_2}(H_1(Y^\infty * I_{\ell_v^1})\tilde{Q}^{-1} + H_1(Y^{N_1} * \pi_{N_2}^\infty)\tilde{Q}^{-1}) + \pi_{N_2}^\infty(H_1(Y * I_{\ell_v^1})\tilde{Q}^{-1}) \\
 &= \pi^{N_2}H_1(Y^\infty * \tilde{Q}^{-1}) + \pi^{N_2}H_1(Y^{N_1} * \pi_{N_2}^\infty\tilde{Q}^{-1}) + \pi_{N_2}^\infty H_1((Y^{N_1} + Y^\infty) * \tilde{Q}^{-1}) \\
 &= H_1(Y^\infty * \tilde{Q}^{-1}) + \pi^{N_2}(H_1(Y^{N_1} * \pi_{N_2}^\infty)) + \pi_{N_2}^\infty(H_1(Y^{N_1} * \tilde{Q}^{-1})).
 \end{aligned}$$

□

5.2 A general-purpose finite computation norm estimate

For a given linear operator $L : X_v \rightarrow X_v$, it is often useful to work with a “block decomposition”,

$$Lh = \begin{bmatrix} T(0) & T_{\dots} \\ U & V \end{bmatrix} \begin{bmatrix} h(0) \\ h_{\dots} \end{bmatrix}.$$

The following lemma facilitates the computation of the norm of such an operator. When $\ker L = X_v^\infty$, the bound of the lemma reduces to a tight, finite computation.

Lemma 5.2.1 *Denote $X_v(0) = \text{span}\{(e_j, 0, \dots, 0) : j = 1, \dots, d\} \subset X_v$ and $\pi(0) : X_v \rightarrow X_v(0)$ the projection onto $X_v(0)$. Let $L : X_v \rightarrow X_v$ be a bounded operator being expressible in the form $L = T + U + V$ with the following specifications:*

- *T has range in $X_v(0)$ and there exists $T(0)$ and $T_{m,j} \in \mathbb{C}^{d \times d}$ for $m = 1 - q, \dots, 0$ and $j \in \mathbb{N}$ such that*

$$(Th)(0) = T(0)h(0) + \sum_{m=1-q}^0 \sum_{j=0}^\infty T_{m,j} h_{m,j},$$

- *$\ker(U) = \text{im}(I_{X_v} - \pi(0))$, U has range in $\text{im}(I_{X_v} - \pi(0))$, and there exist $U_m \in \ell_v^1(\mathbb{C}^{d \times d})$ for $m = 1 - q, \dots, 0$ such that $(Uh)_{m,j} = U_{m,j}h(0)$,*
- *$\ker(V) = X_v(0)$, V has range in $\text{im}(I_{X_v} - \pi(0))$, and there exist $(V_{m,k})_{j,n} \in \mathbb{C}^{d \times d}$ with $m, k \in \{1 - q, \dots, 0\}$ and $j, n \in \mathbb{N}$ such that*

$$(Vh)_{m,j} = \sum_{k=1-q}^0 \sum_{n=0}^\infty (V_{m,k})_{j,n} h_{k,n}.$$

Then $\|L\|_{B(X_v)} \leq \max\{\mathcal{T}, \mathcal{U} + \mathcal{V}\}$, where

$$\mathcal{T}_m = \sup_{j \geq 0} \frac{1}{v^j} \|T_{m,j}\|, \quad \mathcal{T} = \|T(0)\| + \sum_{m=1-q}^0 \mathcal{T}_m$$

$$\mathcal{V}_{m,k} = \sup_{n \geq 0} \frac{1}{v^n} \sum_{j=0}^{\infty} \|(V_{m,k})_{j,n}\| v^j, \quad \mathcal{U} + \mathcal{V} = \max \left\{ \|U_m\|_v + \sum_{k=1-q}^0 \mathcal{V}_{m,k} : m = 1 - q, \dots, 0 \right\}.$$

Proof By definition of the norm on X_v , we have

$$\|L\|_{B(X_v)} = \sup_{\|h\|_{X_v} \leq 1} \max\{\|(Lh)(0)\|, \|(Lh)_0\|_v, \dots, \|(Lh)_{1-q}\|_v\}. \tag{62}$$

Making use of the decomposition $L = T + U + V$, the contribution from $\|(Lh)(0)\|$ comes solely from T . We bound this term first. First, observe that by definition of \mathcal{T}_m we have $\|T_{m,j}\| \leq v^j \mathcal{T}_m$ for all $j \geq 0$. Then

$$\begin{aligned} \|Th(0)\| &\leq \|T(0)h(0)\| + \sum_{m=1-q}^0 \sum_{j=0}^{\infty} \|T_{m,j}h_{m,j}\| \\ &\leq \|T(0)\| + \sum_{m=1-q}^0 \sum_{j=0}^{\infty} \mathcal{T}_m v^j \|h_{m,j}\| \\ &= \|T(0)\| + \sum_{m=1-q}^0 \mathcal{T}_m \|h_m\| \\ &\leq \mathcal{T}. \end{aligned}$$

Next, since $(Lh)_m = (Uh)_m + (Vh)_m$ for $m = 1 - q, \dots, 0$, we will bound $\|(Lh)_m\|_v$ using the triangle inequality. Clearly $\|(Uh)_m\|_v \leq \|U_m\|_v$. As for the V terms, first observe that by definition of $\mathcal{V}_{m,k}$,

$$\sum_{j=0}^{\infty} \|(V_{m,k})_{j,n}\| v^j \leq \mathcal{V}_{m,k} v^n$$

for all $n \geq 0$. Then

$$\begin{aligned} \|(Vh)_m\|_v &= \sum_{j=0}^{\infty} \|(Vh)_{m,j}\| v^j \\ &\leq \sum_{j=0}^{\infty} \sum_{k=1-q}^0 \sum_{n=0}^{\infty} \|(V_{m,k})_{j,n}\| \cdot \|h_{k,n}\| v^j \\ &= \sum_{k=1-q}^0 \sum_{n=0}^{\infty} \left(\sum_{j=0}^{\infty} \|(V_{m,k})_{j,n}\| v^j \right) \|h_{k,n}\| \\ &\leq \sum_{k=1-q}^0 \sum_{n=0}^{\infty} \mathcal{V}_{m,k} v^n \|h_{k,n}\| \\ &= \sum_{k=1-q}^0 \mathcal{V}_{m,k}, \end{aligned}$$

where in the third line we make use of Fubini’s theorem. Combining the previous two estimates, it follows that $\|(Lh)_m\|_v \leq \|U_m\|_v + \sum_k \mathcal{V}_{m,k}$. Taking the maximum over m and applying (62), we obtain the bound $\|L\|_{B(X_v)} \leq \max\{\mathcal{T}, \mathcal{U} + \mathcal{V}\}$. \square

5.3 Finite convolutions and the operator H_1

Let \mathbf{L} be a $d \times (N_2 + 1) \times d(N_2 + 1)$ matrix, and define $L : \ell_v^1 \rightarrow \ell_v^1$ by

$$(Lh)_n = \begin{cases} \sum_{k=0}^{N_2} \mathbf{L}_{n,k} h_k, & n \leq N_2 \\ 0 & n > N_2, \end{cases}$$

where $\mathbf{L}_{n,k}$ denotes the $d \times d$ block with row-column index (n, k) with indexing from zero (that is, $n = 0$ corresponds to the first row). We write $L = i \circ \mathbf{L}$.

We are will later need to bound operators of the form $\pi_{N_2}^\infty H_1(Y^{N_1} * L)$ in norm. To accomplish this, we first make two observations.

1. The image of $Y^{N_1} * L$ is finite-dimensional and equal to $\pi^{N_1+N_2}(\ell_v^1)$.
2. The kernel of $\pi_{N_2}^\infty H_1$ is equal (for $N_2 \geq 1$) to $\pi^{N_2-1}(\ell_v^1)$.

To proceed, we will therefore represent $(Y^{N_1} * L)$ as an infinite matrix with a finite nonzero block and multiply it with a matrix representation of $\pi_{N_2}^\infty H_1$ on the left. Let ζ^{N_2-1} be the matrix associated to the linear map

$$\mathbb{C}^{d(N_1+N_2+1)} \ni (x_0, x_1, \dots, x_{N_1+N_2}) \mapsto (0, \dots, x_{N_2}, \dots, x_{N_1+N_2}).$$

ξ^{N_2-1} is a $d(N_1 + N_2 + 1) \times d(N_1 + N_2 + 1)$ diagonal matrix. Define

$$\mathbf{G}(Y^{N_1}, L) = \zeta^{N_2-1} [DT]_{0:N_1+N_2}^{0:N_1+N_2} \begin{bmatrix} (Y^{N_1} * \mathbf{L})_0 \\ \vdots \\ (Y^{N_1} * \mathbf{L})_{N_2} \\ \vdots \\ (Y^{N_1} * \mathbf{L})_{N_1+N_2} \end{bmatrix}, \tag{63}$$

where $(Y^{N_1} * \mathbf{L})$ is the $d(N_1 + N_2 + 1) \times d(N_2 + 1)$ matrix defined row-wise

$$(Y^{N_1} * \mathbf{L})_j = \sum_{n=-N_1}^{N_1} Y_{|n|}^{N_1} \mathbf{L}_{|n-j|}$$

For $h \in \ell_v^1$, we have by definition of convolution and L that

$$(Y^{N_1} * Lh)_j = \sum_{n=-N_1}^{N_1} Y_{|n|}^{N_1} \sum_{k=0}^{N_2} \mathbf{L}_{|n-j|,k} h_k = (Y^{N_1} * \mathbf{L}h)_j$$

where $\mathbf{h}_n = h_n$ for $n \leq N_2$ and zero otherwise. From this, we conclude that for $h \in \ell_v^1$,

$$\begin{aligned} \pi^{N_1+N_2} \left(\pi_{N_2}^\infty H_1(Y^{N_1} * L)h \right) &= \psi_{N_1+N_2}^{-1} (\mathbf{G}(Y^{N_1}, L)\mathbf{h}), \\ \pi_{N_1+N_2}^\infty \left(\pi_{N_2}^\infty H_1(Y^{N_1} * L)h \right) &= 0, \end{aligned}$$

where $\psi_N : \pi^N(\ell_v^1) \rightarrow \mathbb{C}^{d(N+1)}$ is the isomorphism defined by $(\psi_N h)_{1+nd:(n+1)d} = h_n$. Formally,

$$\psi_N(h_0, \dots, h_N, 0, \dots) = \begin{bmatrix} h_0 \\ \vdots \\ h_N \end{bmatrix}. \tag{64}$$

$d(2N_1 + 1) \times d$ matrix

$$Z_k^{N_1, N_2} = \begin{bmatrix} 0 \\ \vdots \\ 0 \\ I_d \\ 0 \quad I_d \\ \vdots \\ 0 \quad \dots \quad 0 \quad I_d \quad 0 \quad \dots \quad 0 \end{bmatrix}, \quad \mathbf{S}(Y^{N_1}) = \begin{bmatrix} Y_{N_1} \\ Y_{N_1-1} \\ \vdots \\ Y_1 \\ Y_0 \\ Y_1 \\ \vdots \\ Y_{N_1} \end{bmatrix}.$$

where the first nonzero block in $Z_k^{N_1, N_2}$ has row index $N_2 - N_1 + 1 + k$ (and consequently the last nonzero block column has index $N_1 - k$). Let $\tilde{\mathbf{Q}}_j^{-1}(Y)$ and \mathbf{DT}_j denote the j th (d -dimensional block) row of $\tilde{\mathbf{Q}}^{-1}(Y)$ and \mathbf{DT} , and also let $\mathbf{DT}_{j,k}$ denote the row j , column k block of \mathbf{DT} . With a slight abuse of notation, we define $\tilde{\mathbf{Q}}_{j,k}^{-1} = 0$ whenever the indices (j, k) are out of range: that is, $j > N_2$ or $k > N_2$ (recall we index from zero).

6.1 Bounds in the case $p = q = 1$

Let $N_2 > 0$ be given. Making use of the identifications from Sect. 4.4, we can write E and $(I - W)$ as block matrix operators acting on $\mathbb{C}^d \times \ell_v^1$ as follows. If $h = (h(0), \phi)$,

$$Eh = \begin{bmatrix} (I + C_1 + C_2) & (I + C_1)H_2B_1 * I_{\ell_v^1} \\ \mathbf{e}_0 I_{\mathbb{C}^d} & H_1B_1 * I_{\ell_v^1} \end{bmatrix} \begin{bmatrix} h(0) \\ \phi \end{bmatrix} \tag{65}$$

$$(I_{\ell_v^1} - W)h = \begin{bmatrix} I_{\mathbb{C}^d} & -(I + C_1)H_2A_1 * I_{\ell_v^1} \\ 0 & Q(A_1) \end{bmatrix} \begin{bmatrix} h(0) \\ \phi \end{bmatrix} \tag{66}$$

Next, let $N_1 \geq 0$. We can write E_{N_1, N_2} and $I - W_{N_1, N_2}$ using this same notation:

$$E_{N_1, N_2} = \begin{bmatrix} (I + C_1 + C_2) & (I + C_1)H_2B_1^{N_1} * \pi^{N_2} \\ \mathbf{e}_0 I_{\mathbb{C}^d} & \pi^{N_2}H_1B_1^{N_1} * \pi^{N_2} \end{bmatrix} \tag{67}$$

$$I_{\ell_v^1} - W_{N_1, N_2} = \begin{bmatrix} I_{\mathbb{C}^d} & -(I + C_1)H_2A_1^{N_1} * \pi^{N_2} \\ 0 & \tilde{Q}(A_1) \end{bmatrix}, \tag{68}$$

where this time we have suppressed the input h . From here it follows that

$$(I_{\ell_v^1} - W_{N_1, N_2})^{-1} = \begin{bmatrix} I_{\mathbb{C}^d} & (I + C_1)H_2A_1^{N_1} * \pi^{N_2} \tilde{Q}^{-1}(A_1) \\ 0 & \tilde{Q}^{-1}(A_1) \end{bmatrix}. \tag{69}$$

We have included the explicit domains on the identity operators for clarity. We can now express the truncated monodromy operator $M_{N_1, N_2} = (I - W_{N_1, N_2})^{-1}E_{N_1, N_2}$ in block operator form:

$$M_{N_1, N_2} = \begin{bmatrix} M_{N_1, N_2}^{11} & M_{N_1, N_2}^{12} \\ M_{N_1, N_2}^{21} & M_{N_1, N_2}^{22} \end{bmatrix},$$

$$M_{N_1, N_2}^{11} = C_2 + (I_{\mathbb{C}^d} + C_1)(I_{\mathbb{C}^d} + H_2A_1^{N_1} * \pi^{N_2} \tilde{Q}^{-1}(A_1)\mathbf{e}_0 I)$$

$$M_{N_1, N_2}^{12} = (I_{\mathbb{C}^d} + C_1)(H_2B_1^{N_1} * \pi^{N_2} + H_2A_1^{N_1} * \pi^{N_2} \tilde{Q}^{-1}(A_1)\pi^{N_2}H_1B_1^{N_1} * \pi^{N_2})$$

$$M_{N_1, N_2}^{21} = \tilde{Q}^{-1}(A_1)\mathbf{e}_0 I_{\mathbb{C}^d}$$

$$M_{N_1, N_2}^{22} = \tilde{Q}^{-1}(A_1)\pi^{N_2} H_1 B_1^{N_1} * \pi^{N_2}. \tag{70}$$

Remark 6.1.1 When we want to use the computer to calculate eigenvalues of our impulsive delay differential equation, we implement the matrix representation of the restriction of the linear operator M_{N_1, N_2} to the finite-dimensional vector space $X_v^{N_2}$.

Lemma 6.1.1 (Truncated monodromy operator, $p = q = 1$) Define $M_{N_1, N_2} = (I - W_{N_1, N_2})^{-1} E_{N_1, N_2}$. Suppose ϕ is an eigenvector of M_{N_1, N_2} with eigenvalue λ . If $\lambda \neq 0$ then with $\phi = \phi^{N_2} + \phi^\infty$, we have $\phi^\infty = 0$. Also, each of X_v^∞ and $X_v^{N_2}$ is an invariant subspace for M_{N_1, N_2} and for $r > 0$ we have

$$\|(M_{N_1, N_2} - r e^{i\theta})^{-1}\|_{B(X_v^\infty)} \leq \frac{1}{r}.$$

If $\lambda \in \mathbb{C}$, $0 < r < |\lambda|$ and $0 < \omega < \pi$, then for $U \in \{D_r(\lambda), R_\lambda(r, \omega)\}$,

$$\sup_{z \in \partial U} \|(M_{N_1, N_2} - zI)^{-1}\|_{B(X_v^\infty)} \leq \frac{1}{|\lambda| - r}.$$

Proof The assertions concerning the eigenvalues, eigenvectors and invariant subspaces follow directly from the definition of E_{N_1, N_2} and $(I - W_{N_1, N_2})^{-1}$. As for the bound, we have $M_{N_1, N_2} \phi^\infty = 0$, which implies $(M_{N_1, N_2} - r e^{i\theta})^{-1} \phi^\infty = \frac{1}{r} e^{-i\theta} \phi^\infty$ and subsequently, $\|(M_{N_1, N_2} - r e^{i\theta})^{-1} \phi^\infty\|_{X_v} \leq \frac{1}{r} \|\phi^\infty\|_{X_v}$. For the proof concerning the closed ball $D_r(\lambda)$, observe that $(M_{N_1, N_2} - (\lambda + r e^{it})I)^{-1} \phi^\infty = (\lambda + r e^{it})^{-1} \phi^\infty$ for $t \in [0, 2\pi]$, so that

$$\|(M_{N_1, N_2} - (\lambda + r e^{it})I)^{-1}\|_{X_v} \leq \sup_{t \in [0, 2\pi]} \frac{1}{|\lambda + r e^{it}|} \|\phi^\infty\|_{X_v}.$$

which attains its maximum when $t = -\arg \lambda$, resulting in the bound claimed in the lemma. As for the radial sector, we have

$$(M_{N_1, N_2} - z(t; \lambda, r, \omega)I)^{-1} \phi^\infty = \frac{1}{z(t; \lambda, r, \omega)} \phi^\infty$$

for the parameterization in (44). Taking norms and suprema for $t \in [0, 4]$, the upper bound stated in the lemma is attained for $t \in [0, 1]$. □

Remark 6.1.2 For fixed $\lambda \in \mathbb{C}$ and $r \in (0, |\lambda|)$, the coarse bound for $\sup_{z \in \partial U} \|(M_{N_1, N_2} - zI)^{-1}\|_{B(X_v^\infty)}$ is attained at a single point in the boundary parameterization for a closed ball $D_\lambda(r)$, whereas it is attained on a continuum for a given radial sector $R_\lambda(r, \cdot)$. In this sense, $\sup_{z \in \partial U} \|(M_{N_1, N_2} - zI)^{-1}\|_{B(X_v^\infty)}$ can be more conservatively bounded on a radial sector (of a given width) than it can for a closed ball (of radius equal to the prior width).

This lemma gives preliminary justification for why M_{N_1, N_2} is a reasonable choice for a truncated monodromy operator. It also guarantees that the nonzero eigenvalues of the truncation can in principle be computed from the finite (and generally nontrivial) part of M_{N_1, N_2} . The following theorems gives computable bounds c_2 and c_3 .

Theorem 6.1.1 (c_2 bound, $p = q = 1$) Let $N_2 > N_1 \geq 0$. Denote $A_1^{N_1} = (A_{1,0}, \dots, A_{1,N_1}, 0, \dots)$ and $A_1^\infty = A_1 - A_1^{N_1}$. Define

$$K_0 = \max_{k=0, \dots, N_2} \frac{1}{v^k} \sum_{j=0}^{N_2} \|\tilde{Q}_{j,k}^{-1}(A_1^{N_1})\| v^j$$

$$\begin{aligned}
 K_0^\circ &= \max_{k=0,\dots,N_2} \frac{1}{v^k} \sum_{j=0}^{N_2} \|(I + C_1)\tilde{\mathbf{Q}}_{j,k}^{-1}(A_1^{N_1})\|v^j \\
 K_1 &= \max_{k=0,\dots,N_1} \frac{1}{v^{N_2+1+k}} \sum_{j=0}^{N_2} \left(\frac{\|A_1^{N_1}\|_\omega}{(N_2 + 1 - N_1)^2 - 1} \|\tilde{\mathbf{Q}}_{j,0}^{-1}(A_1^{N_1})\| \right. \\
 &\quad \left. + \|\tilde{\mathbf{Q}}_j^{-1}(A_1^{N_1})\mathbf{DTZ}_k^{N_1,N_2}\mathbf{S}(A_1^{N_1})\| \right) v^j \\
 m_{j,k} &= \left(\frac{\|A_1^{N_1}\|_\omega}{(N_2 + 1 - N_1)^2 - 1} \|(I + C_1)\tilde{\mathbf{Q}}_{j,0}^{-1}(A_1^{N_1})\| \right. \\
 &\quad \left. + \|(I + C_1)\tilde{\mathbf{Q}}_j^{-1}(A_1^{N_1})\mathbf{DTZ}_k^{N_1,N_2}\mathbf{S}(A_1^{N_1})\| \right) \\
 K_2 &= \max_{k=0,\dots,N_1} \frac{1}{v^{N_2+1+k}} m_{j,0} + \sum_{j=2}^{N_2} \frac{(-1)^j + 1}{j^2 - 1} \left(\max_{k=0,\dots,N_1} \frac{1}{v^{N_2+1+k}} m_{j,k} \right) \\
 J_0(A_1^{N_1}) &= \max_{k=0,\dots,N_2} \frac{1}{v^k} \sum_{j=N_2}^{N_2+N_1} \|\mathbf{G}(A_1^{N_1}, i \circ I_{\mathbb{C}^{d(N_2+1)}})_{j,k}\|v^j \\
 \alpha(A_1^{N_1}) &= \frac{1}{4(N_2 + 1)} \left(\left(v + \frac{2}{v} + \frac{1}{v^3} \right) \|A_1^{N_1}\|_v - \left(\frac{1}{v} + \frac{1}{v^3} \right) \|A_{1,0}^{N_1}\| \right) \\
 \beta &= \max \left\{ J_0(A_1^{N_1}), K_1 + \alpha(A_1^{N_1}) \right\}
 \end{aligned}$$

and introduce the quantities

$$\begin{aligned}
 \rho_1 &= \left(K_0 \left(1 + \frac{v}{2} \right) + \frac{v + v^{-1}}{2(N_2 + 1)} \right) \|A_1^\infty\|_\omega + \beta \\
 \rho(0) &= g(v)K_0^\circ \left(1 + \frac{v}{2} \right) \|A_1^\infty\|_\omega \\
 &\quad + \max \left\{ 2g(v)\|I + C_1\| \cdot \|A_1^\infty\|_\omega, \frac{2\|(I + C_1) \odot A_1^{N_1}\|_v}{v^{N_2+1}} + K_2 \right\}
 \end{aligned}$$

Suppose $\rho := \max\{\rho_1, \rho(0)\} < 1$. Then, with

$$c_2 := \frac{\|(I - W_{N_1,N_2})^{-1}\|_{B(X_v)}}{1 - \rho} = \frac{\max\{1, \|(I - W_{N_1,N_2})^{-1}\|_{B(X_v^{N_2})}\}}{1 - \rho}, \tag{71}$$

the operator $I - W$ satisfies $\|(I - W)^{-1}\|_{B(X_v)} \leq c_2$.

Proof Define the operator $\Lambda = I - (I - W_{N_1,N_2})^{-1}(I - W)$. By construction,

$$\|(I_{\ell_v^1} - W)^{-1}\|_{B(\ell_v^1)} \leq \|(I_{\ell_v^1} - W_{N_1,N_2})^{-1}\|_{B(\ell_v^1)} \cdot \|(I - \Lambda)^{-1}\|_{B(\ell_v^1)},$$

so if we can estimate the norm of Λ and prove that this is less than one, a Neumann series argument will give a constructive bound for c_2 , since the norm $\|(I_{\ell_v^1} - W_{N_1,N_2})^{-1}\|_{B(\ell_v^1)}$ can be approximated (or rigorously enclosed) on a computer: in particular, it is bounded above by $\max\{1, \|(I - W_{N_1,N_2})^{-1}\pi^{N_2}\|_{B(X_v^{N_2})}\}$.

Moving on to the estimation of the operator norm of Λ , a careful multiplication shows

$$\Lambda = \begin{bmatrix} 0 & (I + C_1)\Lambda_{12} \\ 0 & I_{\ell_v^1} - \tilde{Q}^{-1}(A_1)Q(A_1) \end{bmatrix},$$

with the upper right block given by

$$\begin{aligned} \Lambda_{12} &= H_2 A_1^{N_1} * \pi^{N_2} \tilde{Q}^{-1}(A_1)Q(A_1) - H_2 A_1 * I_{\ell_v^1} \\ &= H_2 \left(A_1^{N_1} * \pi^{N_2} \tilde{Q}^{-1}(A_1)Q(A_1) - A_1 * I_{\ell_v^1} \right) \\ &= H_2 \left(A_1^{N_1} * \pi^{N_2} (\tilde{Q}^{-1}(A_1)Q(A_1) - I_{\ell_v^1}) + A_1^{N_1} * \pi^{N_2} - A_1 * (\pi^{N_2} + \pi_{N_2}^\infty) \right) \\ &= H_2 \left(A_1^{N_1} * \pi^{N_2} (\tilde{Q}^{-1}(A_1)Q(A_1) - I_{\ell_v^1}) - A_1^\infty * \pi^{N_2} - A_1^{N_1} * \pi_{N_2}^\infty \right). \end{aligned}$$

By definition of the norm on $X_v = \mathbb{C}^d \times \ell_v^1$, it follows that

$$\|\Lambda\|_{B(X_v)} \leq \max\{\|(I + C_1)\Lambda_{12}\|_{B(\ell_v^1)}, \|I_{\ell_v^1} - \tilde{Q}^{-1}(A_1)Q(A_1)\|_{B(\ell_v^1)}\}.$$

We will estimate these two norms separately. For brevity, write $\tilde{Q} = \tilde{Q}(A_1^{N_1})$ and $Q = Q(A_1)$. First, we use Lemma 5.1.3 to write

$$\begin{aligned} I_{\ell_v^1} - \tilde{Q}^{-1}Q &= \tilde{Q}^{-1}\pi^{N_2}H_1(A_1^\infty * I_{\ell_v^1}) + \tilde{Q}^{-1}\pi^{N_2}H_1(A_1^{N_1} * \pi_{N_2}^\infty) + \pi_{N_2}^\infty H_1(A_1^\infty * I_{\ell_v^1}) \\ &\quad + \pi_{N_2}^\infty H_1(A_1^{N_1} * \pi^{N_2}) + \pi_{N_2}^\infty H_1(A_1^{N_1} * \pi_{N_2}^\infty). \end{aligned}$$

We will now bound this linear operator using (58) to consider the maximum of the contribution from the body $\pi^{N_2}(\ell_v^1)$ and tail $\pi_{N_2}^\infty(\ell_v^1)$. Using Propositions 4.1.1, 5.3.1 and rows 3, 4, and 8 of Table A, we can get the bound

$$\|(I_{\ell_v^1} - \tilde{Q}^{-1}Q)\pi^{N_2}\|_{B(\ell_v^1)} \leq K_0 \left(1 + \frac{\nu}{2}\right) \|A_1^\infty\|_\omega + \frac{\nu + \nu^{-1}}{2(N_2 + 1)} \|A_1^\infty\|_\omega + J_0(A_1^{N_1}). \tag{72}$$

Similarly, using Proposition 4.1.1 and rows 3, 4, 8, 12 and 14 of Table A, we get

$$\|(I_{\ell_v^1} - \tilde{Q}^{-1}Q)\pi_{N_2}^\infty\|_{B(\ell_v^1)} \leq K_0 \left(1 + \frac{\nu}{2}\right) \|A_1^\infty\|_\omega + K_1 + \frac{\nu + \nu^{-1}}{2(N_2 + 1)} \|A_1^\infty\|_\omega + \alpha(A_1^{N_1}). \tag{73}$$

Taking into account (58), it follows that $\|I_{\ell_v^1} - \tilde{Q}^{-1}Q\|_{B(\ell_v^1)} \leq \rho_1$.

Next, we deal with Λ_{12} . We begin by splitting $\pi^{N_2}(\tilde{Q}^{-1}Q - I_{\ell_v^1})$ into two separate terms:

$$\pi^{N_2}(\tilde{Q}^{-1}Q - I_{\ell_v^1}) = -\pi^{N_2} \tilde{Q}^{-1}(H_1(A_1^\infty * I_{\ell_v^1})) - \pi^{N_2} \tilde{Q}^{-1}H_1(A_1^{N_1} * \pi_{N_2}^\infty).$$

With this decomposition, we can write $-\Lambda_{12}$ as follows:

$$\begin{aligned} -\Lambda_{12} &= H_2(A_1^\infty * \pi^{N_2} + \pi^{N_2} \tilde{Q}^{-1}(H_1(A_1^\infty * I_{\ell_v^1}))) + H_2(A_1^{N_1} * \pi_{N_2}^\infty \\ &\quad + \pi^{N_2} \tilde{Q}^{-1}(H_1(A_1^{N_1} * \pi_{N_2}^\infty))). \end{aligned}$$

This decomposition has the effect of separating the terms that are asymptotically $O(\|A_1^\infty\|_\omega)$ from everything else. After distributing through the $I + C_1$ matrix term using the elementwise product operand \odot , we use Proposition 4.1.1, rows 1, 2, 3, 4 and 15 and (59) to obtain the bound

$$\|(I + C_1)\Lambda_{12}\|_{B(\ell_v^1)}$$

$$\begin{aligned} &\leq g(v)K_0^\circ \left(1 + \frac{v}{2}\right) \|A_1^\infty\|_\omega + \max \{2g(v)\|I \\ &\quad + C_1\| \cdot \|A_1^\infty\|_\omega, \frac{2\|(I + C_1) \odot A_1^{N_1}\|_v}{v^{N_2+1}} + K_2 \} \\ &= \rho(0) \end{aligned} \tag{74}$$

Combining the previous estimates, we conclude $\|\Lambda\|_{B(\ell_1^v)} \leq \max\{\rho_1, \rho(0)\} = \rho$. By Neumann series, $\|(I - \Lambda)^{-1}\|_{B(\ell_1^v)} \leq \frac{1}{1-\rho}$, which combined with the discussion at the beginning completes the proof. \square

Remark 6.1.3 The matrix $\tilde{Q}^{-1}(A_1^{N_1})$ can be identified with the nontrivial, finite block of

$$\tilde{Q}^{-1}(A_1^{N_1})\pi^{N_2} = [0 \ \pi^{N_2}](I - W_{N_1, N_2})^{-1} \begin{bmatrix} 0 \\ \pi^{N_2} \end{bmatrix},$$

and is computed explicitly in our numerical scheme. As such, any finite computations involving this can be accomplished on a computer.

Theorem 6.1.2 (c_3 bound, $p = q = 1$) Let $N_2 > 1$ and $N_1 > 0$, and let $K_0, A_1^{N_1}$ and A_1^∞ be defined as in Theorem 6.1.1. Denote $B_1^{N_1} = (B_{1,0}, \dots, B_{1,N_1}, 0, \dots)$ and $B_1^\infty = B_1 - B_1^{N_1}$. Let \mathbf{M} be the $d(N_2 + 1) \times d(N_2 + 1)$ matrix such that for all $h \in \pi^{N_2}(\ell_1^v)$,

$$\psi_{N_2} \left(\tilde{Q}^{-1}(A_1)\pi^{N_2} H_1 B_1^{N_1} * h \right) = \mathbf{M}\psi_{N_2}(h)$$

where ψ the isomorphism defined by in (64). Introduce the quantities

$$\begin{aligned} \|\mathbf{M}\|_v &= \max_{k=0, \dots, N_2} \frac{1}{v^k} \sum_{j=0}^{N_2} \|\mathbf{M}_{j,k}\| v^j \\ K_0^0 &= \sum_{j=0}^{N_2} \|\mathbf{Q}_{j,0}^{-1}(A_1^{N_1})\| \\ L_0 &= \max_{k=0, \dots, N_2} \frac{1}{v^k} \sum_{j=N_2}^{N_2+N_1} \|\mathbf{G}(A_1^{N_1}, i \circ \tilde{Q}^{-1}(A_1^{N_1}) \text{diag}(I, 0, \dots, 0))_{j,k}\| v^j \\ L_1 &= \max_{k=0, \dots, N_2} \frac{1}{v^k} \sum_{j=N_2}^{N_2+N_1} \|\mathbf{G}(A_1^{N_1}, i \circ \mathbf{M})_{j,k}\| v^j \\ L_2 &= \max_{k=0, \dots, N_1} \frac{1}{v^{N_2+1+k}} \sum_{j=0}^{N_2} \left(\frac{\|B_1^{N_1}\|_\omega}{(N_2 + 1 - N_1)^2 - 1} \|\mathbb{1}_0(j) + \|\mathbf{DT}_j Z_k^{N_1, N_2} \mathbf{S}(B_1^{N_1})\| \right) v^j \\ J_0(B_1^{N_1}) &= \max_{k=0, \dots, N_2} \frac{1}{v^k} \sum_{j=N_2}^{N_2+N_1} \|\mathbf{G}(B_1^{N_1}, i \circ I_{\mathbb{C}^{d(N_2+1)}})\| v^j \\ \alpha(B_1^{N_1}) &= \frac{1}{4(N_2 + 1)} \left(\left(v + \frac{2}{v} + \frac{1}{v^3} \right) \|B_1^{N_1}\|_v - \left(\frac{1}{v} + \frac{1}{v^3} \right) \|B_{1,0}^{N_1}\| \right) \\ \gamma &= \max \left\{ \left(1 + \frac{v}{2} \right) \|\mathbf{M}\|_v \|A_1^\infty\|_\omega + L_1 + J_0(B_1^{N_1}), L_2 + \alpha(B_1^{N_1}) \right\} \\ \kappa_1 &= \left(1 + \frac{v}{2} \right) (K_0^0 \|A_1^\infty\|_\omega + \|B_1^\infty\|_\omega) + L_0 + \gamma \end{aligned}$$

$$\begin{aligned} \kappa(0) &= 2g(v)\|I + C_1\|K_0^0\|A_1^\infty\|_\omega + \max \left\{ 2g(v)\|I + C_1\| \cdot \|B_1^\infty\|_\omega, \right. \\ &\quad \left. 2g(v)\|I + C_1\| \cdot \|A_1^\infty\|_\omega \|M\|_v + \dots \right. \\ &\quad \left. \frac{1}{v^{N_2+1}} \left(2\|(I + C_1) \odot B_1^{N_1}\|_v + \left(1 + \frac{1}{v^{N_2+1}} \right) \|I + C_1\| \cdot \|B_1^\infty\|_\omega \right) \right\} \end{aligned}$$

Then, with

$$c_3 := \max\{\kappa_1, \kappa(0)\}, \tag{75}$$

we have the estimate $\|(I - W)M_{N_1, N_2} - E\|_{B(X_v)} \leq c_3$.

Proof Define $\bar{\Lambda} = (I - W)M_{N_1, N_2} - E$. Using (65)–(69) one can write $\bar{\Lambda}$ in the form

$$\bar{\Lambda} = - \begin{bmatrix} (I + C_1)\bar{\Lambda}_{11} & (I + C_1)\bar{\Lambda}_{12} \\ \bar{\Lambda}_{21} & \bar{\Lambda}_{22} \end{bmatrix}$$

with the more complicated terms being given by

$$\begin{aligned} \bar{\Lambda}_{11} &= H_2(A_1 * I_{\ell_v^1} - A_1^{N_1} * \pi^{N_2})\tilde{Q}^{-1}(A_1)\mathbf{e}_0 I_{C^d} \\ &= H_2(A_1 * I_{\ell_v^1} - A_1^{N_1} * I_{\ell_v^1})\tilde{Q}^{-1}(A_1)\mathbf{e}_0 I_{C^d} \\ &= H_2 A_1^\infty * \tilde{Q}^{-1}(A_1)\mathbf{e}_0 I_{C^d} \\ \bar{\Lambda}_{12} &= H_2 \left(B_1 * I_{\ell_v^1} - B_1^{N_1} * \pi^{N_2} + (A_1 * I_{\ell_v^1} - A_1^{N_1} * \pi^{N_2})\tilde{Q}^{-1}(A_1)\pi^{N_2} H_1 B_1^{N_1} * \pi^{N_2} \right) \\ &= H_2 \left(B_1^\infty * \pi^{N_2} + B_1 * \pi_{N_2}^\infty + (A_1 * I_{\ell_v^1} - A_1^{N_1} * \pi^{N_2})\pi^{N_2} \tilde{Q}^{-1}(A_1)\pi^{N_2} H_1 B_1^{N_1} * \pi^{N_2} \right) \\ &= H_2 \left(B_1^\infty * \pi^{N_2} + B_1 * \pi_{N_2}^\infty + A_1^\infty * \pi^{N_2} \tilde{Q}^{-1}(A_1)\pi^{N_2} H_1 B_1^{N_1} * \pi^{N_2} \right) \\ \bar{\Lambda}_{21} &= (I - Q(A_1)\tilde{Q}^{-1}(A_1))\mathbf{e}_0 I_{C^d} \\ \bar{\Lambda}_{22} &= H_1 B_1 * I_{\ell_v^1} - Q(A_1)\tilde{Q}^{-1}(A_1)\pi^{N_2} H_1 B_1^{N_1} * \pi^{N_2} \\ &= (I_{\ell_v^1} - Q(A_1)\tilde{Q}^{-1}(A_1))\pi^{N_2} H_1 B_1^{N_1} * \pi^{N_2} + H_1 B_1 * I_{\ell_v^1} - \pi^{N_2} H_1 B_1^{N_1} * \pi^{N_2} \\ &= (I_{\ell_v^1} - Q(A_1)\tilde{Q}^{-1}(A_1))\pi^{N_2} H_1 B_1^{N_1} * \pi^{N_2} \\ &\quad + H_1 B_1^\infty * I_{\ell_v^1} + \pi^{N_2} H_1 B_1^{N_1} * \pi_{N_2}^\infty + \pi_{N_2}^\infty H_1 B_1^{N_1} * I_{\ell_v^1}, \end{aligned}$$

Like in the proof of the previous theorem, we can bound $\|\bar{\Lambda}\|_{B(\ell_v^1)}$ via

$$\|\bar{\Lambda}\|_{B(\ell_v^1)} \leq \max \left\{ \|(I + C_1)\bar{\Lambda}_{11}\| + \|(I + C_1)\bar{\Lambda}_{12}\|, \|\bar{\Lambda}_{21}\| + \|\bar{\Lambda}_{22}\| \right\}, \tag{76}$$

where the norms are norms on appropriate spaces of linear maps. It therefore suffices to compute the individual norm bounds. Starting with $\bar{\Lambda}_{21}$, we can write

$$\bar{\Lambda}_{21} = H_1(A_1^\infty * \tilde{Q}^{-1}\mathbf{e}_0) + \pi_{N_2}^\infty H_1(A_1^{N_1} * \tilde{Q}^{-1}\mathbf{e}_0).$$

This we bound using Propositions 4.1.1, 5.3.1 and rows 3 and 9 of Table A to get

$$\|\bar{\Lambda}_{21}\| \leq \left(1 + \frac{v}{2} \right) K_0^0\|A_1^\infty\|_\omega + L_0.$$

Next, we write down $\bar{\Lambda}_{22}$ with more structure. We have

$$\begin{aligned} \bar{\Lambda}_{22} &= H_1(A_1^\infty * \tilde{Q}^{-1}\pi^{N_2} H_1(B_1^{N_1} * \pi^{N_2})) + \pi_{N_2}^\infty H_1(A_1^{N_1} * \tilde{Q}^{-1}\pi^{N_2} H_1(B_1^{N_1} * \pi^{N_2})) \\ &\quad + H_1(B_1^\infty * I_{\ell_v^1}) + \pi^{N_2} H_1(B_1^{N_1} * \pi_{N_2}^\infty) + \pi_{N_2}^\infty H_1 B_1^{N_1} I_{\ell_v^1} \end{aligned}$$

$$\begin{aligned}
 &= H_1(A_1^\infty * \tilde{Q}^{-1}(A_1)\pi^{N_2}H_1B_1^{N_1} * \pi^{N_2}) \\
 &\quad + \pi_{N_2}^\infty H_1(A_1^{N_1} * \tilde{Q}^{-1}(A_1)\pi^{N_2}H_1B_1^{N_1} * \pi^{N_2}) + H_1(B_1^\infty * I_{\ell_v^1}) \\
 &\quad + H_1(B_1^{N_1} * \pi_{N_2}^\infty) + \pi_{N_2}^\infty H_1(B_1^{N_1} * \pi^{N_2}).
 \end{aligned}$$

We can bound the individual terms with Propositions 4.1.1, 5.3.1, Lemma 5.2.1 and rows 3, 4, 13 and 14 of Table A. Additionally taking into account the tail-body split inequality (58), we get

$$\|\bar{\Lambda}_{22}\| \leq \left(1 + \frac{\nu}{2}\right) \|B_1^\infty\|_\omega + \gamma.$$

Combining the two previous estimates, we have $\|\bar{\Lambda}_{21}\| + \|\bar{\Lambda}_{22}\| \leq \kappa_1$. Next we bound $(I + C_1)\bar{\Lambda}_{11}$. Using Proposition 4.1.1 and rows 1 and 9 of Table A, We have

$$\|(I + C_1)\bar{\Lambda}_{11}\| \leq \|I + C_1\|2g(\nu)K_0^0\|A_1^\infty\|_\omega.$$

To handle $(I + C_1)\bar{\Lambda}_{12}$, we use Propositions 4.1.1, 5.3.1, Lemma 5.2.1, rows 1 and 2 of Table A and inequality (59) to get

$$\begin{aligned}
 \|(I + C_1)\bar{\Lambda}_{12}\| \leq \max &\left\{2g(\nu)\|I + C_1\| \cdot \|B_1^\infty\|_\omega, 2g(\nu)\|I + C_1\| \cdot \|A_1^\infty\|_\omega\|\mathbf{M}\|_\nu + \dots \right. \\
 &\left. \frac{2}{\nu^{N_2+1}} \left(\|(I + C_1) \odot B_1^{N_1}\|_\nu + \left(1 + \frac{1}{\nu^{N_2+1}}\right) \|I + C_1\| \cdot \|B_1^\infty\|_\nu \right) \right\}
 \end{aligned}$$

It follows that $\|(I + C_1)\bar{\Lambda}_{11}\| + \|(I + C_1)\bar{\Lambda}_{12}\| \leq \kappa(0)$. Combining these with the previous inequality (76) for $\|\bar{\Lambda}\|_{B(\ell_v^1)}$, we get $\|\bar{\Lambda}\|_{B(\ell_v^1)} \leq c_3$ as claimed.

Remark 6.1.4 \mathbf{M} coincides with the nontrivial $d(N_2 + 1) \times d(N_2 + 1)$ block of M_{N_1, N_2}^{22} from (70). □

6.2 Bounds in the case 1 = p < q

The implicit part W has a particular structure, which in turn induces a structure on $(I - W)$. From (38) and the representations of Sect. 4.4, we can interpret it as being the following block operator acting on X_ν . For $\phi = (\phi(0), \phi_0, \dots, \phi_{1-q})$,

$$(I - W)\phi = \begin{bmatrix} I - (I + C_1)H_2A_1 * I_{\ell_v^1} & 0 & \dots & \dots & 0 \\ 0 & Q(A_1) & 0 & \dots & \dots & 0 \\ 0 & 0 & I_{\ell_v^1} & 0 & \dots & 0 \\ 0 & 0 & 0 & I_{\ell_v^1} & \dots & 0 \\ \vdots & \vdots & \ddots & \ddots & \ddots & \vdots \\ 0 & \dots & \dots & \dots & 0 & I_{\ell_v^1} \end{bmatrix} \phi,$$

where the identity operators I are on the implied spaces: for instance, the first one is on \mathbb{C}^d and the others are on ℓ_v^1 . If we take a direct (N_1, N_2) -mode truncation of W (in the same way

we did for $p = q = 1$), we obtain

$$(I - W_{N_1, N_2})^{-1}\phi = \begin{bmatrix} I(I + C_1)H_2A_1^{N_1} * \pi^{N_2} \tilde{Q}^{-1}(A_1) & 0 & \dots & \dots & 0 \\ 0 & \tilde{Q}^{-1}(A_1) & & & 0 \\ 0 & 0 & I_{\ell_v^1} & 0 & \dots & 0 \\ 0 & 0 & 0 & I_{\ell_v^1} & \dots & 0 \\ \vdots & \vdots & \vdots & \vdots & \ddots & \vdots \\ 0 & \dots & \dots & \dots & \dots & 0 & I_{\ell_v^1} \end{bmatrix} \phi.$$

We can similarly express the explicit part E as a block operator acting on X_v . We have

$$E\phi = \begin{bmatrix} (I + C_1) & 0 & \dots & 0 & C_2S^* & (I + C_1)H_2B_1 * I_{\ell_v^1} \\ \mathbf{e}_0 & 0 & \dots & 0 & 0 & H_1B_1 * I_{\ell_v^1} \\ 0 & I_{\ell_v^1} & 0 & \dots & 0 & 0 \\ \vdots & \vdots & \ddots & \ddots & \vdots & \vdots \\ 0 & \dots & 0 & I_{\ell_v^1} & 0 & 0 \\ 0 & \dots & \dots & 0 & I_{\ell_v^1} & 0 \end{bmatrix} \begin{bmatrix} \phi(0) \\ \phi_0 \\ \vdots \\ \vdots \\ \phi_{2-q} \\ \phi_{1-q} \end{bmatrix}.$$

We can now truncate the sequence B_1 to N_1 modes, while for the second level of truncation we will do something a bit different. We define

$$E_{N_1, N_2}\phi = \begin{bmatrix} (I + C_1) & 0 & \dots & 0 & C_2S^*\pi^{N_2} & (I + C_1)H_2B_1^{N_1} * \pi^{N_2} \\ \mathbf{e}_0 & 0 & \dots & 0 & 0 & \pi^{N_2}H_1B_1^{N_1} * \pi^{N_2} \\ 0 & I_{\ell_v^1} & 0 & \dots & 0 & 0 \\ \vdots & \vdots & \ddots & \ddots & \vdots & \vdots \\ 0 & \dots & 0 & I_{\ell_v^1} & 0 & 0 \\ 0 & \dots & \dots & 0 & I_{\ell_v^1} & 0 \end{bmatrix} \begin{bmatrix} \phi(0) \\ \phi_0 \\ \vdots \\ \vdots \\ \phi_{2-q} \\ \phi_{1-q} \end{bmatrix}.$$

Remark 6.2.1 When we want to use the computer to calculate eigenvalues of our impulsive delay differential equation, we implement the matrix representation of the restriction of the linear operator $M_{N_1, N_2} = (I - W_{N_1, N_2})^{-1}E_{N_1, N_2}$ to the finite-dimensional vector space $X_v^{N_2}$.

Remark 6.2.2 It might be tempting to replace the identity maps $I_{\ell_v^1}$ in the lower diagonal part of E with projections π^{N_2} in the expression for E_{N_1, N_2} . The reason we do not is because if we do, the analogous diagonal terms of $E - E_{N_1, N_2}$ become projections $\pi_{N_2}^\infty$, which have norm 1 for all $N_2 > 0$. This would eliminate our ability to control the bound c_3 by taking more modes, which is undesirable for computer-assisted proofs. It would also imply M_{N_1, N_2} does not converge to M as a bounded operator on X_v as we increase the number of modes, which is completely wrong if we want to think of M_{N_1, N_2} as an approximation of M .

Lemma 6.2.1 (Truncated monodromy operator, $1 = p < q$) Define $M_{N_1, N_2} = (I - W_{N_1, N_2})^{-1}E_{N_1, N_2}$. Suppose ϕ is an eigenvector of M_{N_1, N_2} with eigenvalue λ . If $\lambda \neq 0$ then with $\phi = \phi^{N_2} + \phi^\infty$, we have $\phi^\infty = 0$. Also, each of $X_v^{N_2}$ and X_v^∞ is an invariant subspace for M_{N_1, N_2} and for $r > 0$ we have

$$\|(M_{N_1, N_2} - re^{i\theta})^{-1}\|_{B(X_v^\infty)} \leq \max \left\{ \frac{1}{r}, \frac{1 - r^{-q}}{r - 1} \right\}$$

unless $r = 1$, in which case $\|(M_{N_1, N_2} - r e^{i\theta})^{-1}\|_{B(X_v^\infty)} \leq 1$. If $\lambda \in \mathbb{C}$, $0 < r < |\lambda|$ and $0 < \omega < \pi$, then for $U \in \{D_r(\lambda), R_\lambda(r, \omega)\}$,

$$\sup_{z \in U} \|(M_{N_1, N_2} - zI)^{-1}\|_{B(X_v^\infty)} \leq \max \left\{ \frac{1}{|\lambda| - r}, \frac{1 - (|\lambda| - r)^{-q}}{|\lambda| - r - 1} \right\}.$$

Proof The assertions concerning the eigenvalues, eigenvectors and invariant subspaces follow directly from the definition of E_{N_1, N_2} and $(I - W_{N_1, N_2})^{-1}$. As for the bound, one can verify directly that if ϕ^∞ and h^∞ satisfy $(M_{N_1, N_2} - r e^{i\theta})\phi^\infty = h^\infty$, then

$$\begin{aligned} \phi_0^\infty &= -\frac{1}{r} e^{-i\theta} h_0^\infty, \\ \phi_k^\infty &= -\frac{1}{r} e^{-i\theta} (h_k^\infty - \phi_{k+1}^\infty), \quad 1 - q \leq k \leq -1. \end{aligned}$$

Thus, if $\|h^\infty\|_{X_v} \leq 1$, then $\|\phi_0^\infty\|_v \leq \frac{1}{r}$ and by a quick inductive proof, one can check that

$$\|\phi_k^\infty\|_v \leq \frac{1}{r} (1 + \|\phi_{k+1}^\infty\|_v) \Rightarrow \|\phi_k^\infty\|_v \leq \frac{1 - r^{k-1}}{r - 1} =: w(k),$$

unless $r = 1$, in which case $\|\phi_k^\infty\|_v \leq 1$. To complete the proof, observe that w is strictly decreasing and therefore reaches its maximum at index $k = 1 - q$. The argument for the radial sector and closed ball are similar and omitted. \square

Theorem 6.2.1 (c_2 bound, $1 = p < q$) Let $N_2 > N_1 \geq 0$. With ρ as defined in Theorem 6.1.1, the operator $I - W$ satisfies $\|(I - W)^{-1}\|_{B(X_v)} \leq c_2$ with

$$c_2 := \frac{\|(I - W_{N_1, N_2})^{-1}\|_{B(X_v)}}{1 - \rho} = \frac{\max\{1, \|(I - W_{N_1, N_2})^{-1}\|_{B(X_v^{N_2})}\}}{1 - \rho}. \tag{77}$$

Proof Define $\Omega = I - (I - W_{N_1, N_2})^{-1}(I - W)$. Then

$$\Omega = \begin{bmatrix} 0 & (I + C_1)\Lambda_{12} & \\ 0 & I_{\ell_v^1} - \tilde{Q}^{-1}(A_1)Q(A_1) & \\ & & \mathbf{0} \end{bmatrix},$$

where empty entries are zero (of appropriate spaces of linear maps) and $\mathbf{0} = \text{diag}(0, \dots, 0)$ is the zero operator on $(\ell_v^1)^{q-1}$. The nontrivial part of Ω coincides precisely with Λ from the proof of Theorem 6.1.1. To show that $\|(I - W_{N_1, N_2})^{-1}\|_{B(X_v)} = \max\{1, \|(I - W_{N_1, N_2})^{-1}\|_{B(X_v^{N_2})}\}$, observe that $(I - W_{N_1, N_2})^{-1}$ is still the identity operator when restricted to X_v^∞ . \square

Theorem 6.2.2 (c_3 bound, $1 = p < q$) Let $N_2 \geq N_1 > 0$ and let κ_1 and $\kappa(0)$ be defined as as defined in Theorem 6.1.2. Then, with

$$c_3 := \max \left\{ \kappa_1, \kappa(0) + \frac{2\|C_2\|}{v^{N_2+1}} \right\}, \tag{78}$$

we have the estimate $\|(I - W)M_{N_1, N_2} - E\|_{B(X_v)} \leq c_3$.

Proof Let $\bar{\Omega} = (I - W)(I - W_{N_1, N_2})^{-1}E_{N_1, N_2} - E$. Making use of the previous expressions for $I - W$, $(I - W_{N_1, N_2})^{-1}$, E and E_{N_1, N_2} , we find that in block operator form,

$$\bar{\Omega} = - \begin{bmatrix} (I + C_1)\bar{\Omega}_{11} & 0 \cdots 0 & C_2 S^* \pi_{N_2}^\infty & (I + C_1)\bar{\Omega}_{1+} \\ \bar{\Omega}_{21} & 0 \cdots 0 & 0 & \bar{\Omega}_{2+} \\ 0 & 0 \cdots 0 & 0 & 0 \end{bmatrix},$$

with zeroes representing the zero maps in the appropriate spaces, and

$$\begin{aligned} \overline{\Omega}_{11} &= H_2 A_1 * I_{\ell_v^1} \tilde{Q}^{-1}(A_1) \mathbf{e}_0 I_{\mathbb{C}^d} - H_2 A_1^{N_1} * \pi^{N_2} \tilde{Q}^{-1}(A_1) \mathbf{e}_0 I_{\mathbb{C}^d} \\ &= \overline{\Lambda}_{11} \\ \overline{\Omega}_{1+} &= H_2 B_1 * I_{\ell_v^1} - H_2 B_1^{N_1} * \pi^{N_2} + H_2 (A_1 * I_{\ell_v^1} - A_1^{N_1} * \pi^{N_2}) \tilde{Q}^{-1}(A_1) \pi^{N_2} H_1 B_1^{N_1} * \pi^{N_2} \\ &= \overline{\Lambda}_{12} \\ \overline{\Omega}_{21} &= (I_{\ell_v^1} - Q(A_1) \tilde{Q}^{-1}(A_1)) \mathbf{e}_0 \\ &= \overline{\Lambda}_{21} \\ \overline{\Omega}_{2+} &= H_1 B_1 * I_{\ell_v^1} - Q(A_1) \tilde{Q}^{-1}(A_1) \pi^{N_2} H_1 B_1^{N_1} * \pi^{N_2} \\ &= \overline{\Lambda}_{22} \end{aligned}$$

where the $\overline{\Lambda}_{ij}$ are the same as those appearing in the proof of Theorem 6.1.2. The conclusion then follows by the same estimates as in the proof of the aforementioned, together with the bound for the norm of $C_2 S^* \pi_{N_2}^\infty$ being supplied by row 7 of Table A. \square

6.3 Bounds in the case $1 < p < q$

In this final subsection we will compute the bounds c_2 and c_3 in the final case, where $1 < p < q$. This case will be a fair bit more involved than the previous ones and the bounds are significantly more complicated. Like in the last section, we write $I - W$ using (38) and the representations of Sect. 4.4. Making use of the short form $L\phi_j := (L\phi)_j$ and $L\phi(0) := (L\phi)(0)$ for a linear operator $L : X_v \rightarrow X_v$,

$$(I - W)\phi = \begin{bmatrix} (I - W)\phi(0) \\ (I - W)\phi_0 \\ (I - W)\phi_{-1} \\ \vdots \\ (I - W)\phi_{2-p} \\ (I - W)\phi_{1-p} \\ (I - W)\phi_{-p} \\ \vdots \\ (I - W)\phi_{1-q} \end{bmatrix} = \begin{bmatrix} \phi(0) - (I + C_1)H_2 A_p * \phi_0 - (I + C_1)S\phi_{-1} \\ Q_p \phi_0 - \mathbf{e}_0 S\phi_{-1} \\ Q_{p-1} \phi_{-1} - \mathbf{e}_0 S\phi_{-2} \\ \vdots \\ Q_2 \phi_{2-p} - \mathbf{e}_0 S\phi_{1-p} \\ Q_1 \phi_{1-p} \\ \phi_{-p} \\ \vdots \\ \phi_{1-q} \end{bmatrix}, \tag{79}$$

$$(I - W_{N_1, N_2})\phi = \begin{bmatrix} (I - W_{N_1, N_2})\phi(0) \\ (I - W_{N_1, N_2})\phi_0 \\ (I - W_{N_1, N_2})\phi_{-1} \\ \vdots \\ (I - W_{N_1, N_2})\phi_{2-p} \\ (I - W_{N_1, N_2})\phi_{1-p} \\ (I - W_{N_1, N_2})\phi_{-p} \\ \vdots \\ (I - W_{N_1, N_2})\phi_{1-q} \end{bmatrix} = \begin{bmatrix} \phi(0) - (I + C_1)H_2 A_p^{N_1} * \phi_0 - (I + C_1)S\pi^{N_2} \phi_{-1} \\ \tilde{Q}_p \phi_0 - \mathbf{e}_0 S\pi^{N_2} \phi_{-1} \\ \tilde{Q}_{p-1} \phi_{-1} - \mathbf{e}_0 S\pi^{N_2} \phi_{-2} \\ \vdots \\ \tilde{Q}_2 \phi_{2-p} - \mathbf{e}_0 S\pi^{N_2} \phi_{1-p} \\ \tilde{Q}_1 \phi_{1-p} \\ \phi_{-p} \\ \vdots \\ \phi_{1-q} \end{bmatrix}, \tag{80}$$

where we denote $Q_j = Q(A_j)$ and $\tilde{Q}_j = \tilde{Q}(A_j)$. Similarly, we can write down the explicit part operator E and define the truncation E_{N_1, N_2} .

$$\begin{bmatrix} E\phi(0) \\ E\phi_0 \\ E\phi_{-1} \\ \vdots \\ E\phi_{2-p} \\ E\phi_{1-p} \\ E\phi_{-p} \\ E\phi_{-p-1} \\ \vdots \\ E\phi_{1-q} \end{bmatrix} = \begin{bmatrix} C_2 S^* \phi_{1+p-q} + (I + C_1) H_2 B_p * I_{\ell_v^1} \phi_{p-q} \\ H_1 B_p * I_{\ell_v^1} \phi_{p-q} \\ H_1 B_{p-1} * I_{\ell_v^1} \phi_{p-q-1} \\ \vdots \\ H_1 B_2 * I_{\ell_v^1} \phi_{2-q} \\ \mathbf{e}_0 \phi(0) + H_1 B_1 * I_{\ell_v^1} \phi_{1-q} \\ \phi_0 \\ \phi_{-1} \\ \vdots \\ \phi_{1-(q-p)} \end{bmatrix}, \tag{81}$$

$$\begin{bmatrix} E_{N_1, N_2} \phi(0) \\ E_{N_1, N_2} \phi_0 \\ E_{N_1, N_2} \phi_{-1} \\ \vdots \\ E_{N_1, N_2} \phi_{2-p} \\ E_{N_1, N_2} \phi_{1-p} \\ E_{N_1, N_2} \phi_{-p} \\ E_{N_1, N_2} \phi_{-p-1} \\ \vdots \\ E_{N_1, N_2} \phi_{1-q} \end{bmatrix} = \begin{bmatrix} C_2 S^* \pi^{N_2} \phi_{1+p-q} + (I + C_1) H_2 B_p^{N_1} * \pi^{N_2} \phi_{p-q} \\ \pi^{N_2} H_1 B_p^{N_1} * \pi^{N_2} \phi_{p-q} \\ \pi^{N_2} H_1 B_{p-1}^{N_1} * \pi^{N_2} \phi_{p-q-1} \\ \vdots \\ \pi^{N_2} H_1 B_2^{N_1} * \pi^{N_2} \phi_{2-q} \\ \mathbf{e}_0 \phi(0) + \pi^{N_2} H_1 B_1^{N_1} * \pi^{N_2} \phi_{1-q} \\ \phi_0 \\ \phi_{-1} \\ \vdots \\ \phi_{1-(q-p)} \end{bmatrix}. \tag{82}$$

Note that here we are using the short form $L\phi_j := (L\phi)_j$ and $L\phi(0) := (L\phi)(0)$ for $L \in \{E, E_{N_1, N_2}\}$.

Remark 6.3.1 When we want to use the computer to calculate eigenvalues of our impulsive delay differential equation, we implement the matrix representation of the restriction of the linear operator $M_{N_1, N_2} = (I - W_{N_1, N_2})^{-1} E_{N_1, N_2}$ to the finite-dimensional vector space $X_v^{N_2}$.

Lemma 6.3.1 (Truncated monodromy operator, $1 < p < q$) Define $M_{N_1, N_2} = (I - W_{N_1, N_2})^{-1} E_{N_1, N_2}$. Suppose ϕ is an eigenvector of M_{N_1, N_2} with eigenvalue λ . If $\lambda \neq 0$ then with $\phi = \phi^{N_2} + \phi^\infty$, we have $\phi^\infty = 0$. Also, each of X_v^∞ and $X_v^{N_2}$ is an invariant subspace for M_{N_1, N_2} and for $r > 0$ we have

$$\|(M_{N_1, N_2} - r e^{i\theta})^{-1}\|_{B(X_v^\infty)} \leq \max \left\{ \frac{1}{r}, \frac{1 - r^{-\lfloor q/p \rfloor}}{r - 1} \right\}$$

unless $r = 1$, in which case $\|(M_{N_1, N_2} - r e^{i\theta})^{-1}\|_{B(X_v^\infty)} \leq 1$. If $\lambda \in \mathbb{C}$, $0 < r < |\lambda|$ and $0 < \omega < \pi$, then for $U \in \{D_r(\lambda), R_\lambda(r, \omega)\}$,

$$\sup_{z \in \partial B_\lambda(r, \omega)} \|(M_{N_1, N_2} - zI)^{-1}\|_{B(X_v^\infty)} \leq \max \left\{ \frac{1}{|\lambda| - r}, \frac{1 - (|\lambda| - r)^{-\lfloor q/p \rfloor}}{|\lambda| - r - 1} \right\}.$$

Proof The assertions concerning the eigenvalues, eigenvectors and invariant subspaces follow directly from the definition of E_{N_1, N_2} and $(I - W_{N_1, N_2})$. Indeed, it is easy to verify that each

of $X_v^{N_2}$ and X_v^∞ are invariant subspaces for $I - W_{N_1, N_2}$ and its inverse. As for the bound, one can verify directly that if ϕ^∞ and h^∞ satisfy $(M_{N_1, N_2} - re^{i\theta})\phi^\infty = h^\infty$, then

$$\begin{aligned} 0 &= h_k^\infty - re^{i\theta}\phi_k^\infty, & 1 - p \leq k \leq 0 \\ \phi_{k+p}^\infty &= h_k^\infty - re^{i\theta}\phi_k^\infty, & 1 - q \leq k \leq -p \end{aligned}$$

If $\|h^\infty\|_{X_v} \leq 1$ then $\|\phi_k^\infty\|_v \leq \frac{1}{r}$ for $1 - p \leq k \leq 0$, and for $1 - q \leq k \leq -p$, we have

$$\|\phi_k^\infty\|_v \leq \frac{1}{r} \left(1 + \|\phi_{k+p}^\infty\|_v \right).$$

If $r = 1$ we get $\|\phi_k^\infty\|_v \leq 1$ for $k = 1 - q, \dots, 0$. Otherwise, observe that $\|\phi_k^\infty\|_v \leq x_k$, where

$$x_k = \frac{1}{r}(1 + x_{k+p}), \quad 1 - q \leq k \leq -p,$$

with $x_0 = \dots = x_{1-p} = r^{-1}$. It is easy to verify by induction that this sequence is nonincreasing and therefore reaches its maximum at $k = 1 - q$. Also, since the initial conditions x_0, \dots, x_{1-p} are equal, we have $x_{k+jp} = x_k$ for integers $j \leq 0$ and $k \in \{1 - p, \dots, 0\}$. Consequently,

$$x_{k+(j-1)p} = \frac{1}{r}(1 + x_{k+jp}) \Rightarrow x_{k+jp} = \frac{1 - r^{j-1}}{r - 1} := w(j).$$

Since $j^* = 1 - \lfloor q/p \rfloor$ is the most negative integer such that $k + j^*p \geq 1 - q$ for some $k \in \{1 - p, \dots, 0\}$, we conclude $\|\phi^\infty\|_v \leq \max\{1/r, w(j^*)\}$. The proof for the radial sector and closed ball are similar. □

Lemma 6.3.2 *Let $N_1, N_2 > 0$ and suppose $(I - W_{N_1, N_2})^{-1}(I - W)f = \phi$ for some $f, \phi \in X_v$. Denote $Q_j = Q(A_j)$ and $\tilde{Q}_j = \tilde{Q}(A_j)$. Then $\phi_k = f_k$ for $1 - q \leq k \leq -p$ and*

$$\begin{aligned} \phi_{n-p} &= \tilde{Q}_n^{-1} Q_n f_{n-p} + \tilde{Q}_n^{-1} \sum_{k=1}^{n-1} \left(\prod_{j=k+1}^{n-1} \mathbf{e}_0 S \pi^{N_2} \tilde{Q}_j^{-1} \right) \\ &\quad \mathbf{e}_0 \left(S \pi^{N_2} \tilde{Q}_k^{-1} Q_k - S \right) f_{k-p}, \quad n = 1, \dots, p \end{aligned} \tag{83}$$

$$\begin{aligned} \phi(0) &= f(0) - (I + C_1)H_2(A_p * f_0 - A_p^{N_1} * \pi^{N_2}\phi_0) \\ &\quad - (I + C_1)S(f_{-1} - \pi^{N_2}\phi_{-1}) \end{aligned} \tag{84}$$

where product denotes composition from right to left (bottom to top index), the empty product is defined to be the identity and the empty sum to be zero.

Proof The assertion that $\phi_k = f_k$ for $1 - q \leq k \leq -p$ is clear. We next prove the formula for ϕ_{n-p} for $n = 1, \dots, p$. The definition of ϕ and f is equivalent to having

$$(I - W)f = (I - W_{N_1, N_2})\phi.$$

We prove this by induction. Starting with $n = 1$, using (79)–(80) with the above equation implies $Q_1 f_{1-p} = \tilde{Q}_1 \phi_{1-p}$ and consequently, $\phi_{1-p} = \tilde{Q}_1^{-1} Q_1 f_{1-p}$. This is consistent with (83). Taking an inductive step, if $n \geq 1$ we can again use the above equation together with the explicit expressions (79)–(80) to get

$$Q_{n+1} f_{n+1-p} - \mathbf{e}_0 S f_{n-p} = \tilde{Q}_{n+1} \phi_{n+1-p} - \mathbf{e}_0 S \pi^{N_2} \phi_{n-p}.$$

Solving for ϕ_{n+1-p} , we have

$$\begin{aligned} \phi_{n+1-p} &= \tilde{Q}_{n+1}^{-1} \left(Q_{n+1} f_{n+1-p} - \mathbf{e}_0 S f_{n-p} + \mathbf{e}_0 S \pi^{N_2} \phi_{n-p} \right) \\ &= \tilde{Q}_{n+1}^{-1} Q_{n+1} f_{n+1-p} + \tilde{Q}_{n+1}^{-1} \left(-\mathbf{e}_0 S f_{n-p} + \mathbf{e}_0 S \pi^{N_2} \tilde{Q}_n^{-1} Q_n f_{n-p} + \dots \right. \\ &\quad \left. \mathbf{e}_0 S \pi^{N_2} \tilde{Q}_n^{-1} \sum_{k=1}^{n-1} \left(\prod_{j=k+1}^{n-1} \mathbf{e}_0 S \pi^{N_2} \tilde{Q}_j^{-1} \right) \mathbf{e}_0 \left(S \pi^{N_2} \tilde{Q}_k^{-1} Q_k - S \right) f_{k-p} \right) \\ &= \tilde{Q}_{n+1}^{-1} Q_{n+1} f_{n+1-p} + \tilde{Q}_{n+1}^{-1} \left(\mathbf{e}_0 (S \pi^{N_2} \tilde{Q}_n^{-1} Q_n - S) f_{n-p} \right) + \dots \\ &\quad \tilde{Q}_{n+1}^{-1} \left(\sum_{k=1}^{n-1} \left(\prod_{j=k+1}^n \mathbf{e}_0 S \pi^{N_2} \tilde{Q}_j^{-1} \right) \mathbf{e}_0 \left(S \pi^{N_2} \tilde{Q}_k^{-1} Q_k - S \right) f_{k-p} \right) \\ &= \tilde{Q}_{n+1}^{-1} Q_{n+1} f_{n+1-p} \\ &\quad + \tilde{Q}_{n+1}^{-1} \left(\sum_{k=1}^n \left(\prod_{j=k+1}^n \mathbf{e}_0 S \pi^{N_2} \tilde{Q}_j^{-1} \right) \mathbf{e}_0 \left(S \pi^{N_2} \tilde{Q}_k^{-1} Q_k - S \right) f_{k-p} \right), \end{aligned}$$

which is precisely (83) at index $n + 1$. To get Eq. (84) for $\phi(0)$ one uses the same strategy, except we have left the result implicit. \square

Lemma 6.3.3 *Let $N_1, N_2 > 0$ and suppose $(I - W)(I - W_{N_1, N_2})^{-1} f = \phi$ for some $f, \phi \in X_\nu$. Denote $Q_j = Q(A_j)$ and $\tilde{Q}_j = \tilde{Q}(A_j)$. Then $\phi_k = f_k$ for $1 - q \leq k \leq -p$ and*

$$\begin{aligned} \phi_{n-p} &= Q_n \tilde{Q}_n^{-1} f_{n-p} + (Q_n \tilde{Q}_n^{-1} \mathbf{e}_0 S \pi^{N_2} - \mathbf{e}_0 S) \\ &\quad \tilde{Q}_{n-1}^{-1} \sum_{k=1}^{n-1} \left(\prod_{j=k}^{n-2} \mathbf{e}_0 S \pi^{N_2} \tilde{Q}_j^{-1} \right) f_{k-p}, \quad n = 1, \dots, p \end{aligned} \tag{85}$$

$$\begin{aligned} \phi(0) &= f(0) - (I + C_1) H_2 (A_p * I_{\ell_1^1} - A_p^{N_1} * \pi^{N_2}) \\ &\quad \tilde{Q}_p^{-1} \sum_{k=1}^p \left(\prod_{j=k}^{p-1} \mathbf{e}_0 S \pi^{N_2} \tilde{Q}_j^{-1} \right) f_{k-p} - (I + C_1) S \pi_{N_2}^\infty f_{-1} \end{aligned} \tag{86}$$

where product denotes composition from right to left (bottom to top index), the empty product is defined to be the identity and the empty sum to be zero.

Proof The proof here is similar to the one for Lemma 6.3.2, so we will provide only an outline. Set $z = (I - W_{N_1, N_2})^{-1} f$. Then $z_k = f_k$ for $1 - q \leq k \leq -p$, and using (80) one can prove by induction that

$$\begin{aligned} z_{n-p} &= \tilde{Q}_n^{-1} \sum_{k=1}^n \left(\prod_{j=k}^{n-1} \mathbf{e}_0 S \pi^{N_2} \tilde{Q}_j^{-1} \right) f_{k-p}, \quad n = 1, \dots, p \\ z(0) &= f(0) + (I + C_1) (H_2 A_p^{N_1} * \pi^{N_2} f_0 + S \pi^{N_2} f_{-1}). \end{aligned}$$

Next, one computes $\phi = (I - W)(I - W_{N_1, N_2})^{-1} f = (I - W)z$ using (79) and the above expressions. The result is $\phi_k = f_k$ for $1 - q \leq k \leq -p$ and (85) for $n = 1, \dots, p$, while

$$\phi(0) = z(0) - (I + C_1) (H_2 A_p * I_{\ell_1^1} z_0 + S z_{-1})$$

$$\begin{aligned} &= f(0) + (I + C_1)(H_2 A_p^{N_1} * \pi^{N_2} z_0 + S \pi^{N_2} z_{-1}) - (I + C_1)(H_2 A_p * I_{\ell_v^1} z_0 + S z_{-1}) \\ &= f(0) - (I + C_1)(H_2 A_p * I_{\ell_v^1} - H_2 A_p^{N_1} * \pi^{N_2}) z_0 - (I + C_1)(S - S \pi^{N_2}) z_{-1} \\ &= f(0) - (I + C_1)(H_2 A_p * I_{\ell_v^1} - H_2 A_p^{N_1} * \pi^{N_2}) z_0 - (I + C_1) S \pi_{N_2}^\infty z_{-1}. \end{aligned}$$

We obtain (86) by substituting z_0 and z_{-1} into the above, but we will point out one subtlety. Since $\pi_{N_2}^\infty \tilde{Q}_n^{-1} \pi_{N_2}^\infty$ —see Lemma 5.1.2—we have

$$\pi_{N_2}^\infty z_{-1} = \pi_{N_2}^\infty \tilde{Q}_{p-1}^{-1} \sum_{k=1}^{p-1} \left(\prod_{j=k}^{p-2} \mathbf{e}_0 S \pi^{N_2} \tilde{Q}_j^{-1} \right) f_{k-p} = \pi_{N_2}^\infty f_{-1},$$

since all terms in the summation except for the $p - 1$ term contain a \mathbf{e}_0 on the extreme left, which maps into $\pi^{N_2}(\ell_v^1)$, while for the $p - 1$ term the product collapses to the trivial product (identity). □

Theorem 6.3.1 (*c₂ bound, $1 < p < q$*) *Let $N_2 > N_1 \geq 0$. For $m = 1, \dots, p$, define $A_m^{N_1} = (A_{m,0}, \dots, A_{m,N_1}, 0, \dots)$, $A_m^\infty = A_m - A_m^{N_1}$,*

$$\begin{aligned} K_{0,m} &= \max_{k=0,\dots,N_2} \frac{1}{v^k} \sum_{n=0}^{N_2} \|\tilde{Q}_{n,k}^{-1}(A_m^{N_1})\| v^n, & K_{0,m}^0 &= \sum_{n=0}^{N_2} \|\tilde{Q}_{n,0}^{-1}(A_m^{N_1})\| \\ K_{0,m}^{S,k} &= \|\tilde{Q}_{0,k}^{-1}(A_m^{N_1})\| + 2 \sum_{n=1}^{N_2} \|\tilde{Q}_{n,k}^{-1}(A_m^{N_1})\|, & 0 \leq k \leq N_2 \\ K_{0,m}^{S,k,\odot} &= \|(I + C_1)\tilde{Q}_{0,k}^{-1}(A_m^{N_1})\| + 2 \sum_{n=1}^{N_2} \|(I + C_1)\tilde{Q}_{n,k}^{-1}(A_m^{N_1})\|, & 0 \leq k \leq N_2 \\ K_{0,m}^{S,*} &= \max_{k=0,\dots,N_2} \frac{1}{v^k} K_{0,m}^{S,k}, & K_{0,m}^{S,*,\odot} &= \max_{k=0,\dots,N_2} \frac{1}{v^k} K_{0,m}^{S,k,\odot} \\ K_{0,p}^\odot &= \max_{k=0,\dots,N_2} \frac{1}{v^k} \sum_{j=0}^{N_2} \|(I + C_1)\tilde{Q}_{j,k}^{-1}(A_p^{N_1})\| v^j \\ K_{1,m} &= \max_{k=0,\dots,N_1} \frac{1}{v^{N_2+1+k}} \sum_{j=0}^{N_2} \left(\frac{\|A_m^{N_1}\|_\omega}{(N_2 + 1 - N_1)^2 - 1} \|\tilde{Q}_{j,0}^{-1}(A_m^{N_1})\| \right. \\ &\quad \left. + \|\tilde{Q}_j^{-1}(A_m^{N_1})\mathbf{DT}\tilde{Z}_k^{N_1,N_2}\mathbf{S}(A_m^{N_1})\| \right) v^j \\ \mathbf{m}_{j,k}^{(m)} &= \frac{\|A_m^{N_1}\|_\omega}{(N_2 + 1 - N_1)^2 - 1} \|(I + C_1)\tilde{Q}_{j,0}^{-1}(A_m^{N_1})\| + \|(I + C_1)\tilde{Q}_j^{-1}(A_m^{N_1})\mathbf{DT}\tilde{Z}_k^{N_1,N_2}\mathbf{S}(A_m^{N_1})\|, \\ K_{1,m}^\odot &= \max_{k=0,\dots,N_1} \frac{1}{v^{N_2+1+k}} \sum_{j=0}^{N_2} \mathbf{m}_{j,k}^{(m)} v^j \\ K_{2,p} &= \max_{k=0,\dots,N_1} \frac{1}{v^{N_2+1+k}} \mathbf{m}_{j,0}^{(p)} + \sum_{j=2}^{N_2} \frac{(-1)^j + 1}{j^2 - 1} \left(\max_{k=0,\dots,N_1} \frac{1}{v^{N_2+1+k}} \mathbf{m}_{j,k}^{(p)} \right) \\ J_0(A_m^{N_1}) &= \max_{k=0,\dots,N_2} \frac{1}{v^k} \sum_{j=N_2}^{N_2+N_1} \|\mathbf{G}(A_m^{N_1}, i \circ I_{\mathbb{C}^d(N_2+1)})_{j,k}\| v^j \\ \alpha(A_m^{N_1}) &= \frac{1}{4(N_2 + 1)} \left(\left(v + \frac{2}{v} + \frac{1}{v^3} \right) \|A_m^{N_1}\|_v - \left(\frac{1}{v} + \frac{1}{v^3} \right) \|A_{m,0}^{N_1}\| \right) \\ \beta_m &= \max \left\{ J_0(A_m^{N_1}), K_{1,m} + \alpha(A_m^{N_1}) + K_{0,m}^0 \sum_{k=1}^{m-1} \left(\prod_{j=k+1}^{m-1} K_{0,j}^{S,0} \right) \right\} \end{aligned}$$

$$\begin{aligned}
 & \cdot \left(\frac{2}{\nu^{N_2+1}} + \max\{1, 2\nu^{-1}\}K_{1,k} \right) \Big\} \\
 \eta_m &= \frac{2}{\nu^{N_2+1}} + \max\{1, 2\nu^{-1}\}K_{1,m} + K_{0,m}^{S,*} \left(1 + \frac{\nu}{2}\right) \|A_m^\infty\|_\omega \\
 \rho_m &= \left(K_{0,m} \left(1 + \frac{\nu}{2}\right) + \frac{\nu + \nu^{-1}}{2(N_2 + 1)} \right) \|A_m^\infty\|_\omega \\
 &+ K_{0,m}^0 \sum_{k=1}^{m-1} \left(\prod_{j=k+1}^{m-1} K_{0,j}^{S,0} \right) K_{0,k}^{S,*} \left(1 + \frac{\nu}{2}\right) \|A_k^\infty\|_\omega + \beta_m \\
 \\
 \rho^{N_2}(0) &= 2g(\nu)\|I + C_1\| \cdot \|A_p^\infty\|_\omega + 2g(\nu)\|(I + C_1) \odot A_p^{N_1}\|_\omega \\
 &+ K_{0,p}^0 \sum_{k=1}^{p-1} \left(\prod_{j=k+1}^{p-1} K_{0,j}^{S,0} \right) K_{0,k}^{S,*} \left(1 + \frac{\nu}{2}\right) \|A_k^\infty\|_\omega \\
 &+ K_{0,p-1}^{S,* \odot} \left(1 + \frac{\nu}{2}\right) \sum_{k=1}^{p-1} \left(\prod_{j=k+1}^{p-2} K_{0,j}^{S,0} \right) K_{0,k}^{S,*} \|A_k^\infty\|_\omega \\
 \rho^\infty(0) &= \frac{2\|(I + C_1) \odot A_p^{N_1}\|_\nu}{\nu^{N_2+1}} + K_{2,p} + \frac{2\|I + C_1\|}{\nu^{N_2+1}} \\
 &+ \max\{1, 2\nu^{-1}\}K_{1,p-1}^\odot + K_{0,p-1}^{S,* \odot} \left(1 + \frac{\nu}{2}\right) \|A_{p-1}^\infty\|_\omega \\
 &+ 2g(\nu)\|(I + C_1) \odot A_p^{N_1}\|_\omega \sum_{k=1}^{p-1} \left(\prod_{j=k+1}^{p-1} K_{0,j}^{S,0} \right) \cdot \eta_k + K_{0,p-1}^{S,0 \odot} \sum_{k=1}^{p-2} \left(\prod_{j=k+1}^{p-2} K_{0,j}^{S,0} \right) \cdot \eta_k \\
 \rho(0) &= g(\nu)K_{0,p}^\odot \left(1 + \frac{\nu}{2}\right) \|A_p^\infty\|_\omega + \max\{\rho^{N_2}(0), \rho^\infty(0)\}
 \end{aligned}$$

With $\rho := \max\{\rho(0), \rho_1, \dots, \rho_p\}$, the operator $I - W$ satisfies $\|(I - W)^{-1}\|_{B(X_\nu)} \leq c_2$ with

$$c_2 := \frac{\|(I_{X_\nu} - W_{N_1, N_2})^{-1}\|_{B(X_\nu)}}{1 - \rho} = \frac{\max\{1, \|(I - W_{N_1, N_2})^{-1}\|_{B(X_\nu^{N_2})}\}}{1 - \rho}. \tag{87}$$

Proof Define $\Lambda = I - (I - W_{N_1, N_2})^{-1}(I - W)$. Let $h \in X_\nu$ satisfy $\|h\|_{X_\nu} \leq 1$. By Lemma 6.3.2, we have $(\Lambda h)_k = 0$ for $1 - q \leq k \leq -p$, while for $n = 1, \dots, p$,

$$\begin{aligned}
 (\Lambda h)_{n-p} &= (I - \tilde{Q}_n^{-1} Q_n)h_{n-p} + \tilde{Q}_n^{-1} \sum_{k=1}^{n-1} \left(\prod_{j=k+1}^{n-1} \mathbf{e}_0 S \pi^{N_2} \tilde{Q}_j^{-1} \right) \\
 &\quad \mathbf{e}_0 (S - S \pi^{N_2} \tilde{Q}_k^{-1} Q_k) h_{k-p} \\
 &= (I - \tilde{Q}_n^{-1} Q_n)h_{n-p} + \tilde{Q}_n^{-1} \mathbf{e}_0 \sum_{k=1}^{n-1} \left(\prod_{j=k+1}^{n-1} S \pi^{N_2} \tilde{Q}_j^{-1} \mathbf{e}_0 \right) \\
 &\quad S(\pi_{N_2}^\infty + \pi^{N_2}(I - \tilde{Q}_k^{-1} Q_k))h_{k-p}.
 \end{aligned}$$

We separately majorize in norm for $h \in X_\nu^{N_2}$ and $h \in X_\nu^\infty$. From Lemma 5.1.3, we can decompose as follows:

$$(\Lambda \pi^{N_2} h)_{n-p} = (I - \tilde{Q}_n^{-1} Q_n) \pi^{N_2} h_{n-p} + \tilde{Q}_n^{-1} \mathbf{e}_0 \sum_{k=1}^{n-1} \left(\prod_{j=k+1}^{n-1} S \pi^{N_2} \tilde{Q}_j^{-1} \mathbf{e}_0 \right)$$

$$\begin{aligned}
 & S(\tilde{Q}_k^{-1} \pi^{N_2} H_1(A_k^\infty * \pi^{N_2})) h_{k-p} \\
 (\Lambda \pi_{N_2}^\infty h)_{n-p} &= (I - \tilde{Q}_n^{-1} Q_n) \pi_{N_2}^\infty h_{n-p} + \tilde{Q}_n^{-1} \mathbf{e}_0 \sum_{k=1}^{n-1} \left(\prod_{j=k+1}^{n-1} S \pi^{N_2} \tilde{Q}_j^{-1} \mathbf{e}_0 \right) \\
 & S(\pi_{N_2}^\infty + \tilde{Q}_k^{-1} \pi^{N_2} (H_1(A_k * \pi_{N_2}^\infty))) h_{k-p}.
 \end{aligned}$$

Bounding each of $(I - \tilde{Q}_n^{-1} Q_n) \pi_{N_2}^\infty$ and $(I - \tilde{Q}_n^{-1} Q_n) \pi_{N_2}^\infty$ can be accomplished in the same way as in the proof of Theorem 6.1.1; see (72) and (73). We have $\|\tilde{Q}_n^{-1} \mathbf{e}_0\| \leq K_{0,n}^0$ by row 9 of the table, while row 11 gives the estimate $\|S \pi^{N_2} \tilde{Q}_j^{-1} \mathbf{e}_0\| \leq K_{0,j}^{S,0}$. As for the remaining terms, row 3, 5, 6, 10 and 12 give

$$\begin{aligned}
 \|S(\tilde{Q}_k^{-1} \pi^{N_2} H_1(A_k^\infty * \pi^{N_2}))\| &\leq K_{0,k}^{S,*} \left(1 + \frac{\nu}{2}\right) \|A_k^\infty\|_\omega, \\
 \|S(\pi_{N_2}^\infty + \tilde{Q}_k^{-1} \pi^{N_2} (H_1(A_k * \pi_{N_2}^\infty)))\| &\leq \frac{2}{\nu^{N_2+1}} + \max\{1, 2\nu^{-1}\} K_{1,k} \\
 &\quad + K_{0,k}^{S,*} \left(1 + \frac{\nu}{2}\right) \|A_k^\infty\|_\omega.
 \end{aligned}$$

Combining the previous estimates, we apply (60) to get $\|(\Lambda h)_{n-p}\|_\nu \leq \rho_n$.

Also using Lemma 6.3.2, writing $(\Lambda h)(0) = (I + C)(\bar{\Lambda} h)(0)$, we have

$$\begin{aligned}
 (\bar{\Lambda} h)(0) &= H_2 \left(A_p * h_0 - A_p^{N_1} * \pi^{N_2} \left(\tilde{Q}_p^{-1} Q_p h_0 + \tilde{Q}_p^{-1} \sum_{k=1}^{p-1} \left(\prod_{j=k+1}^{p-1} \right. \right. \right. \\
 &\quad \left. \left. \left. \mathbf{e}_0 S \pi^{N_2} \tilde{Q}_j^{-1} \right) \mathbf{e}_0 (S \pi^{N_2} \tilde{Q}_k^{-1} Q_k - S) h_{k-p} \right) \right) \\
 &\quad + S \left(h_{-1} - \pi^{N_2} \tilde{Q}_{p-1}^{-1} Q_{p-1} h_{-1} - \tilde{Q}_{p-1}^{-1} \sum_{k=1}^{p-2} \left(\prod_{j=k+1}^{p-2} \right. \right. \right. \\
 &\quad \left. \left. \left. \mathbf{e}_0 S \pi^{N_2} \tilde{Q}_j^{-1} \right) \mathbf{e}_0 (S \pi^{N_2} \tilde{Q}_k^{-1} Q_k - S) h_{k-p} \right) \\
 &= H_2 \left(A_p^\infty * h_0 + A_p^{N_1} * \pi^{N_2} (I - \tilde{Q}_p^{-1} Q_p) h_0 + A_p^{N_1} * \pi_{N_2}^\infty h_0 \right) \\
 &\quad + S(\pi_{N_2}^\infty + \pi^{N_2} (I - \tilde{Q}_{p-1}^{-1} Q_{p-1})) h_{-1} \\
 &\quad + H_2 \left(A_p^{N_1} * \tilde{Q}_p^{-1} \mathbf{e}_0 \left(\sum_{k=1}^{p-1} \left(\prod_{j=k+1}^{p-1} S \pi^{N_2} \tilde{Q}_j^{-1} \mathbf{e}_0 \right) S(\pi_{N_2}^\infty + \pi^{N_2} (I - \tilde{Q}_k^{-1} Q_k)) h_{k-p} \right) \right) \\
 &\quad + S \left(\tilde{Q}_{p-1}^{-1} \mathbf{e}_0 \sum_{k=1}^{p-2} \left(\prod_{j=k+1}^{p-2} S \pi^{N_2} \tilde{Q}_j^{-1} \mathbf{e}_0 \right) S(\pi_{N_2}^\infty + \pi^{N_2} (I - \tilde{Q}_k^{-1} Q_k)) h_{k-p} \right)
 \end{aligned}$$

We can bound this term in norm using much the same estimates as before. The only differences are that we will need to use (56) to commute $(I + C_1)$ through the operator H_2 , while a bound for

$$\left\| (I + C_1) H_2 \left(A_p^\infty * h_0 + A_p^{N_1} * \pi^{N_2} (I - \tilde{Q}_p^{-1} Q_p) h_0 + A_p^{N_1} * \pi_{N_2}^\infty h_0 \right) \right\|$$

can be constructed by observing that the quantity being bounded symbolically coincides (except for a single projector, which does not effect the norm) with $(I + C_1) \Lambda_{12}$ from the proof of Theorem 6.1.1, so (74) can be re-used. In total, we get

$$\begin{aligned}
 \|\Lambda \pi^{N_2} h\| &\leq g(\nu) K_{0,p}^\odot \left(1 + \frac{\nu}{2}\right) \|A_p^\infty\|_\omega + 2g(\nu) \|I + C_1\| \cdot \|A_p^\infty\|_\omega + 2g(\nu) \|(I + C_1) \odot A_p^{N_1}\|_\omega \\
 &\quad + K_{0,p}^0 \sum_{k=1}^{p-1} \left(\prod_{j=k+1}^{p-1} K_{0,j}^{S,0} \right) K_{0,k}^{S,*} \left(1 + \frac{\nu}{2}\right) \|A_k^\infty\|_\omega
 \end{aligned}$$

$$\begin{aligned}
 &+ K_{0,p-1}^{S,*,\odot} \left(1 + \frac{\nu}{2}\right) \sum_{k=1}^{p-1} \left(\prod_{j=k+1}^{p-2} K_{0,j}^{S,0}\right) K_{0,k}^{S,*} \|A_k^\infty\|_\omega \\
 \|\Delta \pi_{N_2}^\infty h\| &\leq g(\nu) K_{0,p}^\odot \left(1 + \frac{\nu}{2}\right) \|A_p^\infty\|_\omega + \frac{2\|(I + C_1) \odot A_p^{N_1}\|_\nu}{\nu^{N_2+1}} \\
 &+ K_{2,p} + \frac{2\|I + C_1\|}{\nu^{N_2+1}} + \max\{1, 2\nu^{-1}\} K_{1,p-1}^\odot \\
 &+ K_{0,p-1}^{S,*,\odot} \left(1 + \frac{\nu}{2}\right) \|A_{p-1}^\infty\|_\omega + K_{0,p-1}^{S,0,\odot} \sum_{k=1}^{p-2} \left(\prod_{j=k+1}^{p-2} K_{0,j}^{S,0}\right) \\
 &\left(\frac{2}{\nu^{N_2+1}} + \max\{1, 2\nu^{-1}\} K_{1,k} + K_{0,k}^{S,*} \left(1 + \frac{\nu}{2}\right) \|A_k^\infty\|_\omega\right) \\
 &+ 2g(\nu) \|(I + C_1) \odot A_p^{N_1}\|_\omega \sum_{k=1}^{p-1} \left(\prod_{j=k+1}^{p-1} K_{0,j}^{S,0}\right) \\
 &\left(\frac{2}{\nu^{N_2+1}} + \max\{1, 2\nu^{-1}\} K_{1,k} + K_{0,k}^{S,*} \left(1 + \frac{\nu}{2}\right) \|A_k^\infty\|_\omega\right)
 \end{aligned}$$

We then get $\|\Delta h(0)\| \leq \rho(0)$ and taking into account (60), we conclude $\|\Delta\|_{B(X_\nu)} \leq \rho$. The rest of the proof is nearly identical to the proof of Theorem 6.1.1. Verifying that

$$\|(I_{X_\nu} - W_{N_1, N_2})^{-1}\|_{B(X_\nu)} \leq \max\{1, \|(I - W_{N_1, N_2})^{-1} \pi^{N_2}\|_{B(X_\nu^{N_2})}\}$$

is clear by definition of W_{N_1, N_2} . □

Theorem 6.3.2 (*c₃ bound, 1 < p < q*) *Let $N_2 > N_1 \geq 0$. For $j = 1, \dots, p$, define $A_m^{N_1} = (A_{m,0}, \dots, A_{m,N_1}, 0, \dots)$, $A_m^\infty = A_m - A_m^{N_1}$, $B_m^{N_1} = (B_{m,0}, \dots, B_{m,N_1}, 0, \dots)$ and $B_m^\infty = B_m - B_m^{N_1}$. Let $\mathbf{M}^{(m)}$ be the $d(N_2 + 1) \times d(N_2 + 1)$ matrix such that for all $h \in \pi^{N_2}(\ell_\nu^1)$,*

$$\psi_{N_2} \left(\tilde{Q}^{-1} (A_m^{N_1}) \pi^{N_2} H_1 B_m^{N_1} * h \right) = \mathbf{M}^{(m)} \psi_{N_2}(h)$$

where ψ the isomorphism defined by in (64). Also for $m = 1, \dots, p$ define the quantities

$$\begin{aligned}
 \|\mathbf{M}^{(m)}\|_\nu &= \max_{k=0, \dots, N_2} \frac{1}{\nu^k} \sum_{j=0}^{N_2} \|\mathbf{M}_{j,k}^{(m)}\| \nu^j \\
 K_{0,m} &= \max_{k=0, \dots, N_2} \frac{1}{\nu^k} \sum_{n=0}^{N_2} \|\tilde{Q}_{n,k}^{-1} (A_m^{N_1})\| \nu^n, & K_{0,m}^0 &= \sum_{j=0}^{N_2} \|\mathbf{Q}_{j,0}^{-1} (A_m^{N_1})\| \\
 K_{0,m}^{S,k} &= \|\tilde{Q}_{0,k}^{-1} (A_m^{N_1})\| + 2 \sum_{n=1}^{N_2} \|\tilde{Q}_{n,k}^{-1} (A_m^{N_1})\|, & 0 \leq k \leq N_2 \\
 K_{0,m}^{S,*} &= \max_{k=0, \dots, N_2} \frac{1}{\nu^k} K_{0,m}^{S,k} \\
 L_{0,m} &= \max_{k=0, \dots, N_2} \frac{1}{\nu^k} \sum_{j=N_2}^{N_2+N_1} \|\mathbf{G}(A_m^{N_1}, i \circ \tilde{Q}^{-1} (A_m^{N_1}) \text{diag}(I, 0, \dots, 0))_{j,k}\| \nu^j \\
 L_{1,m} &= \max_{k=0, \dots, N_2} \frac{1}{\nu^k} \sum_{j=N_2}^{N_2+N_1} \|\mathbf{G}(A_m^{N_1}, i \circ \mathbf{M}^{(m)})_{j,k}\| \nu^j
 \end{aligned}$$

$$\begin{aligned}
 L_{2,m} &= \max_{k=0,\dots,N_1} \frac{1}{v^{N_2+1+k}} \sum_{j=0}^{N_2} \left(\frac{\|B_m^{N_1}\|_\omega}{(N_2 + 1 - N_1)^2 - 1} \|\mathbb{1}_0(j) + \|\mathbf{DT}_j Z_k^{N_1, N_2} \mathbf{S}(B_m^{N_1})\| \right) v^j \\
 J_0(B_m^{N_1}) &= \max_{k=0,\dots,N_2} \frac{1}{v^k} \sum_{j=N_2}^{N_2+N_1} \|\mathbf{G}(B_m^{N_1}, i \circ I_{\mathbb{C}^d(N_2+1)})\| v^j \\
 \alpha(B_m^{N_1}) &= \frac{1}{4(N_2 + 1)} \left(\left(v + \frac{2}{v} + \frac{1}{v^3} \right) \|B_m^{N_1}\|_v - \left(\frac{1}{v} + \frac{1}{v^3} \right) \|B_{m,0}^{N_1}\| \right) \\
 \Xi_m &= \left(1 + \frac{v}{2} \right) \|\mathbf{M}^{(m)}\|_v \|A_m^\infty\|_\omega + L_{1,m} + J_0(B_m^{N_1}) \\
 &\quad + \left(1 + \frac{v}{2} \right) [K_{0,m}^0 \|A_m^\infty\|_\omega + L_{0,m}] \sum_{k=1}^{m-1} \left(\prod_{j=k+1}^{m-1} K_{0,j}^{S,0} \right) K_{0,k}^{S,*} \|B_k^{N_1}\|_\omega \\
 \Xi(0) &= 2g(v) \|I + C_1\| \left(\|B_p^\infty\|_\omega + \|A_p^\infty\|_\omega \left(K_{0,p} \left(1 + \frac{v}{2} \right) \right) \right) \\
 &\quad + 2g(v) \|I + C_1\| \cdot \|A_p^\infty\|_\omega K_{0,p}^0 \left(1 + \frac{v}{2} \right) \sum_{k=1}^{p-1} \left(\prod_{j=k+1}^{p-1} K_{0,j}^{S,0} \right) K_{0,k}^{S,*} \|B_k^{N_1}\|_\omega \\
 \kappa_m &= \left(1 + \frac{v}{2} \right) \|B_m^\infty\|_\omega + \max \left\{ L_{2,m} + \alpha(B_m^{N_1}), \Xi_m \right\} \\
 \kappa(0) &= \max \left\{ \Xi(0), \frac{2}{v^{N_2+1}} \left(\|C_2\| + \|I + C_1\| \left(1 + \frac{1}{v^{N_2+1}} \right) \|B_p^\infty\|_v \right. \right. \\
 &\quad \left. \left. + \|(I + C_1) \odot B_2^{N_1}\|_v \right) \right\}.
 \end{aligned}$$

Then, with

$$c_3 := \max\{\kappa(0), \kappa_1, \dots, \kappa_p\}, \tag{88}$$

we have the estimate $\|(I - W)M_{N_1, N_2} - E\|_{B(X_v)} \leq c_3$.

Proof Define $\Omega = (I - W)M_{N_1, N_2} - E$. Let $h \in X_v$ satisfy $\|h\|_{X_v} \leq 1$ and denote $\phi = Eh$ and $\tilde{\phi} = E_{N_1, N_2} h$. Making use of Lemma 6.3.3, we have for $h \in X_v, n = 1, \dots, p$ and $1 - q \leq m \leq -p$,

$$\begin{aligned}
 (\Omega h)_{n-p} &= [Q_n \tilde{Q}_n^{-1} \tilde{\phi}_{n-p} - \phi_{n-p}] + (Q_n \tilde{Q}_n^{-1} - I) \\
 &\quad \mathbf{e}_0 S \pi^{N_2} \tilde{Q}_{n-1}^{-1} \sum_{k=1}^{n-1} \left(\prod_{j=k}^{n-2} \mathbf{e}_0 S \pi^{N_2} \tilde{Q}_j^{-1} \right) \tilde{\phi}_{k-p} \\
 &= [Q_n \tilde{Q}_n^{-1} \tilde{\phi}_{n-p} - \phi_{n-p}] + (Q_n \tilde{Q}_n^{-1} - I) \\
 &\quad \mathbf{e}_0 \sum_{k=1}^{n-1} \left(\prod_{j=k+1}^{n-1} \tilde{S} Q_j^{-1} \mathbf{e}_0 \right) S \pi^{N_2} \tilde{Q}_k^{-1} \tilde{\phi}_{k-p} \\
 (\Omega h)_m &= \tilde{\phi}_m - \phi_m \\
 (\Omega h)(0) &= [\tilde{\phi}(0) - \phi(0)] - (I + C_1) H_2(A_p * I_{\ell_v^1} - A_p^{N_1} * \pi^{N_2}) \\
 &\quad \tilde{Q}_p^{-1} \sum_{k=1}^p \left(\prod_{j=k}^{p-1} \mathbf{e}_0 S \pi^{N_2} \tilde{Q}_j^{-1} \right) \tilde{\phi}_{k-p} - (I + C_1) S \pi_{N_2}^\infty \tilde{\phi}_{-1} \\
 &= -(I + C_1) H_2(A_p * I_{\ell_v^1}
 \end{aligned}$$

$$\begin{aligned}
 & -A_p^{N_1} * \pi^{N_2} \left(\tilde{Q}_p^{-1} \tilde{\phi}_0 + \tilde{Q}_p^{-1} \mathbf{e}_0 \sum_{k=1}^{p-1} \left(\prod_{j=k+1}^{p-1} S \tilde{Q}_j^{-1} \mathbf{e}_0 \right) S \pi^{N_2} \tilde{Q}_k^{-1} \tilde{\phi}_{k-p} \right) \\
 & + [\tilde{\phi}(0) - \phi(0)] - (I + C_1) S \pi_{N_2}^\infty \tilde{\phi}_{-1}
 \end{aligned}$$

To derive a bound for $\|\Omega\|_{B(X_\nu)}$, we will need to separately bound the terms above. First, the easy one: by definition of E and E_{N_1, N_2} we have $\tilde{\phi}_m - \phi_m = 0$ for $1 - q \leq m \leq -p$. Next, observe that $(E_{N_1, N_2} \pi_{N_2}^\infty h)_{k-p} = 0$ for $k = 1, \dots, p$. As such, all of the “product” terms vanish for arguments $h \in X_\nu^\infty$ as they are terminated (at the right) by a $\tilde{\phi}_{k-p}$. This will simplify the application of the direct sum operator norm inequality (60) for $B(X_\nu)$. We will therefore bound each of the above for $h \in X_\nu^\infty$ first.

Let $h^\infty \in X_\nu^\infty$. Replacing h with h^∞ in the above expressions, we get

$$\begin{aligned}
 (\Omega h^\infty)_{n-p} &= -(E h^\infty)_{n-p} = -H_1(B_n * h_{n-q}^\infty) \\
 (\Omega h^\infty)(0) &= -(E h^\infty)(0) = -C_2 S^* h_{1-p-q}^\infty - (I + C_1) H_2(B_p * h_{p-q}^\infty)
 \end{aligned}$$

Row 2 and 7 of Table A and Proposition 4.1.1 can be used to bound the second quantity with geometric decay in N_2 . As for the first, we use row 13 and 14 to handle the body $B_n^{N_1}$ of the sequence B_n , with row 3 and Proposition 4.1.1 to handle the tail B_n^∞ . All together, we get

$$\|\Omega h^\infty\|_{n-p} \leq L_{2,n} + \alpha(B_n^{N_1}) + \left(1 + \frac{\nu}{2}\right) \|B_n^\infty\|_\omega \tag{89}$$

$$\|(\Omega h^\infty)(0)\| \leq \frac{2}{\nu^{N_2+1}} \left(\|C_2\| + \|I + C_1\| \left(1 + \frac{1}{\nu^{N_2+1}}\right) \|B_p^\infty\|_\nu + \|(I + C_1) \odot B_2^{N_1}\|_\nu \right) \tag{90}$$

Now we let $h^{N_2} \in X_\nu^{N_2}$. Replacing h with h^{N_2} in the first set of equations, we will work piece by piece. Making use of (81) and (82),

$$\begin{aligned}
 [Q_n \tilde{Q}_n^{-1} \tilde{\phi}_{n-p} - \phi_{n-p}] &= [Q_n \tilde{Q}_n^{-1} \pi^{N_2} H_1(B_n^{N_1} * \pi^{N_2}) - H_1(B_n * \pi^{N_2})] h_{n-q}^{N_2} \\
 &= -[(I - Q_n \tilde{Q}_n^{-1}) \pi^{N_2} H_1(B_n^{N_1} * \pi^{N_2}) \\
 &\quad + \pi_{N_2}^\infty H_1(B_n^{N_1} * \pi^{N_2}) + H_1(B_n^\infty * \pi^{N_2})] h_{n-q}^{N_2}.
 \end{aligned}$$

These terms all appear in the expression for $\bar{\Lambda}_{22}$ from the proof of Theorem 6.1.2 (modulo some projections that do not alter the norms), so we can bound them using the same methods. Namely, we use Propositions 4.1.1, 5.3.1, Lemma 5.2.1 and rows 3, 4, 13 and 14 of Table A (and some algebra) to get

$$\|[Q_n \tilde{Q}_n^{-1} \tilde{\phi}_{n-p} - \phi_{n-p}]\|_\nu \leq \left(1 + \frac{\nu}{2}\right) \|\mathbf{M}^{(n)}\|_\nu \|A_n^\infty\|_\omega + L_{1,n} + J_0(B_n^{N_1}) + \left(1 + \frac{\nu}{2}\right) \|B_n^\infty\|_\omega. \tag{91}$$

Next, recalling the argument from the proof of Theorem 6.1.2 (see the $\bar{\Lambda}_{21}$ term), we can make the estimate

$$\|(Q_n \tilde{Q}_n^{-1} - I) \mathbf{e}_0\|_{L(\mathbb{C}^d, \ell_\nu^1)} \leq \left(1 + \frac{\nu}{2}\right) K_{0,n}^0 \|A_n^\infty\| + L_{0,n}. \tag{92}$$

For the summation-product part, recall that the $S \tilde{Q}_j^{-1} \mathbf{e}_0$ terms in the products can be bounded individually using row 11, with $\|S \tilde{Q}_j^{-1} \mathbf{e}_0\|_{L(\mathbb{C}^d, \ell_\nu^1)} \leq K_{0,j}^{S,0}$. As for the “external”

terms of the form $S\pi^{N_2} \tilde{Q}_k^{-1} \tilde{\phi}_{k-p}$, since we have replaced h with h^{N_2} , these are given by

$$S\pi^{N_2} \tilde{Q}_k^{-1} \tilde{\phi}_{k-p} = S\pi^{N_2} \tilde{Q}_k^{-1} \pi^{N_2} H_1(B_k^{N_1} * h_k^{N_2-q}).$$

We can bound these using a combination row 3 and 10 of the table and Proposition 4.1.1. We get

$$\|S\pi^{N_2} \tilde{Q}_k^{-1} \tilde{\phi}_{k-p}\|_v \leq K_{0,k}^{S,*} \left(1 + \frac{\nu}{2}\right) \|B_k^{N_1}\|_\omega. \tag{93}$$

Next, expanding $\tilde{\phi}_{k-p}$ in $\tilde{Q}_k^{-1} \tilde{\phi}_{k-p}$ we can get the estimate

$$\|\tilde{Q}_k^{-1} \tilde{\phi}_{k-p}\|_v \leq K_{0,k} \left(1 + \frac{\nu}{2}\right) \|B_k^{N_1}\|_\omega \tag{94}$$

using row 3 and 9 of Table A and Proposition 4.1.1. By combining (91), (92), (93), (94) and the inline estimates, we can finally get the bound

$$\begin{aligned} \|(\Omega h^{N_2})_{n-p}\|_v &\leq \left(1 + \frac{\nu}{2}\right) \|\mathbf{M}^{(n)}\|_v \|A_n^\infty\|_\omega + L_{1,n} + J_0(B_n^{N_1}) + \left(1 + \frac{\nu}{2}\right) \|B_n^\infty\|_\omega \\ &\quad + \left[\left(1 + \frac{\nu}{2}\right) K_{0,n}^0 \|A_n^\infty\| + L_{0,n}\right] \sum_{k=1}^{n-1} \left(\prod_{j=k+1}^{n-1} K_{0,j}^{S,0}\right) K_{0,k}^{S,*} \left(1 + \frac{\nu}{2}\right) \|B_k^{N_1}\|_\omega \end{aligned}$$

Taking the maximum of the above with (89), the result is $\|(\Omega h)_{n-p}\|_v \leq \kappa_n$.

To get a bound for $\|(\Omega h(0))\|$, we will also need to compute and bound $\tilde{\phi}(0) - \phi(0)$. This is straightforward: as we have already obtained a bound for h^∞ , we let $h^{N_2} \in X_v^{N_2}$ so that

$$\begin{aligned} \|\tilde{\phi}(0) - \phi(0)\| &= \|C_2 S^* \pi_{N_2}^\infty h_{1+p-q}^{N_2} + (I + C_1)(H_2(B_p * I_{\ell_v^1}) - H_2(B_p^{N_1} * \pi^{N_2}))\phi_{p-q}\| \\ &= \|(I + C_1)H_2(B_p^\infty * \pi^{N_2})h_{p-q}^{N_2}\| \\ &\leq 2g(\nu)\|I + C_1\| \cdot \|B_p^\infty\|_\omega. \end{aligned}$$

The last thing we need to do is deal with the $H_2(A_p * I_{\ell_v^1} - A_p^{N_1} * \pi^{N_2})$ terms, multiplied on the right by $\tilde{Q}_p^{-1} \tilde{\phi}_0$ or $\tilde{Q}_p^{-1} \mathbf{e}_0$. However, since the latter two have range in $\pi^{N_2}(\ell_v^1)$ (recall we already have a bound for the case $h \in X_v^\infty$, see (90)), this can be equivalently written (for placeholder $z \in \mathbb{C}^d$) as

$$H_2(A_p * I_{\ell_v^1} - A_p^{N_1} * \pi^{N_2}) \left(\tilde{Q}_p^{-1} \tilde{\phi}_0 + \tilde{Q}_p^{-1} \mathbf{e}_0 z\right) = H_2(A_p^\infty * \pi^{N_2}) \left(\tilde{Q}_p^{-1} \tilde{\phi}_0 + \tilde{Q}_p^{-1} \mathbf{e}_0 z\right).$$

The map $H_2(A_p * I_{\ell_v^1} - A_p^{N_1} * \pi^{N_2})$ can without loss of generality be replaced with $H_2(A_p^\infty * \pi^{N_2})$, which gives the bound

$$\|H_2(A_p^\infty * \pi^{N_2})\|_{L(\ell_v^1, \mathbb{C}^d)} \leq 2g(\nu)\|B_p^\infty\|_\omega + \|I + C_1\|$$

Combining the previous estimates again, we finally get the bound

$$\begin{aligned} \|(\Omega h^{N_2})(0)\| &\leq 2g(\nu)\|I + C_1\| \left(\|B_p^\infty\|_\omega + \|A_p^\infty\|_\omega \left(K_{0,p} \left(1 + \frac{\nu}{2}\right)\right)\right) \\ &\quad + 2g(\nu)\|I + C_1\| \cdot \|A_p^\infty\|_\omega K_{0,p}^0 \left(1 + \frac{\nu}{2}\right) \sum_{k=1}^{p-1} \left(\prod_{j=k+1}^{p-1} K_{0,j}^{S,0}\right) K_{0,k}^{S,*} \|B_k^{N_1}\|_\omega. \end{aligned}$$

Applying (60) to take the maximum of the above with (90) we get the bound $\|(\Omega h)(0)\| \leq \kappa(0)$. Finally, applying (60) again but this time to $\Omega : X_v \rightarrow X_v$, we get $\|\Omega\|_{B(X_v)} \leq \max\{\kappa(0), \kappa_1, \dots, \kappa_p\}$. \square

7 MATLAB implementation

To accompany this publication we have implemented the numerical discretization of the monodromy operator in MATLAB. It can be found at the author’s GitHub [9]. The implementation can handle arbitrary period p and delay q , provided these are integers. Rigorous enclosures of the c_2 and c_3 bounds is accomplished with the INTLAB library [24], although at present we have only implemented the case $1 = p \leq q$. In the same way, c_1 bound computation for generalized Morse index and radial sector validation are implemented and handled with INTLAB. The code is general-purpose, taking as input the matrix-valued functions $A(t)$ and $B(t)$ appropriately pre-processed, impulse matrices C_1 and C_2 and various other user-specified data. The code can be found at [9]. INTLAB is required for rigorous proof, but is not required for monodromy operator discretization, so the latter is suitable for eigenvalue (Floquet multiplier) estimation. The validation code can also be run with floating point arithmetic, but in this mode the output should not be considered rigorous (especially the c_1 bound code). At time of writing there are several parts of the code that could be vectorized (specifically some functions that implement block-matrix convolutions), leading to performance improvement.

7.1 Computation of c_1 bounds

For generalized Morse index validation, the c_1 bound must satisfy

$$\max \left(c_1^\dagger, \sup_{\theta \in [0, 2\pi]} \|(M_{N_1, N_2} - r e^{i\theta} I)^{-1}\|_{B(X_\nu^{N_2})} \right) \leq c_1,$$

where $c_1^\dagger = \sup_{\theta \in [0, 2\pi]} \|(M_{N_1, N_2} - r e^{i\theta} I)^{-1}\|_{B(X_\nu^\infty)}$ can be bounded using an explicit formula (Lemmas 6.1.1, 6.2.1 and 6.3.1). Since the eigenvalues of M_{N_1, N_2} come in complex-conjugate pairs, it is enough to perform the former bound over $\theta \in [0, \pi]$. The strategy is therefore to fix a mesh size m , partition $[0, \pi]$ according to

$$0 = \theta_1 < \theta_2 \cdots < \theta_{m-1} < \theta_m = \pi$$

and compute

$$c_1 = \max \left(c_1^\dagger, \max_{j=1, \dots, m} \sup_{\theta \in [\theta_{j-1}, \theta_j]} \|(M_{N_1, N_2} - r e^{i\theta} I)^{-1}\|_{B(X_\nu^{N_2})} \right),$$

where c_1^\dagger is replaced by an appropriate upper bound. The supremums are done using interval arithmetic (INTLAB). If $c_1 c_2 c_3 \geq 1$, one should refine the mesh (to reduce the over-estimation due to interval arithmetic and subsequently decrease c_1), increase the number of modes (to push c_3 closer to zero and decrease the error $\|M - M_{N_1, N_2}\|_{B(X_\nu)}$) or work with ν if such flexibility is afforded by the given problem. It may also be necessary to change the value of the radius r .

The situation is similar for validation in a closed ball. The c_1 bound must satisfy

$$\max \left(c_1^\dagger, \sup_{t \in [0, 2\pi]} \|(M_{N_1, N_2} - (\lambda + r e^{i\theta}) I)^{-1}\|_{B(X_\nu^{N_2})} \right) \leq c_1,$$

where $c_1^\dagger = \sup_{\theta \in [0, 2\pi]} \|(M_{N_1, N_2} - (\lambda + r e^{i\theta}) I)^{-1}\|_{B(X_\nu^\infty)}$. There is no symmetry that can be exploited here, so we must partition the entire interval $[0, 2\pi]$. With m mesh points, we

compute

$$c_1 = \max \left(c_1^\dagger, \max_{j=1, \dots, m} \sup_{\theta \in [\theta_{j-1}, \theta_j]} \|(M_{N_1, N_2} - (\lambda + r e^{i\theta})I)^{-1}\|_{B(X_v^{N_2})} \right)$$

using interval arithmetic. The conditioning guidelines are the same as for generalized Morse index validation.

For radial sector validation, the c_1 bound must satisfy

$$\max \left(c_1^\dagger, \sup_{t \in [0, 4]} \|(M_{N_1, N_2} - z(t; \lambda, r, \omega)I)^{-1}\|_{B(X_v^{N_2})} \right) \leq c_1$$

for the radial sector parameterization z from (44), where $c_1^\dagger = \sup_{t \in [0, r]} \|(M_{N_1, N_2} - z(t; \lambda, r, \omega)I)^{-1}\|_{B(X_v^\infty)}$ can once again be bounded using an explicit formula (Lemmas 6.1.1, 6.2.1 and 6.3.1). By choosing mesh sizes m_k and partitioning the intervals $[k, k + 1]$ for $k = 0, 1, 2, 3$ according to

$$k = t_{k,1} < t_{k,2} < \dots < t_{k,m_k} = k + 1,$$

one can then compute

$$c_1 = \max \left(c_1^\dagger, \max_{k=0,1,2,3} \max_{j=1, \dots, m_k} \sup_{t \in [t_{k,j-1}, t_{k,j}]} \|(M_{N_1, N_2} - z(t; \lambda, r, \omega)I)^{-1}\|_{B(X_v^{N_2})} \right),$$

where c_1^\dagger is replaced by an appropriate upper bound and all suprema are calculated using interval arithmetic (INTLAB). Conditioning guidelines are the same as the previous case, except that generally it might also be necessary to change the value of the width r or sweep ω of the radial sector.

Remark 7.1.1 In all cases, an appropriate bound for c_1^\dagger is available from one of Lemmas 6.1.1, 6.2.1 or Lemma 6.3.1.

7.1.1 Mesh generation

In our implementation of the c_1 bound we have allowed two options for the mesh. The first is a uniform grid, and the second one is a pre-specified mesh. A script is included to generate a (nonuniform) mesh in one of two ways. The first, which is generally very slow, involves first computing

$$s \mapsto \|(M_{N_1, N_2} - z(s)I)^{-1}\|_{B(X_v^{N_2})}$$

at a specified number of equally-spaced points throughout the domain $\text{dom}(z)$ of the parameterization for ∂U (for U the set to validated) with floating point arithmetic (for speed). A mesh $0 = s_1 < \dots < s_m = \max(\text{dom}(z))$ for specified m is then computed so that

$$\int_{s_{i-1}}^{s_i} \|(M_{N_1, N_2} - z(s)I)^{-1}\|_{B(X_v^{N_2})} ds$$

is (nearly) equal for $i = 1, \dots, m$. A much faster way is to instead take $\{\sigma_1, \dots, \sigma_N\} = \sigma(M_{N_1, N_2})$ the eigenvalues of M_{N_1, N_2} and compute

$$s \mapsto \frac{1}{\min_k (|\sigma_k - z(s)|)}$$

at a specified number of equally-spaced points throughout the domain $\text{dom}(z)$, and then generate the mesh in such a way that

$$\int_{s_{i-1}}^{s_i} \frac{1}{\min_k (|\sigma_k - z(s)|)} ds$$

is (nearly) equal for $i = 1, \dots, m$

7.2 Handling arbitrary period and delay in the absence of validation

Our basic implementation of the discretized monodromy operator is built on the premise that the the period p and delay q are coprime and $p \leq q$. In this section we explain how the implementation handles the other cases. If p and q are not coprime but $p \leq q$, one can interpret the monodromy operator M as being a product:

$$M = U(p, p - 1)U(p - 1, p - 2) \cdots U(2, 1)U(1, 0),$$

with $U(t_1, t_0)$ denoting the solution operator from time t_0 to time t_1 for (12)–(13). Each of $U(k, k - 1)$ for $k = 1, \dots, p$ can be discretized using our scheme, since these operators can, themselves, be interpreted as the monodromy operator for a system of the type (12)–(13) except with period $p_0 = 1$ and delay q . This is not optimal, and implementing the discretization from the ground up treating arbitrary $p \leq q$ would improve efficiency by reducing the amount of large matrix multiplications.

Depending on the relationship between p and q and the regularity of the matrix-valued functions $A(t)$ and $B(t)$, one might be able to write M using fewer than p factors. Suppose $p \leq q$ have a common factor m . Then $p = jm$ for some $j \geq 0$, and we can write

$$M = U(p, (j - 1)m)U((j - 1)m, (j - 2)m) \cdots U(2m, m)U(m, 0).$$

Provided the matrix-valued functions $A(t)$ and $B(t)$ are piecewise-analytic with respect to the intervals $(km, (k + 1)m)$ for $k \in \mathbb{Z}$, we can apply our discretization scheme by interpreting each factor as the monodromy operator of a system of the type (12)–(13) with period $p_0 = m$ and delay q . After an appropriate time rescaling (since the new period m divides q) we can rescale the period to 1. However, since this is problem-specific, we do not implement it directly in our MATLAB code and instead implement the worst-case fallback option outlined in the previous paragraph.

Suppose now that $p > q$: that is, the period is greater than the delay. We can write $p = jq + k$ for some positive integer j and a remainder $k \in \{0, \dots, q - 1\}$. We can then write the monodromy operator M as

$$M = U(p, jq)U(jq, (j - 1)q) \cdots U(2q, q)U(q, 0).$$

In the same way as last time, we can interpret $U(mq, (m - 1)q)$ as being a monodromy operator for a system of the type (12)–(13) except with period and delay both equal to q , while $U(p, jq)$ can be interpreted as a monodromy operator for a system of the same type, except with period equal to $p_0 = k$ and delay equal to q . This is handled automatically in our MATLAB implementation, where each of the $M(mq, (m - 1)q)$ operators are discretized using the worst-case product fallback approach from the first paragraph.

At a theoretical level, the discretization M_{N_1, N_2} resulting from this construction converges to M (although with a generally worse rate) in $B(X_\nu)$ just as it does for the coprime cases $p \leq q$; namely, the convergence is achieved as $N_1, N_2 \rightarrow \infty$ provided $N_2 - N_1 \rightarrow \infty$. This can be proven by careful analysis of the bounds c_2 and c_3 . Namely, c_2 is uniformly bounded

and c_3 is $O(1/(N_2 - N_1))$. One can then apply the error bound (42). However, the validated numerics of Sect. 4.3 no longer apply. The proof of the main lemma and theorem in the latter section explicitly uses the decomposition of M in terms of a single implicit and explicit part operator, and if $p > q$ or they are not coprime it is generally necessary to split M into several such operators. We briefly demonstrate the problem at the end of Sect. 10. While the result can indeed be generalized to the case $p > q$ or non-coprime p and q , the estimation of the analogous bounds (such as c_2 and c_3) quickly become rather involved. Thus, while these cases could be handled using our validated numerics setup, we do not do so at this time.

7.3 Optimizations for some special scalar problems

Some additional preprocessing can improve the speed of computer-assisted proofs if $q = kp$ for a natural number k and the impulsive delay differential equation is scalar. First recall [10] that μ is a Floquet multiplier if and only if to $\lambda := p^{-1} \log \mu$ there is associated a nontrivial complex-valued p -periodic function $\phi(t)$ such that $t \mapsto \phi(t)e^{t\lambda}$ is a solution of (10)–(11). One can then check directly that ϕ is a periodic solution of

$$\begin{aligned} \dot{\phi}(t) &= (A(t) - \lambda I)\phi(t) + e^{-\lambda q} B(t)\phi(t - q), & t \notin p\mathbb{Z} \\ \Delta\phi(t) &= C_1\phi(t^-) + e^{-\lambda q} C_2\phi(t - q), & t \in p\mathbb{Z}. \end{aligned}$$

However, since $q = kp$ for p the period of ϕ , the above is equivalent to

$$\begin{aligned} \dot{\phi}(t) &= (A(t) - \lambda I)\phi(t) + e^{-\lambda q} B(t)\phi(t), & t \notin p\mathbb{Z} \\ \Delta\phi(t) &= C_1\phi(t^-) + e^{-\lambda q} C_2\phi(t), & t \in p\mathbb{Z}. \end{aligned}$$

Let $\bar{A} = p^{-1} \int_0^p A(t)dt$ and $\bar{B} = p^{-1} \int_0^t \bar{B}(t)dt$. If ϕ is scalar, ϕ is periodic with period p and nontrivial if and only if

$$1 = (1 + C_1) \exp(p(\bar{A} + e^{-\lambda q} \bar{B} - \lambda)) + C_2 e^{-\lambda q},$$

as can be verified by solving the ordinary impulsive differential equation and imposing the equality $\phi(0) = \phi(p)$. However, this is the exact same equation one obtains upon substituting the ansatz $y(t) = \phi(t)e^{t\lambda}$ into

$$\begin{aligned} \dot{y} &= \bar{A}y(t) + \bar{B}y(t - q), & t \notin p\mathbb{Z} \\ \Delta y &= C_1y(t^-) + C_2y(t - q), & t \in p\mathbb{Z} \end{aligned}$$

and imposing periodicity of ϕ . The above impulsive DDE and (10)–(11) therefore have the same Floquet multipliers, so in the computation of the bounds c_1 , c_2 and c_3 , it is sufficient to replace the inputs A and B with rigorous interval enclosures of the mean over the entire interval $[0, p]$. The tail terms can also be rolled into this rigorous enclosure of the means, so that in the bound computations one can take them to be zero.

8 Examples and applications: rigorous numerics

The following sections demonstrate the strengths (and weaknesses) of our numerical monodromy operator discretization scheme and the rigorous numerics approach to eigenvalue validation. The models of the first two sections (Sects. 8.1, 8.2) are motivated in part by existing mathematical models or well-known equations. In the first of these sections we

exploit the robustness of INTLAB to prove results that are uniform with respect to model parameters. In particular, we prove some robust stability and bifurcation enclosure results. Section 8.3 demonstrates the importance of eigenvalue validation by way of a family of simple examples.

In all proofs of this section, the periodic coefficients of our delay equations will be entire. By Corollary 4.1.1, we can therefore use any $\nu > 1$ in proofs that we want. For the most part we will use $\nu = 1.17$, but when we need to take N_2 very large as we do in the proof of Theorem 8.2.1, it will be necessary to use a smaller ν to balance the interval arithmetic.

Remark 8.0.1 [Disclosure] All references to computing time in the computer-assisted proofs were as performed on a Windows 10 machine with an AMD Ryzen 5 1500X processor and 16gb of memory in MATLAB R2019b with INTLAB v12 unless otherwise stated. The times are for the entire runtime of the proof (e.g. they include interval arithmetic computations of M_{N_1, N_2}), not just the c_1, c_2 and c_3 bound calculation. Times were done using the `tic/toc` MATLAB function. These times are not necessarily optimal. Different choices of modes (N_1, N_2) and weight (ν) can have a significant impact on computing time while still yielding correct proofs. The computation times include negligible overhead associated to the computation of the mesh (generated using the “fast” method from Sect. 7.1.1) for the c_1 bound. The number of points in this mesh has a significant impact on computation time, and this number is generally different for each proof. See the associated MATLAB code [9] for documentation.

8.1 Time-delay predator-prey model with impulsive harvesting

The following predator-prey system is modeled off of one considered in [22]:

$$\dot{x} = rx(t) \left(1 - \frac{x(t)}{K} \right) - \beta x(t)y(t) \tag{95}$$

$$\dot{y} = \rho\beta e^{-d_1\tau} x(t - \tau)y(t - \tau) - d_2y(t), \quad t \notin \mathbb{Z} \tag{96}$$

$$\Delta y = -hy(t^-), \quad t \in \mathbb{Z}. \tag{97}$$

The difference between the above system and one cited is that instead of impulsive harvesting of prey (x), we consider impulsive harvesting of the mature predator (y). Predator age structure is taken into account, but the juvenile dynamics do not have an influence on the remaining population classes and have been neglected here. One may consult [22] for details.

There is a predator-free equilibrium, $(x^*, y^*) = (K, 0)$. The linearization at this equilibrium is

$$\dot{z} = \begin{bmatrix} -r & -\beta K \\ 0 & -d_2 \end{bmatrix} z(t) + \begin{bmatrix} 0 & 0 \\ 0 & \rho\beta K e^{-d_1\tau} \end{bmatrix} z(t - \tau), \quad t \notin \mathbb{Z}$$

$$\Delta z = \begin{bmatrix} 0 & 0 \\ 0 & -h \end{bmatrix} z(t^-), \quad t \in \mathbb{Z}.$$

This system is upper triangular and it is easy to verify that its stability (and, consequently, the dimension of the unstable manifold of (x^*, y^*)) is entirely determined by the following scalar equation:

$$\dot{v} = -d_2v(t) + \rho\beta K e^{-d_1\tau} v(t - \tau), \quad t \notin \mathbb{Z} \tag{98}$$

$$\Delta v = -hv(t^-), \quad t \in \mathbb{Z}. \tag{99}$$

Table 1 Numerical outputs from the proof of Theorems 8.1.1 and 8.1.2

τ	h	N_2	ν	c_1	c_2	c_3	$c_1c_2c_3$	Computing time (s)
1	0.075	30	1.17	219.4946	1.0278	0.0016013	0.36126	11
1	0.060	30	1.17	247.2036	1.0283	0.0016013	0.40704	14
1	[0,0.050]	40	1.17	326.7163	1.0300	0.0013785	0.46387	32
1	[0.050,0.060]	40	1.17	359.694	1.0285	0.0013785	0.50996	36
2	0.075	30	1.17	133.5642	1.0278	0.0015696	0.21547	28
2	0.060	40	1.17	368.8167	1.0282	0.0011863	0.44983	47
3	0.075	40	1.17	135.1902	1.0277	0.0011628	0.16155	105
3	0.060	70	1.3	723.1795	1.0280	0.00068617	0.51012	430

Making use of this observation, our numerical implementation of the discretized monodromy operator and implementations of the c_1 , c_2 and c_3 bounds, we can prove the following.

Theorem 8.1.1 (Pointwise stability) *Suppose $\tau \in \{1, 2, 3\}$. With the parameters $\beta = 0.1$, $\rho = 1$, $K = 1$, $d_1 = 0.02$ and $d_2 = 0.03$, the predator-free equilibrium $(x^*, y^*) = (K, 0)$ of (95)–(97) is:*

- *unstable if $h = 0.060$ with a one-dimensional unstable manifold,*
- *locally asymptotically stable if $h = 0.075$.*

Proof (Outline) For each choice of τ and h , we compute the interval enclosures of the discretized monodromy operator \mathbb{M} (with a suitable number of nonconstant Chebyshev modes) with INTLAB. We then compute c_2 and c_3 bounds, as well as the c_1 bound for Morse index validation. Following this, we count the eigenvalues of the interval matrix \mathbb{M} with absolute value at least one. We do this using the radii polynomial approach from [6]. This count then gives the number of Floquet multipliers of (98)–(99) with absolute value greater than (and, by robustness, greater than or equal to) one. By previous observations, these results carry over to the linearization of the full system (95)–(97) at the predator-free equilibrium. \square

The results of the computer-assisted proof are tabulated in Table 1 and the approximate spectrum for $h = 0.060$ and $\tau = 3$ is plotted in Fig. 3.

We can also prove the following “robust instability” result for the system with $\tau = 1$. The results of the computer-assisted proof can be found in Table 1.

Theorem 8.1.2 (Robust instability) *Suppose $\tau = 1$. With the parameters $\beta = 0.1$, $\rho = 1$, $K = 1$, $d_1 = 0.02$ and $d_2 = 0.03$, the predator-free equilibrium $(x^*, y^*) = (K, 0)$ of (95)–(97) is unstable with a one-dimensional unstable manifold for all $h \in [0, 0.060]$.*

Proof (Outline) Let $M_{N_1, N_2}(h)$ denote discretized the monodromy operator of (98)–(99) for harvesting parameter h (and all others fixed as in the theorem), and let $M(h)$ be the (undiscretized) monodromy operator. We compute an interval enclosure \mathbb{M} of the discretized monodromy operator with $N_2 = 40$ nonconstant Chebyshev modes and interval parameters $h_0 = [0, 0.050]$ and $h_1 = [0.050, 0.060]$. Consequently, for each $h \in h_0$, we have $M_{0, N_2}(h) \in \mathbb{M}(h_0)$ and for each $h \in h_1$, $M_{0, N_2}(h) \in \mathbb{M}(h_1)$. We therefore compute upper estimates for the c_1 , c_2 and c_3 bounds for the interval matrices $\mathbb{M}(h_0)$ and $\mathbb{M}(h_1)$ using INTLAB, for Morse index validation (i.e. radius $r = 1$). If $c_1c_2c_3 < 1$, then $M(h)$ and $M_{0, N_2}(h)$ have the same number of eigenvalues in the complement $B_1(0)$ for all $h \in [0, 0.060]$. By

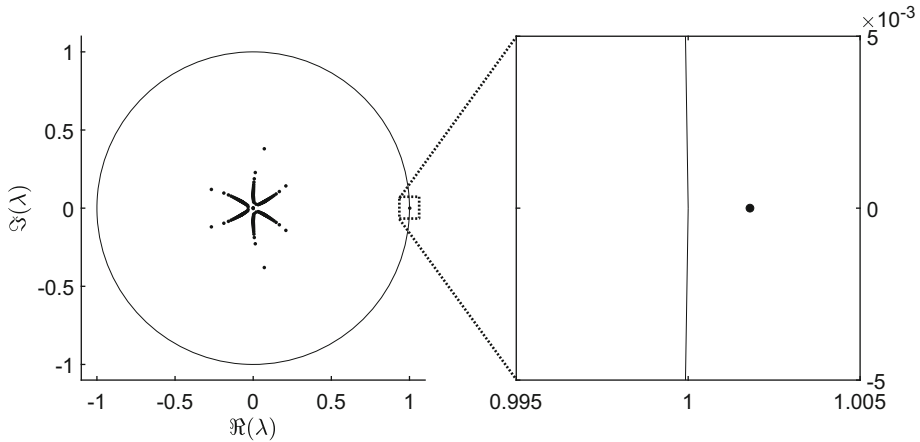


Fig. 3 Left: Approximate spectrum of monodromy operator for the linearized predator-prey model (98)–(99) with parameters from Theorem 8.1.1, $\tau = 3$ and $h = 0.060$, with a unit circle for scale and visual instability reference. Right: zoomed in portion of the region in the dashed box showing the unstable Floquet multiplier (black dot)

Theorem 8.1.1, we already know this number of eigenvalues is exactly one. The supplied MATLAB code completes all these calculations. \square

Finally, we can accurately enclose the possible bifurcation that is identified by Theorem 8.1.1. Doing this requires:

- selection of an interval \mathbf{h} in which the bifurcation is contained,
- validation of a generalized Morse index (of an appropriate radius $r < 1$) uniformly over \mathbf{h} ,
- validation of a radial sector (of appropriate radius and sweep), uniformly over \mathbf{h} ,
- two sets of rigorous interval eigenvalue enclosures, one for each endpoint of \mathbf{h} ,
- two additional Morse index validations (at radius $r = 1$) at the endpoints of \mathbf{h} .

The computer-assisted proof took 1155 s (19 min, 15 s) to complete. The following theorem summarizes the result, and we outline the proof in a similar manner to the previous one. Figure 4 provides a visual depiction of the combined validation structure and output of the code, while Table 2 provides the c_1, c_2 and c_3 bounds for each step.

Theorem 8.1.3 (Bifurcation) *Suppose $\tau = 1$. Let $\mathbf{h} = [0.065, 0.066]$. With $\beta = 0.1, \rho = 1, K = 1, d_1 = 0.02$ and $d_2 = 0.03$, the predator-free equilibrium $(x^*, y^*) = (K, 0)$ of (95)–(97) enjoys the following properties.*

- For all $h \in \mathbf{h}$, it has a single Floquet multiplier $\lambda(h)$ that satisfies $|\lambda(h)| \geq 0.8$, and all other multipliers are strictly contained in the interior of the ball $B_{0.8}(0) \subset \mathbb{C}$.
- $\lambda(h) \in R_{\lambda^*}(r, \omega)$ with $\lambda^* = 1, r = 5 \times 10^{-3}$ and $\omega = 2.5 \times 10^{-3}$ for all $h \in \mathbf{h}$.
- $|\lambda(0.066)| < 1 < |\lambda(0.065)|$. That is, $\lambda(h)$ crosses the unit circle at some $h \in \mathbf{h}$.

Proof (Outline) Similar to the previous proof, we let $M_{N_1, N_2}(h)$ denote the discretized the monodromy operator of (98)–(99) for harvesting parameter h (and all others fixed as in the theorem), and $M(h)$ the (undiscretized) monodromy operator. We compute an interval enclosure We compute an interval enclosure \mathbb{M} of the discretized monodromy operator with

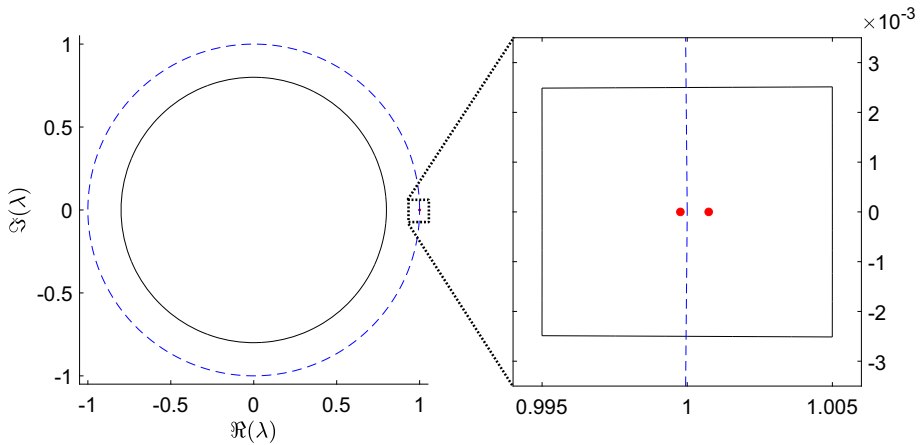


Fig. 4 Visual depiction of the content of Theorem 8.1.3 generated by the computer-assisted proof. Left: the Morse index at radius 0.8 is validated and is represented by the solid black circle. The dashed blue circle has radius 1 and is provided for comparison. At the extreme right are two eigenvalues (one for $h = 0.065$ and another for $h = 0.066$) and the radial sector $R_{\lambda^*}(r, \omega)$ that are too small to resolve at this level of magnification. Right: zoomed in portion of a region within the dotted black square. The radial sector appears as a solid black curve, and the individual eigenvalues (red dots, $h = 0.065$ on the right and $h = 0.066$ on the left) can be resolved. Note that the exact location of the eigenvalues is only known up to inclusion within this radial sector and the ordering $|\lambda(0.066)| < 1 < |\lambda(0.065)|$ (Color figure online)

$N_2 = 150$ nonconstant Chebyshev modes and *interval* parameter \mathbf{h} . As such, for each $h \in \mathbf{h}$ we have $M_{0,N_2}(h) \in \mathbb{M}$. We therefore compute upper estimates for the c_2 and c_3 bounds for the interval matrix \mathbb{M} . Next, we compute c_1 bounds for two validation structures:

1. the ball $B_{0.8}(0)$, for generalized Morse index validation at radius 0.8,
2. the radial sector $R_{\lambda^*}(r, \omega)$ with $\lambda^* = 1, r = 5 \times 10^{-3}$ and $\omega = 2.5 \times 10^{-3}$, for compact eigenvalue validation.

If $c_1 c_2 c_3 < 1$ for the Morse index structure, we can conclude that for all $h \in \mathbf{h}$, the number of eigenvalues of $M(h)$ and $M_{N_2,0}(h)$ in the complement of $B_{0.8}(0)$ are constant and equal. If $c_1 c_2 c_3 < 1$ for the radial sector structure, the number of eigenvalues of $M(h)$ and $M_{N_2,0}(h)$ in $R_{\lambda^*}(r, \omega)$ is constant and equal for all $h \in \mathbf{h}$. This proves the first two points. For the final point, we need to compute $\mathbb{M}(0.065)$ and $\mathbb{M}(0.066)$, validate their eigenvalues and ensure that the eigenvalues with absolute value greater than 0.8 have rigorous enclosures contained in $R_{\lambda^*}(r, \omega)$ and satisfy $|\lambda(0.066)| < 1 < |\lambda(0.065)|$. To ensure that this ordering is correct for the exact eigenvalues, we need to validate the Morse index at radius 1 for $h = 0.065$ and also at $h = 0.066$. Verifying rigorously that the eigenvalues (of the discretized operator) are contained within $R_{\lambda^*}(r, \omega)$ is accomplished with Proposition 4.3.1 and the radii polynomial approach for enclosure of eigenvalues of interval matrices from [6]. The supplied MATLAB code completes all these calculations, and we use $\nu = 1.17$ to complete the proof. As a final remark, the c_2 and c_3 bounds for \mathbb{M} can be used for all validation proofs since they are by definition over-estimates for the associated c_2 and c_3 bounds for the interval matrices $M_{0,N_2}(0.065)$ and $M_{0,N_2}(0.066)$. \square

Table 2 Numerical outputs from the proof of Theorem 8.1.3

h	N_2	ν	Validation structure	c_1	c_2	c_3	$c_1c_2c_3$
[0.065, 0.066]	150	1.17	Morse index, radius 0.8	67.5127	1.0277	0.00032858	0.022798
	150	1.17	Radial sector	653.4255	1.0277	0.00032858	0.22066
0.065	150	1.17	Morse index, radius 1	1851.0522	1.0277	0.00032858	0.62508
0.066	150	1.17	Morse index, radius 1	1763.5515	1.0277	0.00032858	0.59554

The bifurcation proven in Theorem 8.1.3 corresponds to a transcritical bifurcation of periodic solutions. There is some $h^* \in [0.065, 0, 066]$ at which a nontrivial periodic solution of (95)–(97) collapses onto the equilibrium solution $(K, 0)$. Its distance to $(K, 0)$ is $O(|h - h^*|)$ and it is locally asymptotically stable when $h < h^*$. For visualization, we have provided in Fig. 5 a numerical integration of the system at the parameters where this solution is stable.

8.2 Hopf bifurcation “normal form” with symmetry-breaking delays

Consider the following planar delay differential equation with real parameter β and integer delay $\tau \in \mathbb{N}$:

$$\dot{x} = \beta x(t) - \pi y(t) - x(t)(x^2(t - \tau) + y^2(t)) \tag{100}$$

$$\dot{y} = \pi x(t) + \beta y(t) - y(t)(x^2(t) + y^2(t - \tau)). \tag{101}$$

The system (100)–(101) is qualitatively similar to the normal form of the Hopf bifurcation for ODEs with angular velocity π , except we have inserted two delays $\tau > 0$ into the nonlinear terms. The solutions of the traditional Hopf normal form are invariant under rotation about zero, but this is not the case for the system above.

$(x, y) = (0, 0)$ is an equilibrium solution and as β crosses through zero, a supercritical Hopf bifurcation occurs. The bifurcating periodic solution is explicitly available: for given parameter $\beta > 0$ it is precisely

$$(x^*(t), y^*(t)) = (\sqrt{\beta} \cos(\pi t), \sqrt{\beta} \sin(\pi t)).$$

This follows almost immediately from the observation that $x^*(t - \tau) = (-1)^\tau x^*(t)$ and $y^*(t - \tau) = (-1)^\tau y^*(t)$. We are interested in the stability and possible bifurcations that can occur on this branch of periodic orbits. After some algebraic simplifications and use of trigonometric identities, one can show that the linearization at (x^*, y^*) is

$$\begin{aligned} \dot{z} = & \begin{bmatrix} 0 & -\pi - \beta \sin(2\pi t) \\ \pi - \beta \sin(2\pi t) & 0 \end{bmatrix} z(t) \\ & + (-1)^{\tau+1} \begin{bmatrix} \beta(1 + \cos(2\pi t)) & 0 \\ 0 & \beta(1 - \cos(2\pi t)) \end{bmatrix} z(t - \tau) \end{aligned} \tag{102}$$

for $z \in \mathbb{R}^2$. Note that even though the original periodic solution has period two, we can see that the linearization has period one. If we let $U(t, s) : C([-\tau, 0], \mathbb{R}^2) \rightarrow C([-\tau, 0], \mathbb{R}^2)$ denote the associated solution operator, the monodromy operator $M := U(2, 0)$ can be factored: if we define $\tilde{M} := U(1, 0)$, then

$$M = U(2, 0) = U(2, 1)U(1, 0) = U(1, 0)U(1, 0) = \tilde{M}^2 \tag{103}$$

due to the periodicity of the coefficients. By the spectral mapping theorem, the eigenvalues of M are the squares of the eigenvalues of \tilde{M} . Thus, to investigate the stability of (x^*, y^*) it suffices to work with the monodromy operator for (102) interpreted as a periodic system with period $p = 1$ and delay $q = \tau$, rather than period two. Also, recall that since (x^*, y^*) is a periodic solution of an autonomous delay differential equation, $\mu = 1$ will always be a Floquet multiplier [14, Section XIV.2, Proposition 2.6], so we will always have $\sqrt{\mu} \in \pm 1$ as an eigenvalue of \tilde{M} . Stability of (x^*, y^*) is determined by the remaining Floquet multipliers.

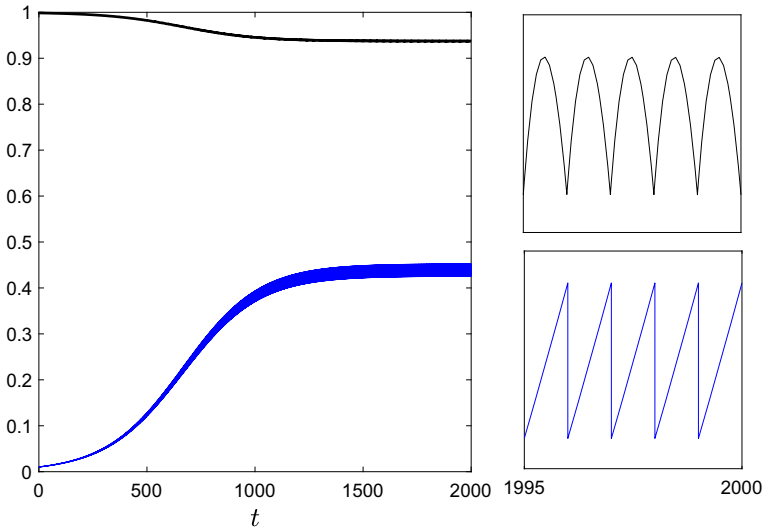


Fig. 5 Left: numerical simulation of the system (95)–(97) at the parameters $\tau = 1, \beta = 0.1, \rho = 1, K = 1, d_1 = 0.02, d_2 = 0.03, r = 0.7$ and $h = 0.06$ from the constant initial condition $(x_0, y_0) = (1, 0.01)$ for $t \in [0, 2000)$. The equilibrium $(x, y) = (1, 0)$ is unstable by Theorem 8.1.2. The x component is the top curve (black) and y is the blue curve (bottom). The discontinuities occurring at the integers make the y curve difficult to resolve (note the varying “thickness” of the curve with respect to t). Top right: x component windowed to $t \in [1995, 2000)$. Bottom right: y component with the same windowing. At this resolution the converged periodic solution (of period 1) is easily discernible

Namely, orbital asymptotic stability with asymptotic phase (i.e. asymptotic stability modulo phase difference) occurs if all other multipliers have modulus less than one, and instability occurs if there is a multiplier with modulus greater than one.

Since each of $\cos(2\pi t)$ and $\sin(2\pi t)$ (the nontrivial time-varying coefficients in (102)) can be generated as solutions of the two-dimensional linear ODE

$$\dot{u} = \begin{bmatrix} 0 & -2\pi \\ 2\pi & 0 \end{bmatrix} u, \tag{104}$$

we can:

- get the terms of the truncated Chebyshev series of $\cos(\pi(s - 1))$ and $\sin(\pi(s - 1))$ with rigorous interval enclosures (for a partial level of discretization) using monodromy operator discretization on (104);
- obtain bounds for the absolute error in the truncated coefficients using the discretization error c_2c_3 ;
- bound the tails using the discretization error.

This information is then used to obtain interval enclosures of the truncated Chebyshev series of the matrices in (102) (after transforming the time domain from $t \in [-1, 0]$ to $s \in [-1, 1]$) and bounds on the tails. Using our rigorous numerical method, we can prove then prove the following theorem.

Theorem 8.2.1 *Let $\tau = 1$. The unstable manifold of the nontrivial periodic solution $(x^*(t), y^*(t))$ of the two-dimensional Hopf-like normal form (100)–(101) at parameter $\beta = \frac{3}{2}$ is at least two-dimensional.*

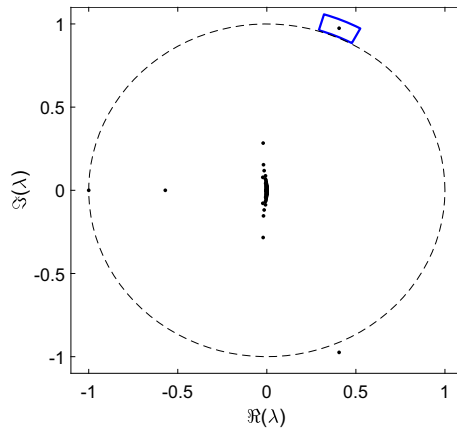


Fig. 6 The black dots are the eigenvalues of the finite (matrix) part of the operator \tilde{M}_{N_1, N_2} . Observe that -1 is a (numerical) eigenvalue, which is consistent with the discussion following (103). The radial sector $R_{\lambda^*}(r, \omega)$ from the proof of Theorem 8.2.1 appears in blue. The unit circle is provided for relative scale, and is delineated by a black dashed curve. The gap between the radial sector and the unit circle is very small and difficult to resolve in the figure: in the radial direction the length of the gap is bounded below by 3.4×10^{-3}

Table 3 Numerical outputs from the proof of Theorem 8.2.1

c_1	c_2	c_3	$c_1 c_2 c_3$
85.79436	5.70375	0.0020193	0.98813

Proof (Outline) We validated the radial sector $R_{\lambda^*}(r, \omega)$ with

$$\lambda^* = 0.405828912008976 + 0.974191597102970i, \quad r = 0.055, \quad \omega = 0.1.$$

The validation was done at $N_1 = 65, N_2 = 1000$ and $\nu = 1.04$. We used the radii polynomial method and Proposition 4.3.1 to prove that \tilde{M}_{N_1, N_2} has exactly one eigenvalue within this radial sector. As the non-real eigenvalues of the monodromy operator come in complex-conjugate pairs and $R_{\lambda^*}(r, \omega)$ does not intersect the real axis, we conclude that there is also a conjugate eigenvalue. By Lemma 4.3.2, the (undiscretized, true) monodromy operator \tilde{M} has a pair of complex-conjugate eigenvalues contained in the union of $R_{\lambda^*}(r, \omega)$ and its reflection over the real axis. This sector is strictly outside of the unit disc in the complex plane, so the eigenvalues have absolute value greater than one. From our observations above concerning the spectral mapping theorem and the relationship between the eigenvalues of M and \tilde{M} , we conclude the unstable manifold of the periodic solution $(x^*(t), y^*(t))$ is at least two-dimensional. See Fig. 6 for the validation structure and approximate eigenvalues. \square

The proof is computationally expensive. Based on some heuristics, we would expect an unparallelized version of the proof to take approximately 23 days to complete on our machine. Almost all of this time is due to the lengthy c_1 bound calculation. To speed up the computation for the proof, we distributed the load over our primary machine and a laptop running an Intel Core i7 5950HQ with 32GB of memory. Each machine then ran five simultaneous instances of MATLAB, and each instance was tasked with 1/10 of the load associated to the c_1 bound. The script at [9] includes a parameter that controls which section of the proof is to be completed, and it was this script that was simultaneously run on the ten MATLAB instances. Doing the proof this way, it took a bit over two days to complete. The results are found in Table 3.

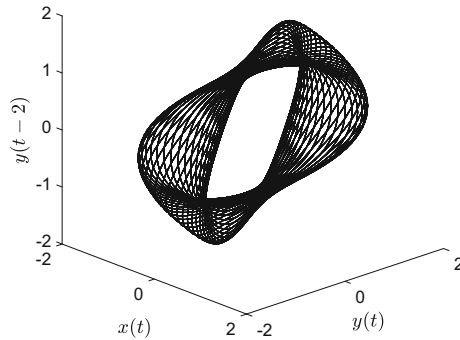


Fig. 7 The attractor of the planar system (100)–(101) at $\tau = 1$ and $\beta = \frac{3}{2}$. Computed by forward integration in dde23 for $t \in [0, 2000]$ and truncated to $[1000, 2000]$. The delayed variable $y(t - 2)$ is included to realize the embedding of the two-dimensional manifold (equivalent to a torus) in three-dimensional space

This theorem provides strong evidence for the existence of an invariant torus, since the two unstable Floquet multipliers would need to have crossed through the unit circle between $\beta = 0$ and $\beta = \frac{3}{2}$. The likely scenario is that this would have occurred at a Neimark-Sacker bifurcation. Numerical integration of the delay differential equations does indeed reveal an attracting, invariant torus: see Fig. 7.

8.3 Spurious flower petals

This final example demonstrates the importance of validated numerics. It also provides some aesthetically pleasing figures. Consider the following piecewise-constant delay equation:

$$\dot{x} = (-1)^{\lfloor t \rfloor} \begin{bmatrix} 0 & -c \\ c & 0 \end{bmatrix} x(t - \tau), \tag{105}$$

where τ is a nonnegative integer and $c \in \mathbb{R}$. It is worth mentioning that this equation is notoriously difficult to integrate to high precision.

Proposition 8.3.1 *For any nonnegative integer delay τ and $c \in \mathbb{R}$, the only nonzero Floquet multiplier of (105) is $\mu = 1$.*

Proof Let $x(t) = \phi(t)e^{t\lambda}$ be a Floquet eigensolution—that is, $\lambda \in \mathbb{C}$ and ϕ complex-valued with period 2. Let $V(\lambda) = \begin{bmatrix} 0 & -ce^{-\lambda\tau} \\ ce^{-\lambda\tau} & 0 \end{bmatrix}$. Then

$$\dot{\phi} = -\lambda\phi(t) + (-1)^{\lfloor t \rfloor} V(\lambda)\phi(t - \tau).$$

Case 1: τ is even. Then $\phi(t - \tau) = \phi(t)$ since ϕ is periodic with period 2. Then

$$\dot{\phi} = (-\lambda I + (-1)^{\lfloor t \rfloor} V(\lambda))\phi.$$

One can verify that the matrices $-\lambda I + V(\lambda)$ and $-\lambda I - V(\lambda)$ commute, from which it follows that the solution $\phi(t)$ of the above differential equation satisfies

$$\phi(2) = \exp(-\lambda I - V(\lambda)) \exp(-\lambda I + V(\lambda)) \phi(0) = \exp(-\lambda I) \phi(0).$$

Since ϕ is nontrivial, we must have $\lambda = 0$. Therefore $\mu = e^0 = 1$ is the only nonzero Floquet multiplier.

Case 2: τ is odd. Define $\phi_0(t) = \phi(t)$ and $\phi_1(t) = \phi(t - 1)$. Since ϕ is periodic with period 2, we have $\phi_0(t - \tau) = \phi_1(t)$ and $\phi_1(t - \tau) = \phi_0(t)$. The pair (ϕ_0, ϕ_1) therefore satisfies the ODE

$$\begin{aligned} \dot{\phi}_0 &= -\lambda \phi_0 + (-1)^{\lfloor t \rfloor} V(\lambda) \phi_1 \\ \dot{\phi}_1 &= -\lambda \phi_1 - (-1)^{\lfloor t \rfloor} V(\lambda) \phi_0 \end{aligned}$$

The matrices $M_1 = -\lambda I_{4 \times 4} + \text{diag}^\perp(V(\lambda), -V(\lambda))$ and $M_2 = -\lambda I_{4 \times 4} - \text{diag}^\perp(V(\lambda), -V(\lambda))$ commute, where $\text{diag}^\perp(A, B) = \begin{bmatrix} 0 & A \\ B & 0 \end{bmatrix}$. It follows that $\mathbf{\Phi}(t) = (\phi_0(t), \phi_1(t))$ satisfies

$$\mathbf{\Phi}(2) = \exp(M_2) \exp(M_1) \mathbf{\Phi}(0) = \exp(-2\lambda I_{4 \times 4}) \mathbf{\Phi}(0).$$

As ϕ is nontrivial, we must have $\lambda = 0$. Therefore $\mu = e^0 = 1$ is the only nonzero Floquet multiplier. □

Even though $\mu = 1$ is the only Floquet multiplier, the discretized operator M_{N_1, N_2} has some rather interesting flower petal-shaped numerical eigenvalue patterns that are present for seemingly arbitrarily high level of modes N_2 (note: $N_1 = 0$ for this problem). The latter is a common element of the *spurious eigenvalue* phenomenon [12]. We provide plots of the eigenvalues of M_{N_1, N_2} in Fig. 8 for $c = 10$, $\tau = 3, 5, 7$ and various values of N_2 . We should also emphasize that neither the radii polynomial method [6] nor `verifyeig` (applied to validation of distinct eigenvalues) from INTLAB [24] are able to verify *any* of the eigenvalues of the associated matrices M_{N_1, N_2} , so even if we were able to numerically verify $c_1 c_2 c_3 < 1$ for for the closed circle with radius $r = 0.99$ (which seems bounded away from the all of the discretized spectra), we would be unable to prove using a computer that there is an eigenvalue with absolute value greater than 0.99.

Another interesting observation is that the diameter of the “flower” portion of the eigenvalue pattern seems to be proportional to the parameter c . We do not provide figures demonstrating this scaling but refer the reader to the MATLAB code [9] where they may adjust the parameters τ , c and N_2 as desired. Even with $c = 10^{-2}$, none of the eigenvalues (treated as distinct, as opposed to clusters) can be validated with the radii polynomial method or `verifyeig`.

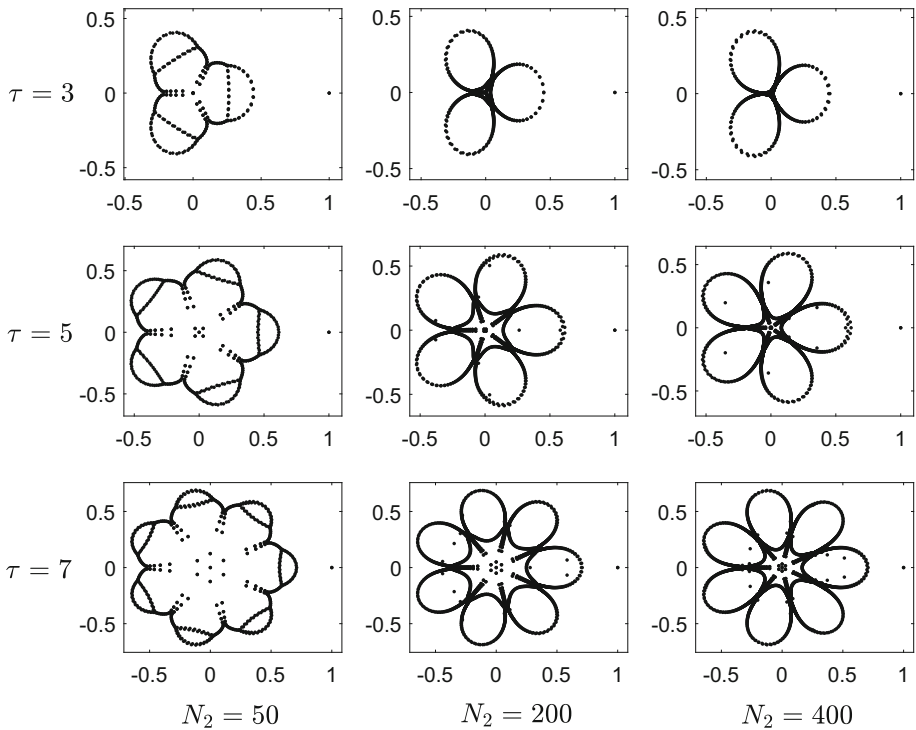


Fig. 8 Eigenvalues in the complex plane (horizontal axis real, vertical axis imaginary) of the discretized monodromy operator M_{N_1, N_2} as computed by `eig` in MATLAB for the two-dimensional system (105) with $c = 10$. Since the periodic coefficient $(-1)^{\lfloor t \rfloor}$ is piecewise-constant, $N_1 = 0$. Plots are provided for $\tau = 3, 5, 7$ and $N_2 = 50, 200, 400$. Though the figures are not reported here, we did the same calculation with $N_2 = 1000$ and the same “flower petal” patterns were present

9 Examples with floating point arithmetic

It is worthwhile doing some large-scale tests of our numerical method for monodromy operator discretization of impulsive delay differential equations in floating point arithmetic. In particular, we are interested in how fast our implementation is for larger systems.

9.1 Methodology: examples with periodic coefficients

We generated six systems of the form (10)–(11) for each dimension $d = 10, 50$. The delays were $q \in \{1, 2, 3\}$ and the periods $p \in \{1, 2\}$, so that each combination of delay and period is seen at each dimension. The systems were constructed as follows.

- 1 The matrices $A(t)$ and $B(t)$ were designed at the Chebyshev level. After transformation to the $s \in [-1, 1]$, suppose we write truncated Chebyshev series for the restriction of one of $A(t)$ or $B(t)$ to an integer-length interval $t \in [n, n + 1]$ as

$$S_0 + 2 \sum_{k=1}^{N_1} S_k T_k(s)$$

for $d \times d$ matrices S_k and T_k the k th Chebyshev polynomial. The entries of S_k are drawn from the uniform distribution on $2^{-k}[-1, 1]$ to simulate analytic coefficients with geometric decay rate 2. We took $N_1 = 50$ so that all remaining terms of this (presumably) analytic function would have norm bounded above by 9×10^{-16} . The coefficients are then rescaled by a random number drawn from uniform $[0, 1]$.

- 2 The C_1 matrices was designed to induce contraction (or at least non-expansion). We first generate a random matrix D by sampling entries from the uniform distribution on $[-1, 1]$. We then take k to be sampled from the uniform $[0, 1]$ and define

$$C_1 = \frac{k}{\|D\|} D - I_{d \times d}.$$

By construction, $\|I + C_1\| = k \leq 1$, so the effect of the impulse due to C_1 is nonexpansive (contractive if $k < 1$).

- 3 The C_2 matrices was taken to be a (relatively) small and random. Their entries were drawn from the normal distribution with mean $\mu = 0$ and variance $\sigma^2 = 10^{-1}$, truncated to the interval $[-10^{-1}, 10^{-1}]$.

9.2 Methodology: examples with piecewise-constant coefficients

With constant coefficient systems it makes sense to look at lower-mode discretizations (since we do not need to take into account the standing hypothesis $N_2 > N_1$). This also gives us more flexibility (in terms of computer memory) to look at systems of higher dimension. We look this time at systems of dimension $d = 10, 50$ and also 100. Our design methodology is identical to the periodic coefficients case except that we take $N_1 = 0$ so that our Chebyshev series for $A(t)$ and $B(t)$ have zero nonconstant modes (i.e. $A(t)$ and $B(t)$ are piecewise constant).

9.3 Results

Remark 9.3.1 All references to computing time were as performed on a Windows 10 machine with an AMD Ryzen 5 1500X processor and 16gb of memory in MATLAB R2019b. All operations were completed in 64-bit floating point arithmetic. Times were done using the `tic/toc` MATLAB function. While this is relatively accurate for long computations, short computations are subject to jitter and the actual computation time might be shorter.

Before we begin presenting the results, we should briefly mention that due to how we have designed the matrices $A(t)$, $B(t)$, C_1 and C_2 , it is expected that higher-dimensional problems we study will be unstable (in the sense of Lyapunov stability) and therefore have larger spectral radii $\sigma(M_{N_1, N_2})$. Intuitively, this is because since these have been generated randomly there is greater potential for multilayered feedback mechanisms to overwhelm the contraction generated by $I + C_1$.

The time needed to compute M_{N_1, N_2} in floating point arithmetic for each tuple of dimension, period, delay and number of modes (d, p, q, N_2) is stated in Tables 4 and 5 for the systems with periodic coefficients. The systems with constant coefficients have the results stated in Tables 6, `reftablespsfp50c` and 8. The spectral radius of M_{N_1, N_2} for each tuple is also stated, so that one can compare the predicted spectral radius (and inferred stability) as the order (i.e. number of modes) increases. We should emphasize that the part of M_{N_1, N_2} that lives in memory (i.e. the finite part) is a $qd(N_2 + 1) \times qd(N_2 + 1)$ matrix. The construction

Table 4 Computation time for M_{N_1, N_2} and spectral radius for the 10-dimensional periodic coefficient examples

p	q	N_2	Time	$\sigma(M_{N_1, N_2})$	p	q	N_2	Time	$\sigma(M_{N_1, N_2})$
1	1	50	0.1823	0.260300268572241	2	1	50	0.3669	1.716890539322859
1	1	100	0.8171	0.260300268572240	2	1	100	1.8684	1.716890539322860
1	1	200	4.6518	0.260300268572241	2	1	200	10.6391	1.716890539322858
1	2	50	0.3009	0.862657110762436	2	2	50	0.8336	0.962102756266976
1	2	100	1.5717	0.862657110762425	2	2	100	4.6179	0.962102756266973
1	2	200	10.5377	0.862657110762449	2	2	200	30.3392	0.962102756266975
1	3	50	0.5769	0.835260513721166	2	3	50	0.7818	1.301687998067846
1	3	100	3.4762	0.835260513721170	2	3	100	4.2526	1.301687998067844
1	3	200	24.7049	0.835260513721173	2	3	200	25.8714	1.301687998067849

Table 5 Computation time for M_{N_1, N_2} and spectral radius for the 50-dimensional periodic coefficient examples

p	q	N_2	Time	$\sigma(M_{N_1, N_2})$	p	q	N_2	Time	$\sigma(M_{N_1, N_2})$
1	1	50	7.1569	2.007711242747832	2	1	50	16.1546	10.407570266516226
1	1	100	48.5008	2.007711242747846	2	1	100	115.242	10.407570266516256
1	1	200	348.3643	2.007711242747829	2	1	200	789.033	OOM
1	2	50	17.6226	3.790193289898586	2	2	50	52.8226	1.592405342469769
1	2	100	119.2017	3.790193289898596	2	2	100	400.6249	1.592405342469754
1	2	200	OOM	OOM	2	2	200	OOM	OOM
1	3	50	44.8359	1.146527675417064	2	3	50	50.2296	7.557587755604763
1	3	100	330.5872	1.146527675417057	2	3	100	378.5051	7.557587755604715
1	3	200	OOM	OOM	2	3	200	OOM	OOM

of each such matrix requires storing other large matrices in memory and multiplying them. In those instances where we were unable to complete the calculation because we ran out of memory, the associated entry in the table is flagged “OOM” (Out Of Memory).

From the point of view of spectral radius approximation, we see that computing more than $N_2 = 50$ nonconstant modes does not improve precision. For example, comparing the results for the systems with periodic coefficients, the estimations of $\sigma(M_{N_1, N_2})$ agree to 10^{-13} precision for each problem (i.e. fixed p and q). Thus, at least insofar as stability verification is concerned, there is no reason to use more than $N_2 = 50$ nonconstant modes. The same trend is present for the systems with piecewise-constant coefficients. Going further, comparing from $N_2 = 10$ to $N_2 = 50$ modes, we see that the spectral radius calculations agree to 10^{-8} for all problems of dimension $d = 10, 50$, and to 10^{-4} for the 100-dimensional problems.

Table 6 Computation time for M_{N_1, N_2} and spectral radius for the 10-dimensional constant coefficient examples

p	q	N_2	Time	$\sigma(M_{N_1, N_2})$	p	q	N_2	Time	$\sigma(M_{N_1, N_2})$
1	1	10	0.0204	0.556128844229585	2	1	10	0.0478	2.185758750606892
1	1	50	0.2339	0.556128849778831	2	1	50	0.3671	2.185758750607603
1	1	100	0.5561	0.556128849778835	2	1	100	1.6692	2.185758750607603
1	2	10	0.0265	0.663276863767956	2	2	10	0.0329	0.661060805093243
1	2	50	0.2693	0.663276863768000	2	2	50	0.6227	0.661060805093239
1	2	100	1.2452	0.663276863768000	2	2	100	3.6868	0.661060805093245
1	3	10	0.0183	0.657019981757325	2	3	10	0.0494	1.762876266177592
1	3	50	0.5016	0.657019981765232	2	3	50	0.6014	1.762876266179832
1	3	100	3.0095	0.657019981765237	2	3	100	3.2392	1.762876266179832

Table 7 Computation time for M_{N_1, N_2} and spectral radius for the 50-dimensional constant coefficient examples

p	q	N_2	Time	$\sigma(M_{N_1, N_2})$	p	q	N_2	Time	$\sigma(M_{N_1, N_2})$
1	1	10	0.1289	1.431806607392872	2	1	10	0.3776	5.889651972534294
1	1	50	6.6510	1.431806607395949	2	1	50	15.2128	5.889651972514686
1	1	100	44.1495	1.431806607395935	2	1	100	103.2565	5.889651972514656
1	2	10	0.2640	3.021066383737128	2	2	10	0.7894	55.374021351893155
1	2	50	16.5041	3.021066384401501	2	2	50	47.9067	55.374022020448038
1	2	100	114.8197	3.021066384401488	2	2	100	338.0685	55.374022020448052
1	3	10	0.6170	2.713663289865321	2	3	10	0.7164	6.095605026664076
1	3	50	40.7782	2.713663291176386	2	3	50	46.6918	6.095605037539426
1	3	100	297.4751	2.713663291176395	2	3	100	320.8671	6.095605037539483

Table 8 Computation time for M_{N_1, N_2} and spectral radius for the 100-dimensional constant coefficient examples

p	q	N_2	Time	$\sigma(M_{N_1, N_2})$	p	q	N_2	Time	$\sigma(M_{N_1, N_2})$
1	1	10	1.0073	4.756741912773284	2	1	10	1.9272	694.4431525710570
1	1	50	44.8451	4.756741869532997	2	1	50	103.5975	694.4431388682707
1	1	100	353.0308	4.756741869532950	2	1	100	893.3342	694.4431388682730
1	2	10	1.7046	3.180153198138059	2	2	10	4.9740	7.487399911295219
1	2	50	116.2478	3.180152710155930	2	2	50	366.5735	7.487399886587351
1	2	100	904.2700	3.180152710155918	2	2	100	3000.4027	7.487399886587358
1	3	10	3.8915	5.086753778285468	2	3	10	4.4939	7.141800125000926
1	3	50	310.9164	5.086753811041823	2	3	50	362.3332	7.141800129977383
1	3	100	2640.3295	5.086753811041799	2	3	100	2677.7598	7.141800129977379

10 Conclusions

We have developed a numerical method for the discretization of the monodromy operator associated for impulsive delay differential equations with periodic coefficients. The method is able to accommodate systems where the period and delay are commensurate: that is, their ratio is a rational number. The numerical scheme is based Chebyshev collocation: we identify concrete linear operators that act on Chebyshev series coefficients that represent sufficiently smooth initial conditions to the impulsive delay differential equation. We also represent the periodic coefficients in the Chebyshev polynomial basis (with matrix coefficients). Truncating the number of modes at the level of the inputs (initial conditions) and at the level of the periodic coefficients yields a numerical method.

An advantage of our framework is that it is amenable to computer-assisted proofs concerning the location of Floquet multipliers based on the discretized monodromy operator. In Sect. 6 we proved explicit and computable formulas for quantities c_1 , c_2 and c_3 such that if $c_1 c_2 c_3 < 1$, the location of the Floquet multipliers of the impulsive DDE relative to a specified validation structure has the same location as analogous eigenvalues of the discretized monodromy operator. These structures include specific compact sets in the complex plane that are bounded away from the origin (e.g. radial sector validation) and complements of closed discs centered at zero (i.e. generalized Morse index validation).

We implemented our numerical scheme for arbitrary integer period p and delay q in MATLAB. We also implemented the bounds c_1 , c_2 and c_3 for the cases $p = q = 1$ and $1 = p < q$. We demonstrated the computer-assisted proof techniques on two problems. The first was a scalar problem motivated by a model from mathematical ecology. For this problem we first proved binary stability/instability results by validating a Morse index at radius 1. We then proved some robust stability and bifurcation enclosure results. The second example was a two-dimensional nonlinear system modeled off of the Hopf bifurcation normal form. We linearized about a periodic solution and verified using our method that at a particular parameter value, the unstable manifold of this periodic solution is two-dimensional.

We tested our numerical implementation in floating point arithmetic on several problems. The implementation is fast for problems of moderate (≤ 50) dimension and a reasonable number ($N_2 \leq 50$) of modes provided p and q are fairly small. For the test problem of calculating the spectral radius of the monodromy operator, there was not a significant difference in relative accuracy when the number of modes N_2 was dramatically increased (i.e. from 50 to 100 or from 100 to 200), so fewer modes (e.g. 10 to 50) may be perfectly suitable for situations where validated numerics are not needed. As should be expected, the computing time and memory requirements become steep as the (rescaled, relative to period) delay q increases. Some of the matrices needed to compute M_{N_1, N_2} are sparse, so memory could be saved with a sparse matrix implementation at the cost of speed. Moreover, our implementation for arbitrary period and delay outlined in Sect. 7.2 has some inefficiencies and could certainly be improved.

It should be emphasized that the extra dimensions (of which there are $(q - 1)(N_2 + 1)$) in the discretization due to the delay q are only present because of our stated goal of developing not only a rigorous numerical method, but also techniques for computer-assisted proof of Floquet multiplier location. Indeed, the extra dimensions are necessary to ensure that all eigenfunctions can be represented as uniformly convergent Chebyshev series with coefficients in X_p . However, if one were to expand the solutions in terms of other basis functions and the form of convergence was taken to be more coarse (e.g. L^2 convergence), a faster numerical method could be developed that does not suffer from this drawback. However, such a method

would likely not be as well-suited to computer-assisted proof of eigenvalue location and proving its convergence might be difficult.

We have claimed that our approach to computer-assisted proof could be extended to the case where the period is greater than the delay: $p > q$. We elaborate on this briefly now by way of an example. Suppose that $p = 2$ and $q = 1$. Let $M_1 = (I - W_1)^{-1}E_1$ denote the operator that sends an initial condition at time $t = 0$ to its value at time $t = 1$ after flowing along the dynamical system (10)–(11). Similarly, Let $M_2 = (I - W_2)E_2$ be the operator that an initial condition from time $t = 1$ forward to time $t = 2$. Then $M = M_2M_1$ is the monodromy operator. If $\tilde{E}_1, \tilde{W}_1, \tilde{E}_2$ and \tilde{W}_2 are approximations of E_1, W_1, E_2 and W_2 , then one may be interested in adapting Lemma 4.3.1 to the operator M and its “approximation” $\tilde{M} = \tilde{M}_2\tilde{M}_1$, with $\tilde{M}_2 = (I - \tilde{W}_2)^{-1}\tilde{E}_2$ and $\tilde{M}_1 = (I - \tilde{W}_1)^{-1}\tilde{E}_1$. Observe that

$$\begin{aligned} \tilde{M} - M &= (I - W_2)^{-1} \left[(I - W_2)(I - \tilde{W}_2)^{-1}\tilde{E}_2(I - \tilde{W}_1)^{-1}\tilde{E}_1 - E_2(I - W_1)^{-1}E_1 \right] \\ &= (I - W_2)^{-1} \left\{ \left[(I - W_2)(I - \tilde{W}_2)^{-1}\tilde{E}_2 - E_2 \right] (I - \tilde{W}_1)^{-1}\tilde{E}_1 \right. \\ &\quad \left. + E_2 \left[(I - \tilde{W}_1)^{-1}\tilde{E}_1 - (I - W_1)^{-1}E_1 \right] \right\} \\ &= (I - \tilde{W}_2)^{-1} \left\{ \left[(I - W_2)\tilde{M}_2 - E_2 \right] \tilde{M}_1 + E_2 \left[\tilde{M}_1 - M_1 \right] \right\} \end{aligned}$$

The norm of \tilde{M}_1 can (presumably) be obtained precisely using a computer. Each of $(I - \tilde{W}_2)^{-1}$ and $(I - W_2)\tilde{M}_2 - E_2$ are formally analogous to operators that are bounded above by c_2 and c_3 in our present proof of Lemma 4.3.1. The latter lemma can technically be applied as stated to obtain a bound on the norm of $\tilde{M}_1 - M_1$. As for E_2 , its norm can in principle be estimated by writing

$$E_2 = \tilde{E}_2 + (E_2 - \tilde{E}_2),$$

computing a bound for the norm of \tilde{E}_2 on a computer, and deriving a computable bound for the norm of the error $E_2 - \tilde{E}_2$ by careful inspection. In summary, there should be an explicit computable bound for the norm of $\tilde{M} - M$ and its computation will involve similar estimates to those involved in the statement of Lemma 4.3.1, so we would expect many of the bounds from Sect. 6 to be applicable. The rest of the proof could be carried out essentially verbatim. The above argument can be extended to general commensurate period-delay pairs.

Acknowledgements The author thanks Jean-Philippe Lessard for some helpful technical discussions. Kevin E. M. Church acknowledges the support of NSERC (Natural Sciences and Engineering Research Council of Canada) through the NSERC Postdoctoral Fellowships Program.

A Table of useful norm bounds

The two linear operators expressed in Lemma 5.1.3 appear often in estimates concerning the c_2 and c_3 bound, and they are often accompanied by a projection operator. Several other auxiliary operator norms are also required. Here, we list such operators and upper bounds on their norms (in the appropriate spaces of linear maps) in the form of a table. We then prove each bound directly. In what follows, we always have $\nu > 1$, $U, Y \in \ell^1_\nu(\mathbb{C}^d)$ and $N_2 > N_1 \geq 0$. Also, let $\mathbf{Q}^{-1}(Y)$, \mathbf{DT} , \mathbf{H}_1^0 , $Z_k^{N_1, N_2}$ and $S(Y^{N_1})$ be defined as at the beginning of Sect. 6.

Row	Linear map $F : X \rightarrow Y$	Bound for $\ F\ _{L(X,Y)}$
1	$H_2 : \ell_v^1 \rightarrow \mathbb{C}^d$	$2 + \left(\frac{1}{v} - v\right) \tanh^{-1}\left(\frac{1}{v}\right) \equiv g(v)$
2	$H_2(Y * \pi_{N_2}^\infty) : \ell_v^1 \rightarrow \mathbb{C}^d$	$\frac{2}{v^{N_2+1}} \left(\ Y^{N_1}\ _v + \left(1 + \frac{1}{v^{N_2+1}}\right) \ Y^\infty\ _v \right)$
3	$H_1 : \ell_v^1 \rightarrow \ell_v^1$	$\frac{1}{2} + \frac{v}{4}$
4	$\pi_{N_2}^\infty H_1 : \ell_v^1 \rightarrow \ell_v^1$	$\frac{v + v^{-1}}{4(N_2 + 1)}$
5	$S : \ell_v^1 \rightarrow \mathbb{C}^d$	$\max\{1, 2v^{-1}\}$
6	$S\pi_{N_2}^\infty : \ell_v^1 \rightarrow \mathbb{C}^d$	$2v^{-(N_2+1)}$
7	$S^*\pi_{N_2}^\infty : \ell_v^1 \rightarrow \mathbb{C}^d$	$2v^{-(N_2+1)}$
8	$\tilde{Q}^{-1}(Y^{N_1})\pi^{N_2} : \ell_v^1 \rightarrow \ell_v^1$	$\max_{k=0,\dots,N_2} \frac{1}{v^k} \sum_{j=0}^{N_2} \ \tilde{Q}_{j,k}^{-1}(Y^{N_1})\ _v^j$
9	$\tilde{Q}^{-1}(Y^{N_1})\mathbf{e}_0 : \mathbb{C}^d \rightarrow \ell_v^1$	$\sum_{j=0}^{N_2} \ \tilde{Q}_{j,0}^{-1}(Y^{N_1})\ _v^j$
10	$S\tilde{Q}^{-1}(Y^{N_1})\pi^{N_2} : \ell_v^1 \rightarrow \mathbb{C}^d$	$\max_{k=0,\dots,N_2} \frac{1}{v^k} \left(\ \tilde{Q}_{0,k}^{-1}(Y^{N_1})\ + 2 \sum_{n=1}^{N_2} \ \tilde{Q}_{n,k}^{-1}(Y^{N_1})\ \right)$
11	$S\tilde{Q}^{-1}(Y^{N_1})\mathbf{e}_0 : \mathbb{C}^d \rightarrow \mathbb{C}^d$	$\ \tilde{Q}_{0,0}^{-1}(Y^{N_1})\ + 2 \sum_{j=1}^{N_2} \ \tilde{Q}_{j,0}^{-1}(Y^{N_1})\ $
12	$\tilde{Q}^{-1}(Y^{N_1})\pi^{N_2}H_1(U^{N_1} * \pi_{N_2}^\infty) : \ell_v^1 \rightarrow \ell_v^1$	$\max_{k=0,\dots,N_1} \frac{1}{v^{N_2+1+k}} \sum_{j=0}^{N_2} \left(\frac{\ U^{N_1}\ _\omega}{(N_2 + 1 - N_1)^2 - 1} \ \tilde{Q}_{j,0}^{-1}\ + \ \tilde{Q}_j^{-1} \mathbf{DT} Z_k^{N_1, N_2} \mathbf{S}(U^{N_1})\ \right) v^j$
13	$\pi^{N_2}H_1(Y^{N_1} * \pi_{N_2}^\infty) : \ell_v^1 \rightarrow \ell_v^1$	$\max_{k=0,\dots,N_1} \frac{1}{v^{N_2+1+k}} \sum_{j=0}^{N_2} \left(\frac{\ U^{N_1}\ _\omega}{(N_2 + 1 - N_1)^2 - 1} \mathbf{1}_0(j) + \ \mathbf{DT}_j Z_k^{N_1, N_2} \mathbf{S}(U^{N_1})\ \right) v^j$
14	$\pi_{N_2}^\infty H_1(Y^{N_1} * \pi_{N_2}^\infty) : \ell_v^1 \rightarrow \ell_v^1$	$\frac{1}{4(N_2 + 1)} \left(\left(v + \frac{2}{v} + \frac{1}{v^3} \right) \ Y^{N_1}\ _v - \left(\frac{1}{v} + \frac{1}{v^3} \right) \ Y_0^{N_1}\ \right) + \mathbf{m}_0 + \sum_{k=2}^{N_2} \frac{(-1)^k + 1}{k^2 - 1} \mathbf{m}_k,$
15	$H_2(\pi^{N_2} \tilde{Q}^{-1}(Y^{N_1})H_1(U_1^{N_1} * \pi_{N_2}^\infty)) : \ell_v^1 \rightarrow \mathbb{C}^d$	$\mathbf{m}_k = \max_{j=0,\dots,N_1} \frac{1}{v^{N_2+1+j}} \left(\frac{\ U^{N_1}\ _\omega}{(N_2 + 1 - N_1)^2 - 1} \ \tilde{Q}_{k,0}^{-1}\ + \ \tilde{Q}_k^{-1} \mathbf{DT} \tilde{Z}_j^{N_1, N_2} \mathbf{S}(U^{N_1})\ \right)$

A.1 Proofs of the bounds from the table in Appendix A

This subsection will be structured with proofs being completed by row. The row number will be stated and a proof will immediately follow.

A.1.1 Proof of Row 1

Let $h \in \ell_v^1$ satisfy $\|h\|_v \leq 1$. Then

$$\begin{aligned} \|H_2h\| &\leq \|h_0\| + \sum_{j=1}^{\infty} \frac{2}{(2j)^2 - 1} \|h_{2j}\| \leq 1 + \sum_{j=1}^{\infty} \frac{2v^{-2j}}{(2j)^2 - 1} \\ &= 1 + \frac{v + (1 - v^2) \tanh^{-1}(v^{-1})}{v} = g(v). \end{aligned}$$

A.1.2 Proof of Row 2

Let $h \in \ell_v^1$ satisfy $\|h\|_v \leq 1$. Then with $h^\infty = \pi_{N_2}^\infty h$,

$$\begin{aligned} \|H_2(Y^\infty * h^\infty)\|_v &= \|(Y^\infty * h^\infty)_0\| + \sum_{j=1}^{\infty} \frac{2}{(2j)^2 - 1} \|(Y^\infty * h^\infty)_{2j}\| v^{2j} \\ &\leq 2 \sum_{n \geq N_2+1} \|Y_n^\infty\| \cdot \|h_n\| + \sum_{j=1}^{\infty} \frac{2}{(2j)^2 - 1} \sum_{|m| \geq N_2+1} \|Y_{|m-2j}^\infty\| \cdot \|h_{|m|}\| \\ &\leq \frac{2\|Y^\infty\|_v}{v^{2(N_2+1)}} + \sum_{j=1}^{\infty} \frac{2}{(2j)^2 - 1} \|Y^\infty\|_v \frac{1}{v^{N_2+1}} \sum_{|m| \geq N_2+1} \|h_{|m|}\| v^{|m|} \\ &\leq \frac{2\|Y^\infty\|_v}{v^{2(N_2+1)}} + \frac{2}{v^{N_2+1}} \sum_{j=1}^{\infty} \frac{2}{(2j)^2 - 1} \|Y^\infty\|_v \\ &= \frac{2}{v^{N_2+1}} \|Y^\infty\|_v \left(1 + \frac{1}{v^{N_2+1}}\right). \end{aligned}$$

Conversely, one can check that $\|H_2(Y^{N_1} * h^\infty)\| \leq \frac{2}{v^{N_2+1}} \|Y^{N_1}\|_v$ by a similar argument.

A.1.3 Proof of Row 3

$$\begin{aligned} \|H_1\|_{B(\ell_v^1)} &\leq \sup_{n \geq 0} \frac{1}{v^n} \sum_{j=0}^{\infty} \|H_{1,(j,n)}\| v^j \\ &\leq \max \left\{ \frac{1}{2} + \frac{1}{4}v, \frac{1}{v} \left(\frac{1}{4} + \frac{1}{8}v^2 \right), \right. \\ &\quad \left. \sup_{n \geq 2} \frac{1}{v^n} \left(\frac{1}{n^2 - 1} + \frac{v^{n-1}}{4(n-1)} + \frac{v^{n+1}}{4(n+1)} \right) \right\} = \frac{1}{2} + \frac{v}{4}. \end{aligned}$$

A.1.4 Proof of Row 4

Let $h \in \ell_v^1$ satisfy $\|h\|_v \leq 1$.

$$\|\pi_{N_2}^\infty H_1(h)\| \leq \sum_{k=N_2+1}^{\infty} v^k \sum_{j=0}^{\infty} \|H_{1,(k,j)} h_j\| = \sum_{k=N_2+1}^{\infty} \frac{v^k}{4k} (\|h_{k-1}\| + \|h_{k+1}\|)$$

$$\begin{aligned} &\leq \frac{1}{4(N_2 + 1)} \sum_{k=N_2+1}^{\infty} v^{k-1} \|h_{k-1}\|_v + v^{k+1} \|h_{k+1}\|_v^{-1} \\ &\leq \frac{1}{4(N_2 + 1)} \left(v + \sum_{i \geq 0} v^i \|h_i\| + v^{-1} \sum_{j \geq 0} v^j \|h_j\| \right) \\ &= \frac{v + v^{-1}}{4(N_2 + 1)} \|h\|_v. \end{aligned}$$

A.1.5 Proof of Row 5

Write $h \in \ell_v^1$ with $\|h\|_v = 1$ as $h = h^0 + h^\infty$, where $h^0 = (h_0, 0, \dots)$. Set $\lambda = \|h^0\|$. Then $\|h^\infty\|_v = 1 - \lambda$ and

$$\|Sh\| \leq \|h_0\| + 2 \sum_{j=1}^{\infty} \|h_j\| \leq \lambda + \frac{2}{v} \sum_{j=1}^{\infty} \|h_j\| v^j = 1 \cdot \lambda + \frac{2}{v} (1 - \lambda) \leq \max\{1, 2v^{-1}\}.$$

A.1.6 Proof of Row 6/7

$$\|S\pi_{N_2}^\infty h\| \leq 2 \sum_{k \geq N_2+1} \|h_k\| \leq \frac{2}{v^{N_2+1}} \sum_{k \geq N_2+1} \|h_k\| v^k \leq \frac{2}{v^{N_2+1}} \|h\|_v.$$

The proof for S^* is essentially identical.

A.1.7 Proof of Row 8

We will apply Lemma 5.2.1 to the operator $L : X_v \rightarrow X_v$ for $X_v = \mathbb{C}^d \times \ell_v^1$, with $Lh = (0, \tilde{Q}^{-1} \pi^{N_2} h_0)$. By construction,

$$(\tilde{Q}^{-1} \pi^{N_2} h)_j = \sum_{n=0}^{\infty} \tilde{Q}_{j,n}^{-1} h_n,$$

for $0 \leq j \leq N_2$ and is zero for all other indices. In that notation L consists of only a V -type operator. Then $\|L\|_{B(X_v)}$ is bounded above by

$$\sup_{n \geq 0} \frac{1}{v^n} \sum_{j=0}^{\infty} \|\tilde{Q}_{j,n}^{-1}\| v^n = \max_{n=0, \dots, N_2} \frac{1}{v^n} \sum_{j=0}^{N_2} \|\tilde{Q}_{j,n}^{-1}\| v^n.$$

and we obtain the bound for $\|\tilde{Q}^{-1} \pi^{N_2}\|_{B(\ell_v^1)}$ by restriction.

A.1.8 Proof of Row 9

Let $z \in \mathbb{C}^d$. Then

$$(\tilde{Q}^{-1} e_0 z)_j = \begin{cases} \tilde{Q}_{j,0}^{-1} z, & 0 \leq j \leq N_2 \\ 0 & j \geq N_2 + 1. \end{cases}$$

$N_2 + 1$ rows correspond precisely to $\tilde{Z}_k^{N_1, N_2} \mathbf{S}(U^{N_1})$ for $N_2 + 1 \leq k \leq N_2 + 1 + N_1$. Finally, we already know that $(U^{N_1} * \pi_{N_2}^\infty)_k = 0$ for $0 \leq k \leq N_2$.

We now combine all of the previous discussion. Our bound becomes

$$\begin{aligned} & \| \tilde{Q}^{-1} \pi^{N_2} H_1(U^{N_1} * \pi_{N_2}^\infty) \|_{B(\ell_v^1)} \\ & \leq \sup_{k \geq 0} \frac{1}{v^k} \sum_{j=0}^\infty (\| \tilde{Q}_j^{-1} H_1^0(U^{N_1} * \pi_{N_2}^\infty)_k \| + \| \tilde{Q}_j^{-1} DT(U^{N_1} * \pi_{N_2}^\infty)_k \|) v^j \\ & \leq \max_{k=0, \dots, N_1} \frac{1}{v^{N_2+1+k}} \sum_{j=0}^{N_2} \left(\frac{\|U^{N_1}\|_\omega}{N^2 - 1} \| \tilde{Q}_{j,0}^{-1} \| + \| \tilde{Q}_j^{-1} \mathbf{DT} \tilde{Z}_k^{N_1, N_2} \mathbf{S}(U^{N_1}) \| \right) v^j. \end{aligned}$$

The proof for row 13 follows by formally replacing \tilde{Q}^{-1} with the identity.

A.1.11 Proof of Row 14

Denote $e^k \in L(\mathbb{C}^d, \ell_v^1)$ the map defined by $(e^k z)_n = \delta_{k,n} z$ for δ the Kronecker delta. The operator $\pi_{N_2}^\infty H_1(A_1^{N_1} * \pi_{N_2}^\infty)$ satisfies for $\pi_{N_2}^\infty H_1(A_1^{N_1} * \pi_{N_2}^\infty) e^k = 0$ for $k \leq N_2$, while for $k \geq N_2 + 1$,

$$\begin{aligned} (\pi_{N_2}^\infty H_1(Y^{N_1} * \pi_{N_2}^\infty) e^k)_j &= \frac{1}{4j} \left((Y^{N_1} * e^k)_{j-1} - (Y^{N_1} * e^k)_{j+1} \right) \\ &= \frac{1}{4j} \sum_{|n| \geq N_2+1} \left(Y_{|j-1-n|}^{N_1} - Y_{|j+1-n|}^{N_1} \right) e^k_{|n|} \\ &= \frac{1}{4j} \left(Y_{|j-1-k|}^{N_1} - Y_{|j+1-k|}^{N_1} \right) \\ &\equiv \frac{1}{4j} c_{j,k} \end{aligned}$$

for $j \geq N_2 + 1$, while it is identically zero for $j \leq N_2$ because of the projection $\pi_{N_2}^\infty$ on the left. We can therefore set $c_{j,k} = 0$ without loss of generality whenever $0 \leq j, k \leq N_2$. Since we can write $\ell_v^1 \ni h = \sum_{k \geq 0} e^k h_k$, we have the expression

$$(\pi_{N_2}^\infty H_1(Y^{N_1} * \pi_{N_2}^\infty) h)_j = \sum_{k \geq 0} \frac{1}{4j} c_{j,k} h_k.$$

Next we apply Lemma 5.2.1.

$$\begin{aligned} & \| \pi_{N_2}^\infty H_1(Y^{N_1} * \pi_{N_2}^\infty) \|_{B(\ell_v^1)} \\ & \leq \sup_{k \geq 0} \frac{1}{v^k} \sum_{j=0}^\infty \frac{1}{4j} \| c_{j,k} \| v^j \\ & \leq \sup_{c \geq 1} \frac{1}{v^{N_2+c}} \cdot \frac{1}{4(N_2 + 1)} \left(\sum_{j=c+1-N_1}^{c+1+N_1} \| Y_{|j-1-c|}^{N_1} \| v^{N_2+j} + \sum_{r=c-1-N_1}^{c-1+N_1} \| Y_{|r+1-c|}^{N_1} \| v^{N_2+r} \right) \\ & \leq \sup_{c \geq 1} \frac{1}{4v^c (N_2 + 1)} \left(\sum_{m=-N_1}^{N_1} \| Y_{|m|}^{N_1} \| v^{m+c+1} + \sum_{n=-N_1}^{N_1} \| Y_{|n|}^{N_1} \| v^{r+c-1} \right) \end{aligned}$$

$$\begin{aligned}
 &= \frac{1}{4(N_2 + 1)} \left(\sum_{m_1=-N_1}^{-1} \nu^{2m_1+1} \|Y_{|m_1|}^{N_1}\| \nu^{|m_1|} + \sum_{m_2=0}^{N_1} \nu \|Y_{|m_2|}^{N_1}\| \nu^{|m_2|} \right. \\
 &+ \left. \sum_{r_1=-N_1}^{-1} \nu^{2r_1-1} \|Y_{|r_1|}^{N_1}\| \nu^{|r_1|} + \sum_{r_2=0}^{N_1} \nu^{-1} \|Y_{|r_2|}^{N_1}\| \nu^{|r_2|} \right) \\
 &\leq \frac{1}{4(N_2 + 1)} \left(\frac{1}{\nu} (\|Y^{N_1}\|_{\nu} - \|Y_0^{N_1}\|) + \nu \|Y^{N_1}\|_{\nu} + \frac{1}{\nu^3} (\|Y^{N_1}\|_{\nu} - \|Y_0^{N_1}\|) + \frac{1}{\nu} \|Y^{N_1}\|_{\nu} \right) \\
 &= \alpha(Y^{N_1}).
 \end{aligned}$$

A.1.12 Proof of Row 15

To complete this proof, we determine bounds for $(\pi^{N_2} \tilde{Q}^{-1}(Y^{N_1})H_1(U^{N_1} * \pi_{N_2}^{\infty}))_j, k = 0, \dots, N_2$. An application of the triangle inequality will then supply the bound for row 15. However, since $\pi^{N_2} \tilde{Q}^{-1}(Y^{N_1}) = \pi^{N_2} \tilde{Q}^{-1}(Y^{N_1})\pi^{N_2}$, much of the work has already been done in the proof of row 12/13. Indeed, for fixed $k \in \{0, \dots, N_2\}$, this calculation shows that

$$\begin{aligned}
 &\|(\pi^{N_2} \tilde{Q}^{-1}(Y^{N_1})H_1(U^{N_1} * \pi_{N_2}^{\infty}))_k\|_{L(\ell^1, \mathbb{C}^d)} \\
 &\leq \max_{j=0, \dots, N_1} \frac{1}{\nu^{N_2+1+j}} \left(\frac{\|U^{N_1}\|_{\omega}}{\mathbf{N}^2 - 1} \|\tilde{Q}_{k,0}^{-1}\| + \|\tilde{Q}_k^{-1} \mathbf{DT} \tilde{Z}_j^{N_1, N_2} \mathbf{S}(U^{N_1})\| \right).
 \end{aligned}$$

Note, the roles of j and k are reversed relative to the previous proof.

References

1. Akhmet, M: Principles of discontinuous dynamical systems. Springer, New York, New York, NY (2010)
2. Bainov, D., Simeonov, P.: Impulsive Differential Equations: Periodic Solutions and Applications. Chapman and Hall/CRC, (1993)
3. Breda, D.: Computing the characteristic roots for delay differential equations. IMA Journal of Numerical Analysis **24**(1), 1–19 (2004)
4. Breda D, Maset S, Vermiglio R (2005) Characteristic roots of delay differential. SIAM J. Sci. Comput **27**(22), 482–495
5. Breda, D., Maset, S., Vermiglio, R.: Pseudospectral approximation of eigenvalues of derivative operators with non-local boundary conditions. Appl. Numer. Math., 56:318–331 (2006)
6. Castelli, R., Lessard, J.-P.: A method to rigorously enclose eigenpairs of complex interval matrices. In: Conference Applications of Mathematics 2013 in Honor of the 70th Birthday of Karel Segeth. Institute of Mathematics AS CR, Prague 2013, pp. 1–11 (2013)
7. Cepeda-Gomez R, Michiels W (2015) Special cases in using the matrix Lambert W function for the stability analysis of high-order linear systems with time delay. IFAC-PapersOnLine **28**(12), 7–12
8. Church, K.: Invariant Manifold Theory for Impulsive Functional Differential Equations with Applications. Ph.D. thesis, University of Waterloo (2019)
9. Church, K.E.M.: Codes to accompany Eigenvalues and delay differential equations: periodic coefficients, impulses and rigorous numerics (2020). https://github.com/kemchurch/IFDE_spectral_methods/tree/master/JDDE-2020
10. Church KEM, Liu X (2018) Smooth centre manifolds for impulsive delay differential equations. J. Differ. Equ. **265**(4), 1696–1759
11. Church KEM, Liu X (2019) Computation of centre manifolds and some codimension-one bifurcations for impulsive delay differential equations. J. Differ. Equ. **267**(6), 3852–3921
12. Dawkins PT, Dunbar SR, Douglass RW (1998) The origin and nature of spurious eigenvalues in the spectral Tau method. J. Comput. Phys. **147**(2), 441–462

13. Diamond P (1990) Impulsive evolution equations and population models. In: Vincent TL, Mees AI, Jennings LS (eds) *Dynamics of Complex Interconnected Biological Systems*. Birkhäuser, Boston, pp. 175–203
14. Diekmann O, Verduyn Lunel SM, van Gils SA, Walther H-O (1995) *Delay Equations: Functional-, Complex-, and Nonlinear Analysis*, Applied Mathematical Sciences. Springer, New York
15. Engelborghs, K.: DDE-BIFTOOL: A Matlab Package for Bifurcation Analysis of Delay Differential Equations. Technical report (2000)
16. Gilsinn DE, Potra FA (2006) Integral operators and delay differential equations. *J. Integr. Equ. Appl.* **18**(3), 297–336
17. Ivanov, I.L., Slyn'Ko, V.I.: A stability criterion for autonomous linear time-lagged systems subject to periodic impulsive force. *International Applied Mechanics* **49**(6), 732–742 (2013)
18. Jarlebring E, Meerbergen K, Michiels W (2010) A Krylov method for the delay eigenvalue problem. *SIAM J. Sci. Comput.* **32**(6), 3278–3300
19. Kato T (1995) *Perturbation Theory for Linear Operators* *Classics in Mathematics*, vol. 132. Springer, Berlin
20. Lakshmikantham, V., Bainov, D.D., Simeonov, P.S.: *Theory of Impulsive Differential Equations*. World Scientific, Singapore (1989)
21. Lessard, JP, Mireles James JD (2019) A functional analytic approach to validated numerics for eigenvalues of delay equations. *J. Comput. Dyn.*, 7, 123
22. Meng X, Jiao J, Chen L (2008) The dynamics of an age structured predator-prey model with disturbing pulse and time delays. *Nonlinear Anal. Real World Appl.* **9**(2), 547–561
23. Miyajima S (2017) Verified solutions of delay eigenvalue problems. *Appl. Math. Comput.* **303**, 211–225
24. Rump SM (1999) INTLAB—INTERVAL LABORATORY. In: Tibor C (ed) *Developments in Reliable Computing*. Kluwer Academic Publishers, Dordrecht, pp 77–104
25. Samoilenko AM, Perestyuk NA (1995) *Impulsive Differential Equations*, World Scientific Series on Nonlinear Science Series A. World Scientific, Singapore
26. Sieber J, Szalai RR (2011) Characteristic matrices for linear periodic delay differential equations. *SIAM J. Appl. Dyn. Syst.* **10**(1), 129–147
27. Slynko VI, Tunç C, Erdur S (2020) Sufficient conditions of interval stability of a class of linear impulsive systems with a delay. *J. Comput. Syst. Sci. Int.* **59**(1), 88–18
28. Stamova I (2009) *Stability Analysis of Impulsive Functional Differential Equations*. De Gruyter, Berlin
29. Szalai, R.: *Knut: A Continuation and Bifurcation Software for Delay-differential Equations*
30. Szalai R, Stépán G, John Hogan S (2006) Continuation of bifurcations in periodic delay–differential equations using characteristic matrices. *SIAM J. Sci. Comput.* **28**(4), 1301–1317
31. Trefethen LN (2013) *Approximation Theory and Approximation Practice*. Society for Industrial and Applied Mathematics, Philadelphia
32. Verduyn Lunel, S.M.: Small solutions and completeness for linear functional differential equations. In: *Oscillations and Dynamics in Delay Equations*, Contemporary Mathematics, vol. 129. AMS, Providence, pp. 127–152 (1992)
33. Zhen W, Michiels W (2012) Reliably computing all characteristic roots of delay differential equations in a given right half plane using a spectral method. *J. Comput. Appl. Math.* **236**(9), 2499–2514

Publisher's Note Springer Nature remains neutral with regard to jurisdictional claims in published maps and institutional affiliations.